UNIVERSITÉ DE MONTRÉAL

SYNTHESES AND CHARACTERIZATIONS OF NEW POLYMERS WITH BILE ACID DERIVATIVES AS PENDANT GROUPS

PAR
QIANG WANG
DÉPARTEMENT DE CHIMIE
FACULTÉ DES ARTS ET DES SCIENCES

THÈSE PRÉSENTÉE À LA FACULTÉ DES ÉTUDES SUPÉRIEURES
EN VUE DE L'OBTENTION DU GRADE DE
MAÎTRE ÈS SCIENCE (M. Sc.)
EN CHIMIE

AVRIL 2002

UNIVERSITÉ DE MONTRÉAL

FACULTÉ DES ÉTUDES SUPÉRIEURES

Cette thèse intitulée

SYNTHESES AND CHARACETRIZATIONS OF NEW POLYMERS WITH BILE ACID DERIVATIVES AS PENDANT GROUPS

Présentée par

QIANG WANG

A été évaluée par un jury composé des personnes suivantes:

André Beauchamp, président rapporteur

François Brisse, directeur de recherche

Xiao Xia Zhu, co-directeur de recherche

Michel Lafleur, membre du jury

Thèse acceptée le:

ACKNOWLEDGEMENTS

I would like to thank my directors: Prof. François Brisse and Prof. Julian Zhu who give me kind help, instruction and encouragement during my graduate study and research. Their knowledge, diligence and meticulous scientific approach affect me very much. It should be very beneficial for me in my chemistry research career in the future.

I also want to thank my colleagues for the many discussions and exchange of ideas.

I wish to thank Michel Simard and Francine Bélanger-Gariépy for their help in X-ray diffraction work.

Finally, I would like to thank my family: my parents, wife, brother, daughter. They gave me spiritual encouragement and support so that I could continue and finish my study at University of Montreal when I had difficulties.

ABSTRACT

The purpose of this study was to synthesize and characterize liquid crystalline polymers containing bile acids and determine the crystal structures of some precursors using X-ray diffraction.

New monomers containing three molecular components were synthesized. The methacrylate monomers were polymerized to form the polymer backbone. The mesogenic group of the side chain is a rigid bile acid. The alkyl methylene spacer decouples the motion of the mesogenic groups and the polymer chains, allowing for a regular orientation in the liquid crystalline state. The length of the spacer was varied so as to study its influence on the liquid crystalline properties of the polymer. Recrystallisation was possible for two of the monomers. They were obtained as single crystals and their structures were determined by X-ray diffraction. The methyl 3α-tosyloxy-5β-cholan-24-ate belongs to $P2_12_12_1$ orthorhombic space group. There are 6 independent molecules in the asymmetric unit. The methyacryloyloxy-hexyloxy-3α,7α,12α-trihydroxy-5β-cholan-24-ate has the $P2_1$ monoclinic space group. There are 2 molecules in unit cell.

Liquid crystalline polymers containing bile acid derivatives were synthesized via free radical polymerization. These polymers were typical side-chain liquid crystalline polymers containing methylene side chain spacers, bile acid derived mesogenic groups and methacrylate main chains.

Both homopolymers and copolymers were characterized by the following techniques: nuclear magnetic resonance (NMR), mass spectrometry (MS), Fourier transform infrared spectroscopy (FTIR), size exclusion chromatography (SEC), differential scanning calorimetry (DSC) and X-ray diffraction.

It seems that the short spacer groups did not allow for the existence of mesophases in the presence of bulky bile acid groups. Monomers with longer spacers may be required to reach the liquid crystalline (LC) state.

SOMMAIRE

Le présent travail avait pour but la préparation de polymères liquides cristallins dérivés de l'acide cholique et leur détermination structurale par diffraction des rayons X.

De nouveaux monomères contenant trois composantes moléculaires ont été synthétisés. L'acide cholique rigide est le groupe mésogène de la branche latérale. La chaîne principale est polymérisée à partir du monomère méthacrylate. L'espaceur de méthylène alkyl différencie le mouvement du groupe mésogène de celui de la chaîne principale. Les groupes mésogènes peuvent alors s'aligner régulièrement dans l'état de liquide cristallin. La longueur de l'espaceur a été variée pour que son influence sur les propriétés du liquide cristallin puisse être étudié. Deux monomères ont été recristallisés et forment des cristaux uniques. Les structures sont déterminées par diffraction des rayons X. Le méthyl 3α-tosyloxy-5β-cholan-24-ate appartient au groupe d'espace orthorhombique $P2_12_12_1$ et cristallise avec six molécules indépendantes dans l'unité asymétrique. Le méthyacrylyoyloxy-hexyloxy-3α,7α,12α-trihydroxy-5β-cholan-24-ate appartient au groupe spatial $P2_1$ monoclinique et il cristallise avec deux molécules par maille.

Les polymères dérivés de l'acide cholique sont synthétisés par polymérisation radicalaire. Les polymères sont typiquement des polymères branchés qui contiennent des espaceurs et des groupes mésogènes dérivés de l'acide cholique sur les branches latérales et le méthacrylate comme chaîne principale.

Les polymères ont été étudiés par: la résonance magnétique nucléaire (RMN), la spectrométrie de masse (SM), la spectroscopie infrarouge à transformée de Fourier (FTIR), chromatographie d'exclusion stérique (CES), l'analyse calorimétrique differentielle (DSC) et la diffraction des rayons-X.

Il est démontré que les polymères ne forment pas de cristaux liquides. Il semblerait que les espaceurs courts ne conduisent pas à la formation de mésophases en présence de groupes d'acide cholique encombrants. Des monomères avec des espaceurs longs peuvent être nécessaires pour obtenir l'état liquide cristallin.

TABLE OF CONTENTS

LIST OF TABLES

LIST OF FIGURES

LIST OF SYMBOLS AND ABBREVIATIONS

a, b, c	Three unit cell axes, or their lengths (in Å)
Å	Angström
AIBN	2,2'-azo-bis(isobutyronitrile)
ax	Axial
CA	Cholic acid
CAME	Cholic acid methyl ester
CH_2Cl_2	Dichloromethane
$CHCl_3$	Chloroform
d	d-spacing between two consecutive *hkl* reflection planes (in Å)
d^*	d-spacing in the reciprocal lattice (in $Å^{-1}$)
d	Density of a crystal (in g/cm^3)
D	Fiber to detector distance in X-ray diffraction (in mm)
DMF	Dimethylformamide
DMSO	Dimethylsulfoxide
DSC	Differential scanning calorimetry
EA	Elemental analysis
eq	Equatorial
Et_3N	Triethylamine
EtOH	Ethanol
f_i	Scattering factors
F_{hkl}	The overall amplitude of an X-ray wave diffracted by an *hkl* plane
FTIR	Fourier transform infrared
g	Glass state
h, k, l	Three Miller indices defining a crystallographic plane
Hz	Hertz
I_{hkl}	Diffracted intensity of an *hkl* reflection

I	Isotropic liquid
J	Coupling constant
K	Crystal state
LC	Liquid crystal
LCA	Lithocholic acid
LCAME	Lithocholic acid methyl ester
mL	Millilitre
mmol	Millimole
mol	Mole
M_n	Number average molecular weight
m. p.	Melting point
MS	Mass spectrometry
M_w	Weight average molecular weight
n	Nematic phase
NMR	Nuclear magnetic resonance
ppm	Parts per million
R	The distance of a reflection spot to the center of the film (in mm)
R	Agreement factor
R_w	Weighted agreement factor
s	Smectic phase
S	Disclination strength
S_A	Smectic A phase
S_C	Smectic C phase
SEC	Size exclusion chromatography
$SOCl_2$	Thionyl chloride
T_g	Glass transition temperature
TGA	Thermogravimetric analysis
THF	Tetrahydrofuran
U_{11}, U_{12}..	Anisotropic thermal parameters

V	Volume of a unit cell (in $Å^3$)
Z	Number of molecules in a unit cell
α, β, γ	Three unit cell angles (in °)
ξ	Distance between a reciprocal point and the equator plane (in $Å^{-1}$)
θ	Bragg angle (in °)
λ	Wavelength of the X-radiation (in Å)
ρ	Electron density distribution (in e $Å^{-3}$)
μ	Absorption factor of a crystal (in mm^{-1})
σ	Estimated standard deviation
ω	Torsion angle (in °)

CHAPTER 1

INTRODUCTION

1.1 Liquid crystals and liquid crystalline polymers

Liquid crystalline polymers, which originated from combination of polymers and liquid crystalline property, hold out much promise for the future. They have led to a great upsurge of interest not only because they provide us with more knowledge but also from the standpoint of technological importance. Nowadays, the activity in the field of liquid crystals and liquid crystal polymers (LC polymers) is growing rapidly. LC systems were developed as display materials in many modern fields[1-3] such as opto-electronic materials, non-linear optical (NLO) devices, Laser-writable devices (e.g., strongly scattering smectic textures and optically induced conformation transitions), field-orientation devices etc. It is becoming clear that self-assembly, where molecules are designed so that they organize themselves into larger scale structures in order to achieve some special properties, will be a significant objective in materials science in the years to come.

1.1.1 Low molecular weight systems

The discovery of liquid crystals can be traced to more than 100 years ago. As early as 1888, it was first described by Friedric Reinitzer[4] who observed a peculiar melting behaviour, iridescent colours, and birefringence of cholesterol esters. Reinitzer found that crystals melted sharply to form an opaque melt instead of the usual clear melt. The conclusion he drew is that some type of order still existed in the molten state. Furthermore, the opacity vanished at a higher temperature, called the clearing temperature. Drawing on Greek notes, he introduced the terms[5] ''nematic'', ''smectic'', ''cholesteric'' and discotic (Figure 1.1) according to the type of ordering. The nematic liquid crystalline phase (Figure 1.1 a) possesses long range orientational order but only short range positional order. The cholesteric state (Figure 1.1 b) is equivalent to a

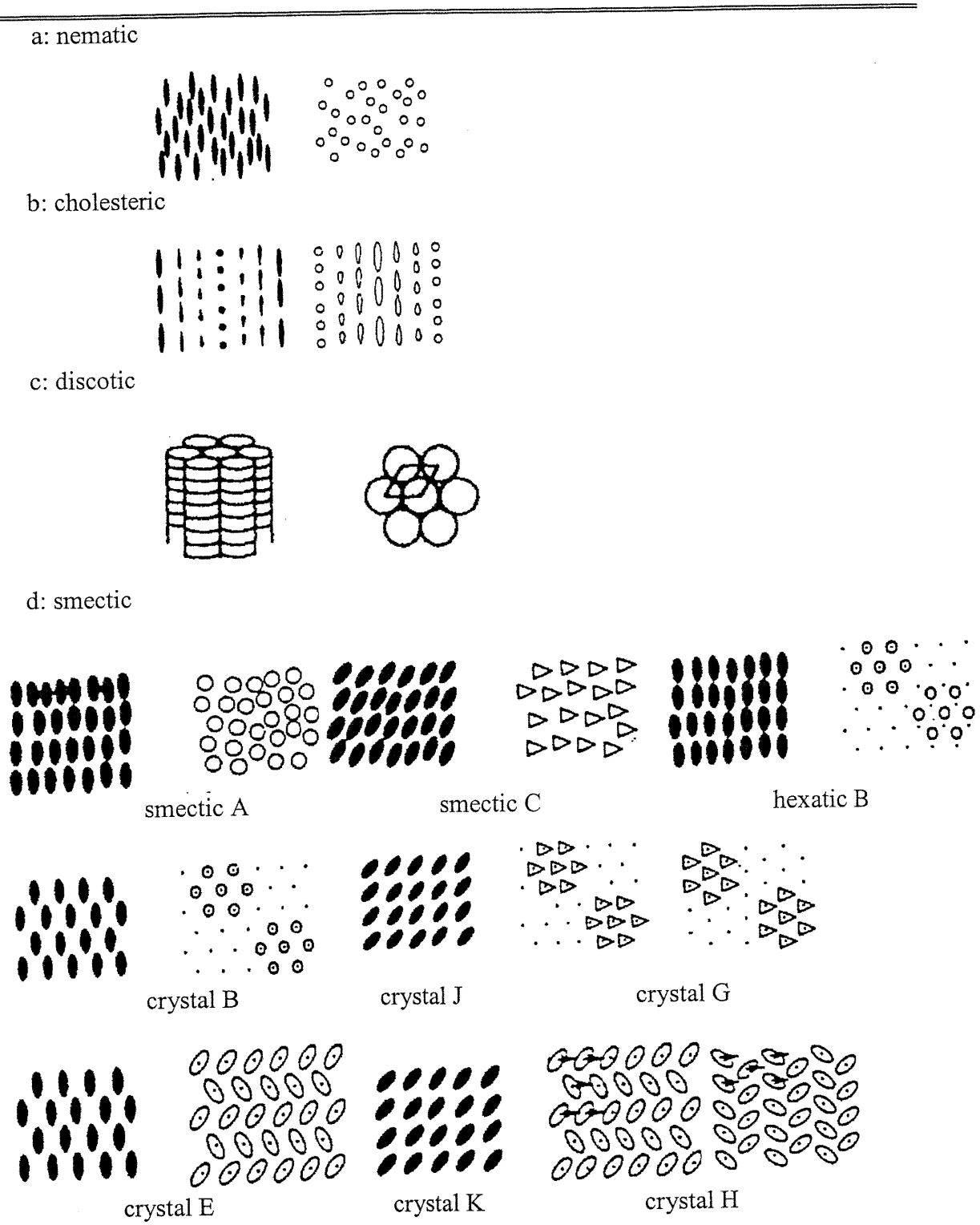

Figure 1.1 Four liquid crystal classes. The smectic modifications are taken from Gray[3]. The black and white circles stand for the molecules viewed from the side and the top respectively.

nematic which has been twisted periodically about an axis. It may be considered as a twist distortion of the nematic state. However, the twist in a cholesteric LC arises spontaneously when the mesogenic molecules have a chiral nature. The discotic mesophase resembles stacks of disks or coins (Figure 1.1 c). Smectic phases are so named because their basic layer structure gives them a soapy feel. There are several variants of smectic, but all consist of a layered structure on account of the segregation of the ends of rod molecules onto common planes. Gray[6] has divided the smectic phases into several sub-types. The two most common sub-types are known as smectic A and smectic C shown in Figure 1.1.

S_A, molecular axes are orthogonal to the layers, random arrangement within the layers;

S_C, molecular axes are tilted to the layers, random arrangement within the layers;

All of the above phases can be called ''mesophases'' which Gray suggested should supplant ''liquid crystal'' to stand for a number of distinct states between conventional crystalline solid and the isotropic liquid phases. Nowadays applications[1-3] of liquid crystals have developed rapidly, especially when the display industry started to expand in the 1970's.

The common feature of liquid crystals is asymmetric shapes. Most mesomorphic molecules are either as rod-shaped, with axial ratio greater than about 3, or form thin platelets of biaxial order. The formation of LC phases is a direct consequence of molecular asymmetry. The well known structure of a mesomorphic molecule[3,7] is shown below

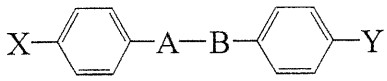

X and Y represent a range of terminal substituents. A typical nematic terminal group efficiency order[3] is:

$$CN > OCH_3 > NO_2 > Cl > Br > N(CH_3)_2 > CH_3 > H$$

However, as the terminal chain becomes longer, it tends to favour and stabilize the smectic phase with respect to other liquid crystalline structures.

A and B represent a rigid linking unit in the central structure. A typical central group nematic efficiency order[3] is:

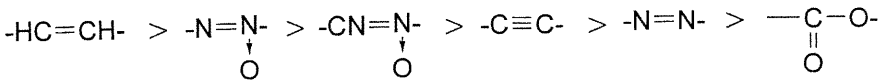

Some typical LC structures of low molecular weight are shown in Figure 1.2.

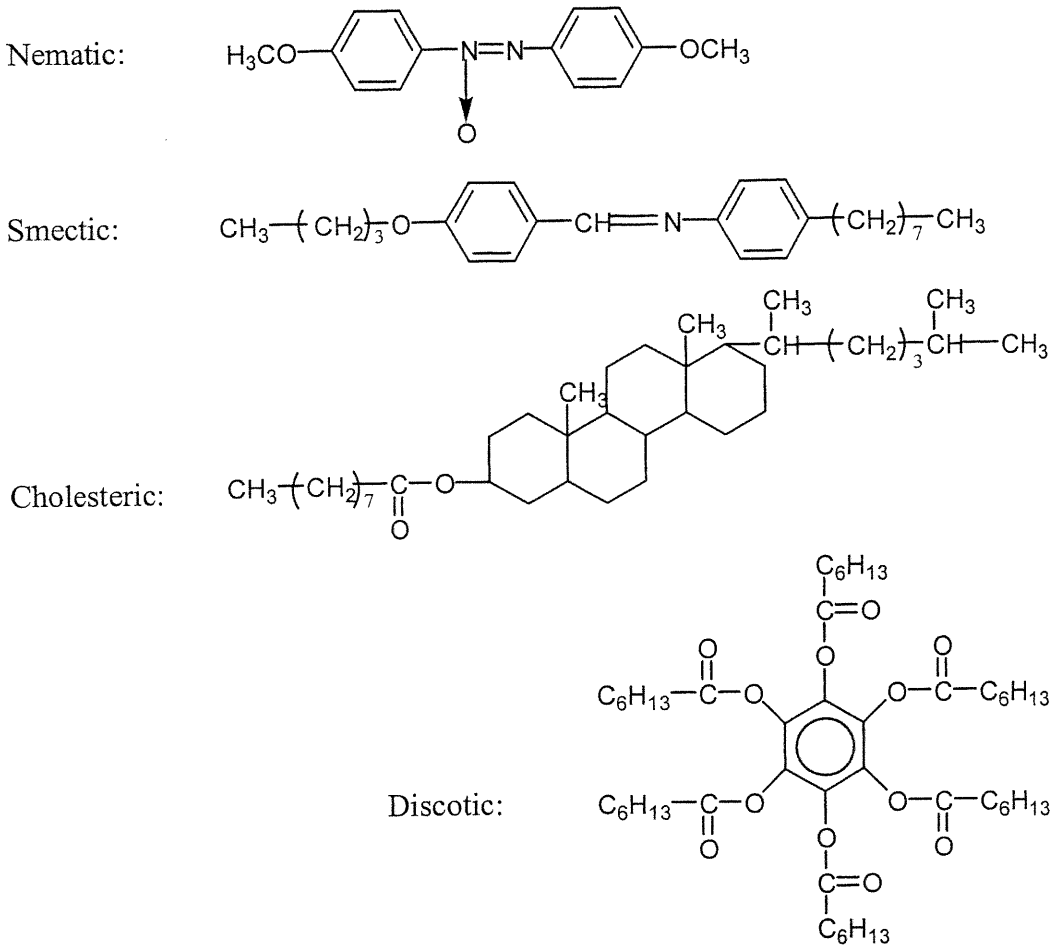

Figure 1.2 Molecules with asymmetric shapes (rods or plates) may form liquid crystals.

Besides the classification by structure, another important approach is to classify liquid crystals into lyotropic and thermotropic. They are distinguished by the way the phase changes take place. For thermotropic liquid crystals, which consist of mesogenic

molecules alone, the phase change occurs following a change of temperature. In lyotropic materials, however, the phase change is controlled by the concentration of the solution to form ordered states. Lyotropic systems are particularly significant in liquid crystalline polymers, as the addition of the solvent is an important means of reducing the melting point to manageable levels.

1.1.2 LC polymers

From the early work[8] on tobacoo mosaic virus (TMV), a stiff rod-like molecule a few thousands angstroms long in solution, to their exploitation as bulk plastic and fiber materials[9,10], the gradual development of LC polymers has been underpinned by advances in theories which explain the detailed observations. Onsager (1949)[11] was the first to introduce a theory of LC polymers by using a virial expansion, while Flory (1956)[12] adapted his lattice model of conventional polymers to the rigid situation. The development of polymeric materials has been largely a matter of adding active rod-like groups, similar to conventional LC molecules, onto flexible polymer chains. They are added either as side chains or into the backbone itself so that one way to classify thermotropic LC polymers is to examine whether the mesogenic unit is part of the main chain or in the side chain[13].

In the main chain polymers, the backbone is generated by linking together suitable functional groups A and B located at the end of the mesogenic monomers. If these monomer units are joined to form the main chain, the polymer backbone itself becomes rigid and rod-like. The rod-like structure causes anisotropic packing of the macromolecules. The strong interactions which exist between chains result in the reduction of the translational and orientational independence of the small units. The combination of chain stiffness and high ordering degree of the liquid crystal polymer in the melt (or in solution) yield ultra-high performance materials[14]. Typical main chain LC polymers are aromatic copolyesters, or terpolymers[15]. Simple homopolymer polyesters generally have too high a melting temperature to form thermotropic mesophases. In order to reduce the melting temperature and lower the transition temperatures, several techniques are available[16], one of which is to incorporate flexible

spacers[17,18], to decrease rigidity. The use of spacers is illustrated schematically for both main chain and side chain mesogenic units in Figure 1.3.

In the case of side chain polymers, the backbone is formed by using mesogenic monomers carrying a terminal group that can give addition polymerization. A number of polymerizable monomers have been synthesized in this manner. They are comprehensively summarized by Blumstein and Hsu (1978)[19] and by Shibaev and

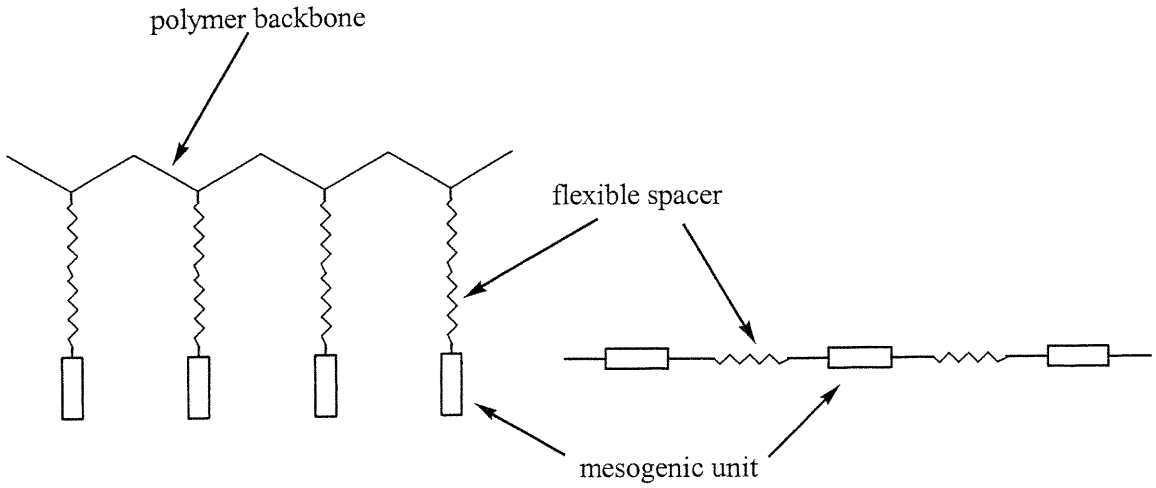

Figure 1.3 Side chain and main chain LC polymers.

Platé (1978)[20]. In most cases, the polymerizable group is a methacrylate or an acrylate, which forms a flexible vinyl backbone. The key advance in the development of side chain LC polymers was the realization by Ringsdorf, Finkelmann and coworkers[21] that rod-like side chains would only readily form mesophases if they were decoupled from the backbone to which they were attached by means of a short length of flexible chain as a spacer. The flexible spacer decouples motions of the main chain and side chain and alleviates steric hindrance. Under these conditions the mesogenic side chains can be

anistropically ordered in the liquid state even though the polymer main chain tends to adopt a statistical chain conformation. Consequently, a variation of the spacer length should clearly influence the LC order of the side chain and change the character of the mesophase. This will be discussed in the later part of this work. For the side chain LC polymers in liquid crystalline state, only original mesogenic side chains are responsible for the liquid crystalline order. This order is more or less independent of the conformation of the polymer main chain. Therefore it may be assumed that the mesogenic side chain of the polymers is very similar to the conventional low molecular weight mesogens.

1.2 Bile acid derivatives and polymers

1.2.1 The structure and importance of bile acid

Bile acids are naturally occurring amphiphilic compounds existing in bile as sodium salt of N-acyl derivatives of glycine and taurine. They can solubilize hydrophobic substances by the formation of micellar aggregates and thus help in the digestion of fats and lipids[22]. Their amphilic properties, the chirality and the rigidity of the backbone, and the unique disposition of hydroxyl groups on one side of the molecule make these compounds interesting starting materials in the synthesis of macrocyclic compounds used in biomedical, molecular recognition studies and other applications[23-26]. The well-known bile acids include cholic acid, lithocholic acid and desoxycholic acid. The cholic acid has a steroid structure with a carboxylic group at position 24 and hydroxyl groups at positions 3, 7 and 12 respectively (Figure 1.4). The four steroid cycles constitute a "plane" from which the methyl groups and hydroxyl groups, carboxylic groups are arranged above and below the plane respectively. The different orientations of the hydrophobic methyl groups and the hydrophilic groups are responsible for the amphiphilic character.

1.2.2 Polymers with bile acid derivatives

In recent years bile acids have attracted considerable research interest in the development of new polymeric materials for drug delivery systems[27], asymmetric

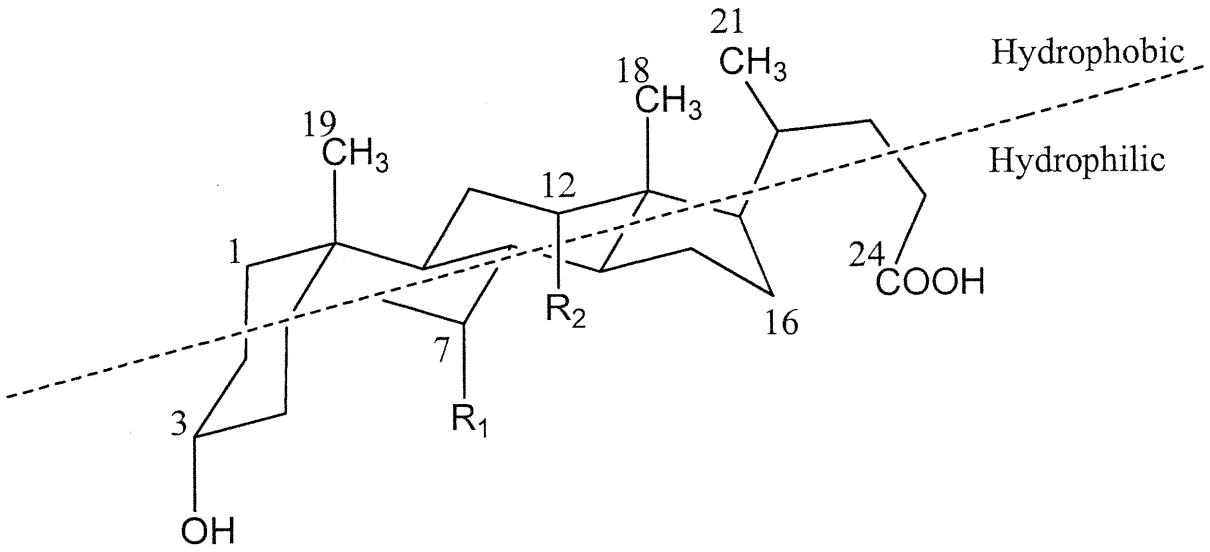

bile acids	R_1	R_2
cholic acid	OH	OH
lithocholic acid	H	H
desoxycholic acid	H	OH

Figure 1.4 Chemical structure and amphiphilic character of bile acids.

syntheses[28-30], molecular recognition[31], and artificial receptors[23]. Various polymers have been made with bile acid residues that are part of the main chain[32] or in the side chain[33,34] as pendent groups. Because of the biological origin of bile acids, their inclusion in polymers could lead to better biocompatibility when the materials are used for biomedical applications. Our group published a series of reports on polymers containing bile acids[35-40].

1.3 Selected methods used to study LC polymers

1.3.1 X-ray diffraction

Among the techniques used to study liquid crystals, X-ray diffraction is the most useful to interpret their structure. The most sophisticated of the current techniques uses the four-circle diffractometer (Figure 1.5).

The regular translation of a molecular unit along three reference axes yields a three dimensional direct lattice. When an X-ray beam is sent onto a crystal, it is diffracted by groups of so called "planes" composed of the electrons of the molecule. This phenomenon can be described by a simple relation known as Bragg's law[41]:

$$2d(hkl).\ \sin\theta(hkl) = \lambda \qquad (1.1)$$

where d(*hkl*) is the spacing (in Å) between the two consecutive planes of a given family which is specified by its Miller indices *hkl* . θ(*hkl*) is the angle between the incident beam and the *hkl* plane and λ is the wavelength of the X-rays (in Å) . The interpretation of an X-ray diffraction pattern is facilitated when the inverse relation between sinθ(*hkl*) and d(*hkl*) is replaced by a direct one. What amounts to this can be achieved by constructing a reciprocal lattice, based on 1/d, a quantity which varies directly with sinθ. The reciprocal lattice may be defined as illustrated in Figure 1.6 where a family of *hkl* planes in direct space is associated to a lattice point in the reciprocal lattice. A point of the reciprocal lattice, *hkl*, is represented by a vector constructed in the following way: the vector's origin is at O, it is normal to the *hkl* plane and terminates at a distance d*=1/d from this origin. Consider a sphere of radius 1/λ (called the Ewald sphere) whose center coincides

with the crystal. The path of the direct X-ray beam meets the Ewald sphere at O. When the *hkl* vector intersects with the Ewald sphere at A, Bragg's law is followed and reflection occurs in the OA direction.

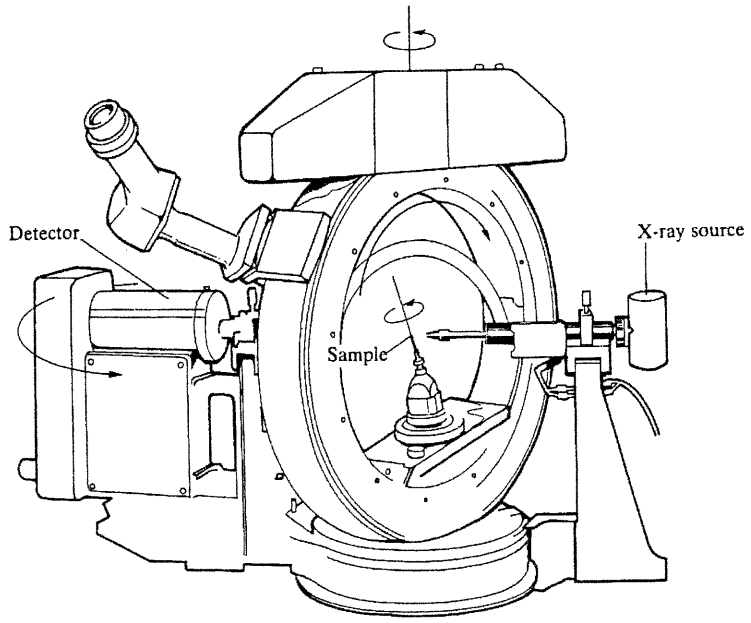

Figure 1.5 A four-circle diffractometer. The settings of the orientations of the crystal is controlled by computer; each (*hkl*) reflection is monitered in turn, and its intensity, I_{hkl}, is recorded[41].

In order to record all accessible diffraction data, the crystal must be moved so that each reflection plane will reach its proper θ angle with respect to the X-ray beam. In other words, all the reciprocal lattice points must be given the chance to intersect the surface of the Ewald sphere.

1.3.1.1 Single crystal diffraction

In a single crystal, a lattice point of reciprocal lattice is associated with a reflection (Figure 1.6). The X-ray diffraction process for this system is well developed

both in theory and technology[42]. A sophisticated piece of equipment called a diffractometer is designed to move a single crystal around three axes. Thus, a large number of reciprocal points will cross the Ewald sphere. A detector will move correspondingly and measures the intensity of each reflection. All accessible reflections can be accurately recorded by the orientation of the associated vector and its magnitude (intensity). The three dimensional vectors are used to deduce the reciprocal lattice. An indexing routine will generate the possible unit cells. In order to establish the crystal

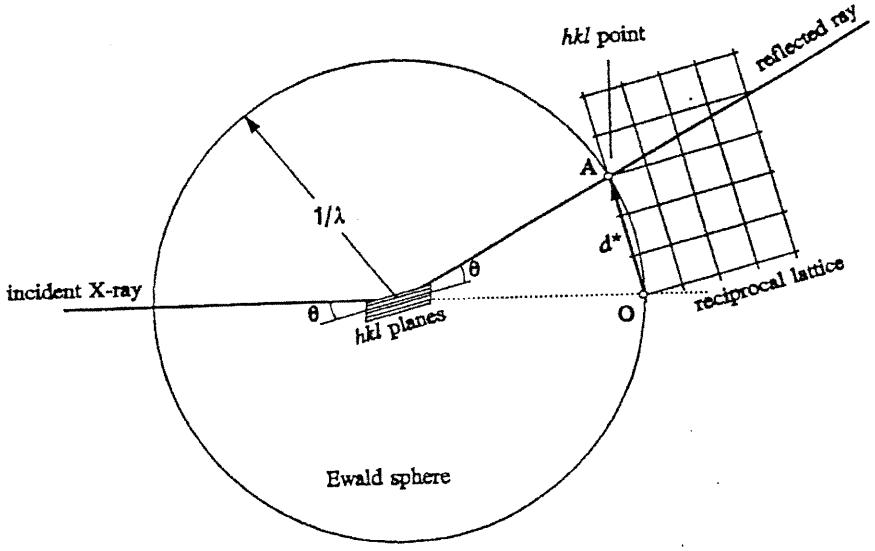

Figure 1.6 Reciprocal lattice and diffraction[43].

structure, one requires accurate measurements of the diffracted intensities. A unit cell contains several atoms j with scattering factors f_j. These factors are related to the electron density distribution in the atom, $\rho_j(r)$, by

$$f_i = 4\pi \int_0^\infty \rho \frac{\sin kr}{kr} r^2 dr \quad , \text{ where } k = \frac{4\pi}{\lambda} \sin\theta \qquad (1.2)$$

and coordinates (x_ja, y_jb, z_jc), the overall amplitude of the wave diffracted by an (*hkl*)

plane is a generalization of the expression:

$$F_{hkl} = \sum_j f_i e^{2\pi i(hx_j + ky_j + lz_j)} \qquad (1.3)$$

The sum is over all the atoms in the unit cell. F_{hkl} is called the structure factor. The intensity of a reflection, $I_{hkl,}$ is proportional to $|F_{hkl}|^2$, thus

$$|F_{hkl}| = \sqrt{I_{hkl}}/k \qquad (1.4)$$

The reciprocal lattice with the point intensities constitute the Fourier transform of the content of a crystal unit cell.

Although there exists a phase problem that prevents one from taking the reverse of the Fourier transform and then obtaining the structure, there are some sophisticated computer programs that can now produce an approximate model very close

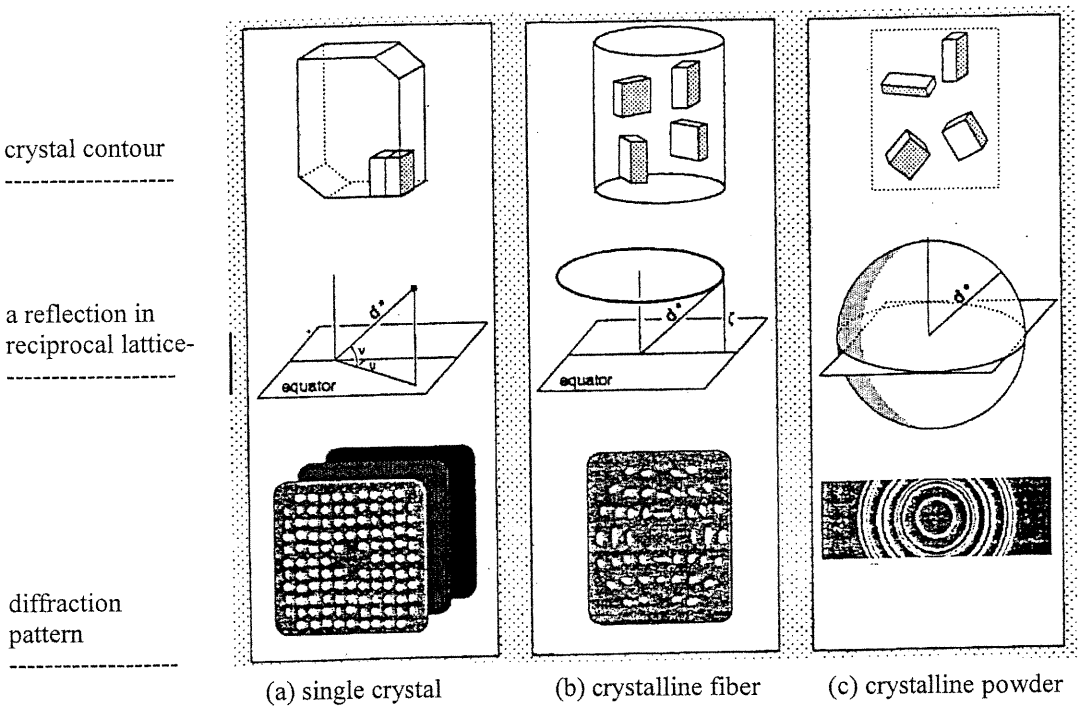

Figure 1.7 Crystal and X-ray diffraction recordings[43].

to the actual structure. This is the direct-methods approach which is applicable to small organic molecules. In subsequent steps, the structure is refined with respect to the atomic positions and thermal parameters by using a least-squares procedure. A structure is usually considered established when the ratio of the sum of the difference between the observed and calculated structure factors to the sum of observed values reaches about 4-6%, for all reflections.

Single crystal X-ray diffraction is a very powerful technique widely used to establish the structure of small and large molecules as long as a single crystal is available. A structure, once solved and refined, contains detailed and accurate information about the molecule itself and the spatial interactions between these molecules.

1.3.1.2 Fiber diffraction

It is very difficult to obtain single crystals of a polymer because of its high molecular weight and the disordered nature of the material. But X-ray diffraction remains nevertheless an important method to study the structure of polymers[44]. When polymers are stretched along one single direction, the small crystalline domains or crystallites may be aligned along the stretch axis. The crystallites within the polymer have one of their crystallographic axes, the fiber axis, parallel to the c-axis. The crystallites are randomly oriented around the fiber axis, a situation that is equivalent to that of a rotating single crystal. In reciprocal space, each reflection, or vector, is represented by as circle defined with two parameters: ξ and d* as shown in Figure 1.7 b and c. In addition, the circle is centred on the F-axis which is parallel to the fiber axis.

Thus, for partially crystalline polymers, with no orientation at the crystals, the X-ray diffraction pattern is made up of concentric circles of various intensities. However, when the crystallites are aligned, usually under tension, the diffraction pattern is made up of diffraction spots or arcs (Figure 1.7 b). The higher the degree of alignment, the shorter the arcs. In other words, the diffraction pattern of a well oriented polymer comprises clearly observed diffraction spots. As shown in Figure 1.8, the two parameters, θ (or d) and ξ, are calculated from its position R and Y using the quantities and the equations (1.5) and (1.6).

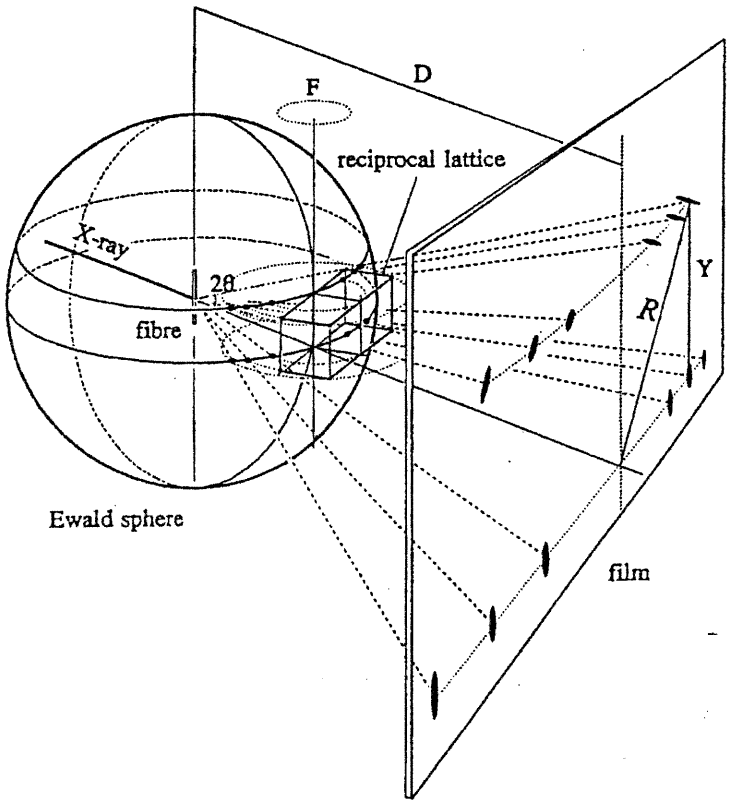

Figure 1.8 Reciprocal lattice and fibre diffraction[43].

$$\text{tg } 2\theta = R/D \qquad (1.5)$$

$$\xi = Y/(\lambda(R^2+D^2)^{1/2}) \qquad (1.6)$$

When the c-axis of the unit cell is parallel to the fiber, all the reflection spots are arranged in layers. The Miller index l can be determined directly since ξ is given by the following relation:

$$\xi = l/c \qquad (1.7)$$

Because the symmetry of the polymer is not high, normally triclinic or monoclinic, the unit-cell parameters are sometimes difficult to obtain.

In order to establish the structure of a polymer, a model is constructed using known values of the bond lengths and bond angles. This model is positioned at best in the unit cell taking into account its symmetry elements. The corresponding diffraction pattern is calculated. It is then checked against the observed X-ray pattern. The translations and orientations of the polymer chain are adjusted until the experimental and the calculated patterns match.

1.3.2 Differential scanning calorimetry (DSC)

A LC-forming polymer may exhibit multiple mesophases at different temperatures or pressures. As the temperature is raised, the polymer goes through a number of first-order transitions from a more ordered to a less ordered state. Scientists speak of a "clearing temperature", when the last LC phase gives way to the isotropic melt or fused polymer. The various mesophase transitions are of the first-order, because the volume and the heat capacity go through discontinuities when plotted against temperature or pressure.

The essential features of the phase transformation of mesogenic polymers may be established by DSC, which turns out to be an appropriate and convenient method. The characteristic DSC trace of a low molecular weight LC with one liquid crystalline phase is shown in Figure 1.9 (a). The first exotherm, as the temperature increases, indicates a first-order transformation from the isotropic phase to a mesophase. The second temperature peak indicates the transformation from a mesophase to the liquid crystal state.

For noncrystallizing polymers (b), only a glass transition can be observed. When a mesogenic group is linked to a polymer chain, the transformation from mesophase to isotropic is seen to occur at a higher temperature and a glass transition appears at lower temperature. It indicates the characteristic combination of the property for the LC polymer material (c):

(I) a glass transition characteristic of the polymer backbone and

(II) a phase transformation from mesophase to isotropic phase due to mesogenic side chains

(a): low molecular weight liquid crystal

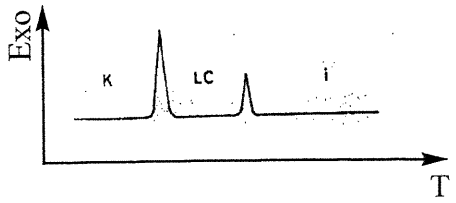

(b): isotropic polymers

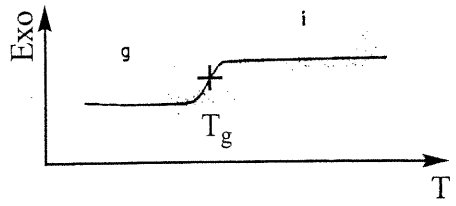

(c): liquid crystal polymers

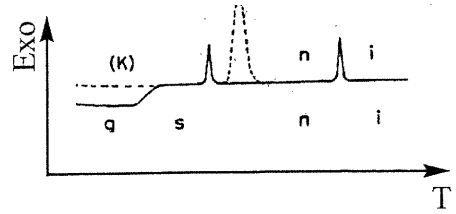

Figure 1.9 Schematic DSC traces of (a) low molecular weight LC (b) isotropic polymer T_g is the glass transition temperature. (c) liquid crystal polymers. k is crystal phase, LC is mesophase, i is isotropic phase, g is glass state, s is smectic phase, n is nematic phase. The dash line shows that mesophase is monotropic which can be observed if the sample is annealed some degree above the T_g extremely slowly.

1.3.3 Polarized microscopy

Optical pattern or texture observations with a polarizing microscope is widely used to identify the appearance of mesophases and transitions between the various mesophases and the isotropic material. Isotropic liquids have no texture, while both

regular crystals and liquid crystals do. However, the texture of each type of phase is different (Figure 1.10).

Many liquid crystalline polymers exhibit Schlieren textures, which display dark brushes. These correspond to extinction positions of the mesophase. At certain points, two or more dark brushes meet at points called disclinations (Figure 1.10). The disclination strength is calculated from the number of dark brushes meeting at one point:

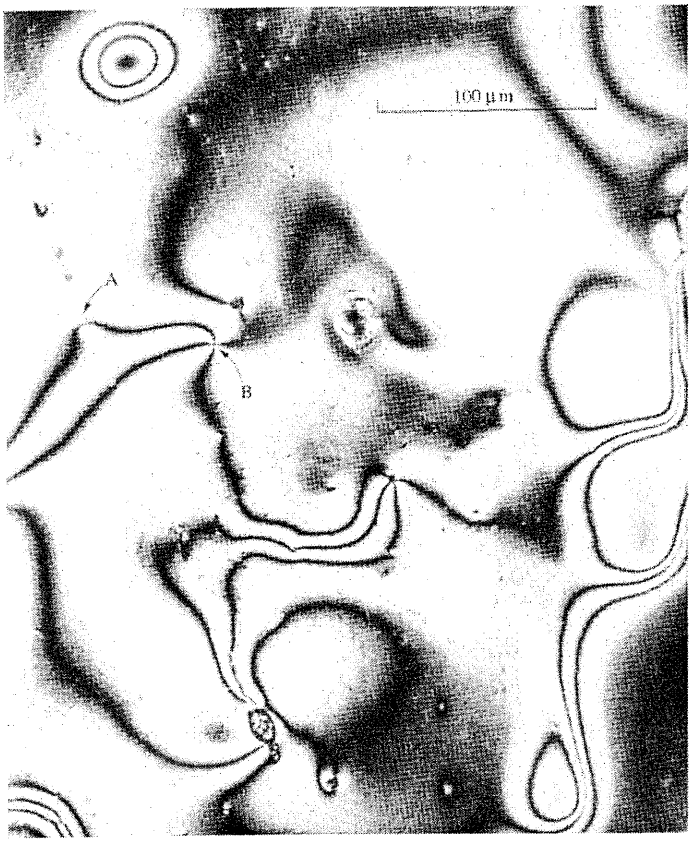

Figure 1.10 Schlieren textures of liquid crystals showing the meeting of dark brushes[45].

$$|S| = (\text{number of brushes meeting})/4$$

The sign of S is positive when the brushes turn in the same direction as the rotated polarizers, and negative when they turn in the opposite direction. Mesophase identification by this procedure requires

Nematic $S = \pm \frac{1}{2}, \pm 1$

Smectic $S = \pm 1$

Thus a nematic phase is indicated by a mixture of two and four disclinations, while a smectic phase exhibits only four disclinations. Disclinations are like dislocations in crystalline solids, where domains of differing orientations meet. The disclinations cause distributions of the director field of the polymer chains, giving rise to an excess free energy of the liquid material.

1.4 The research project:

Some polymers with bile acid derivatives were synthesized in our group. However, their LC properties have never been studied. In the present work we report on some new LC polymers where the bile acid derivatives constitute the mesogenic unit. Meanwhile, many biological systems exhibit the properties of liquid crystals and play an

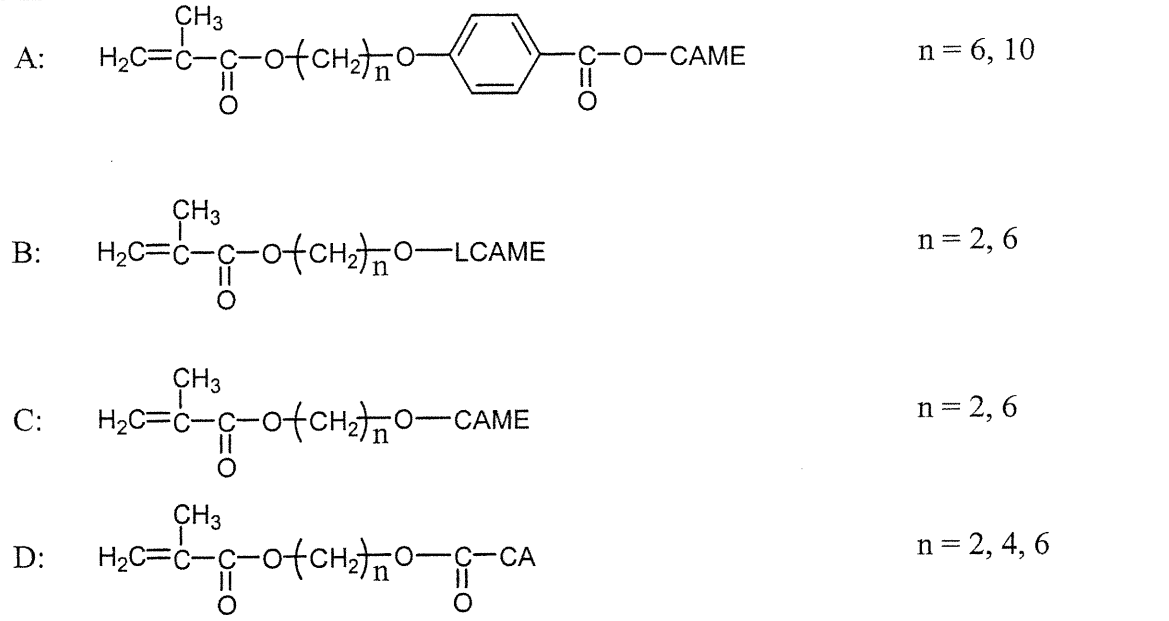

Figure 1.11 The structure of some designed monomers.

important role in the structure and biochemical function of living tissues[46,47], so it is very useful and important to study LC polymers with bile acid derivatives. The structure of some of the designed monomers are shown as Figure 1.11.

Because of the space required by the large mesogenic unit of bile acids (Figure 1.4), the main chain of the LC polymer is forced to take a conformation as extended as possible. However, it is not so clear how the main chain, the side chain spacer and the mesogenic units coordinate and interact to form an ordered structure. In this work, we will try to answer this question.

Then we will synthesize a series of homopolymers and copolymers and characterize them using DSC, SEC, X-ray diffraction, and polarized microscopy. In this project, we will try to find out: 1) how the spacer length influences the liquid crystalline state, 2) the relation of mesophases between the monomers and polymers, 3) the structure and arrangement of massive mesogenic bile acid groups in polymers, and 4) the properties of a series of LC polymers.

CHAPTER 2

EXPERIMENTAL SECTION

2.1 Methods of physical characterization

2.1.1 Nuclear magnetic resonance (NMR)

The ^1H NMR spectra of the monomers were recorded with a Bruker AMX-300 operated at 300 MHz. The deuterated chloroform ($CDCl_3$) was used as solvent and reference. The peak of $CDCl_3$ appears at 7.23 ppm.

The ^1H NMR spectra of the polymers were recorded on a Bruker AMX-400 at 400 MHz. The polymer samples were dissolved in deuterated dimethyl sulfoxide (DMSO). The solvent peak appears at 2.5 ppm. The delay of relaxation was set at 10 seconds and the number of accumulations was 48.

2.1.2 Mass spectrometry (MS)

The high resolution mass spectra of the monomers were obtained with the MS 50 TC TA (Kratos) instrument. The monomers were bombarded by a cluster of high-energy electrons so that some of the molecules converted into ions.

2.1.3 Elemental analysis (EA)

The elemental analyses of the monomers were obtained with the EA 1108 CHN analyzer of Fisons Instruments.

2.1.4 Differential scanning calorimetry (DSC)

The glass transition temperature of the polymers and other thermal events were determined with a DSC 2910 manufactured by TA Instruments.

A precise quantity of polymer, between 5 to 8 mg, was placed in an aluminium cell in an ultra pure helium atmosphere with a flow of 40 mL/min. A 10°C/min heating

rate was adopted to determine the glass transition temperature, T_g. The results were treated using the Thermal Analyst 2100 system of TA Instruments.

The melting point (T_f) of the intermediate products and the final monomers were also measured by the Thermal Analyst 2100 system of TA Instruments.

2.1.5 Thermogravimetric analysis (TGA)

The thermogravimetric behavior of homopolymers and copolymers was recorded with a Hi-Res TGA 2950 Thermogravimetric Analyzer by TA Instruments.

Approximately 1 to 3 mg of the sample was weighted in a platinum cell. The specimen was heated from ambient temperature to 700°C at a rate of 20°C/min. A flow of nitrogen gas was passed over the specimen at a rate of 77 mL/min. The thermogram records the variation of the weight of the specimen as a function of the temperature.

2.1.6 Size exclusion chromatography (SEC)

The molecular weight of polymers were determined by SEC. the polymer 25 mg was dissolved in 10 mL of tetrahydrofuran (THF). The chromatograph was recorded, at the flow of 1 mL/min and the temperature of 25°C, using the differential refractometer Water 410 (Millipore) installed with three columns of porous polystyrene gels. The number-average molecular weight (M_n) and weight-average molecular weight (M_w) were determined from the calibration curve for standard polystyrene (Shodex).

2.1.7 X-ray diffraction

A crystal of about 0.3 mm was selected and mounted on a thin glass fiber which was then placed on a goniometer head. The crystal was adjusted and oriented to meet the requirements of the diffractometer. Intensity data were collected with an Enraf-Nonius CAD-4 single crystal diffractometer. In all cases, the diffraction measurements were carried out with the graphite monochromatized CuK_α radiation ($\lambda = 1.54178$ Å) with a scan range $\Delta\omega = (1.0 + 0.14\ tg\theta)°$ and scan rate of 4°/min. The unit-cell dimensions were obtained after centering 25 strong reflections distributed in 8 octants in the range $40° \leq 2\theta \leq 50°$

The integrated intensities were measured by the $\omega/2\theta$ technique and the orientation of the crystal was verified using 4 standard reflections to check on the stability of the crystal through the measuring process. The crystal data of interest for the model compounds examined and structure refinement are listed in Tables 2.2 and 2.3 respectively.

2.1.8 Polarized microscopy

A Leitz Wetzlar microscope, equipped with a polarizer/analyser and a hot stage was employed. Liquid crystal characteristics as well as the phase transformations could be observed under crossed polarizers as the temperature was varied.

2.1.9 Fourier transform infrared (FTIR) spectroscopy

All monomers and some selected polymers were characterized using the Bomem (MB-series) Hartmann & Braun FTIR instrument. All the samples were ground and pressed with KBr to form a thin transparent round pellet. All the FTIR spectra were analysed by Win-Bomem Easy software.

2.2 Molecular design of different monomers

If rigid mesogenic side chains are directly attached to the polymer backbone, motions of the polymer segments and mesogenic groups are directly coupled. In the liquid state, above T_g, the polymer tends to adopt a statistical chain conformation that hinders anisotropic orientation of the mesogenic side chains. Furthermore, the steric hindrance prevents mesogenic ordering. As the flexible spacer decouples motions of the main and side chains and alleviates steric hindrance under these conditions, we will synthesize the following series of monomers with various spacer lengths in order to establish the influence of the spacer on the molecular structure. We will also study the properties of the liquid crystalline state of LC polymers with bile acid derivatives and determine the structures and their parent model compounds by X-ray diffraction. All the monomers and intermediates that I attempted to synthesize are listed in Table 2.1. The structures of monomers are shown as Figure 2.1.

Table 2.1 The number and name of intermediates and final monomers

Product No.	Product Name
1	4-(6-hydroxyhexyloxy)benzoic acid
2	4-(10-hydroxydecyloxy)benzoic acid
3	4-(6-methacryloyloxy)hexyloxy benzoic acid
4	4-(10-methacryloyloxy)decyloxy benzoic acid
5	4-(6-methacryloyloxy)hexyloxy benzoic acyl chloride
6	4-(10-methacryloyloxy)decyloxy benzoic acyl chloride
7	cholic acid methyl ester
8	4-(6-methacryloyloxy)hexyloxy benzoate cholic acid methyl ester
9	4-(10-methacryloyloxy)decyloxy benzoate cholic acid methyl ester
10	lithocholic acid methyl ester
11	methyl 3α-tosyloxy-5β-cholan-24-ate
12	methyl 3β-(2-hydroxyethoxy)-5β-cholan-24-ate
13	methyl 3β-(6-hydroxyhexyloxy)-5β-cholan-24-ate
14	methyl 3β-(methacryloyloxy)ethoxy-5β-cholan-24-ate
15	methyl 3β-(methacryloyloxy)hexyloxy-5β-cholan-24-ate
16	methyl 3α-tosyloxy-7α,12α-dihydroxy-5β-cholan-24-ate
17	methyl 3β-(2-hydroxyethoxy)-7α,12α-dihydroxy-5β-cholan-24-ate
18	methyl 3β-(6-hydroxyhexyloxy)-7α,12α-dihydroxy-5β-cholan-24-ate
19	methyl 3β-(methacryloyloxy)ethoxy-7α,12α-dihydroxy-5β-cholan-24-ate
20	methyl 3β-(methacryloyloxy)hexyloxy-7α,12α-dihydroxy-5β-cholan-24-ate
21	(2-hydroxyethoxy) 3α,7α,12α-trihydroxy-5β-cholan-24-ate
22	(4-hydroxybutyloxy) 3α,7α,12α-trihydroxy-5β-cholan-24-ate
23	(6-hydroxyhexyloxy) 3α,7α,12α-trihydroxy-5β-cholan-24-ate
24	methacryloyloxy-ethoxy 3α,7α,12α-trihydroxy-5β-cholan-24-ate
25	methacryloyloxy-butyloxy 3α,7α,12α-trihydroxy-5β-cholan-24-ate
26	methacryloyloxy-hexyloxy 3α,7α,12α-trihydroxy-5β-cholan-24-ate

2.3 Syntheses of monomers

The A monomers (A_6, A_{10}), illustrated in Figure 2.1 are synthesized by the traditional way [18-20, 48-52]. The CAME, spacer and methacrylate are linked by ester, *para*-phenyl and so on (Figure 2.1). Monomers B and C are linked respectively by ester and ether structures with methyl ester of lithocholic acid (LCAME) or cholic acid (CAME) in 3 position. Monomers D are compounds that connected purely by ester groups with spacer, methacrylate and cholic acid (CA) in 24 position.

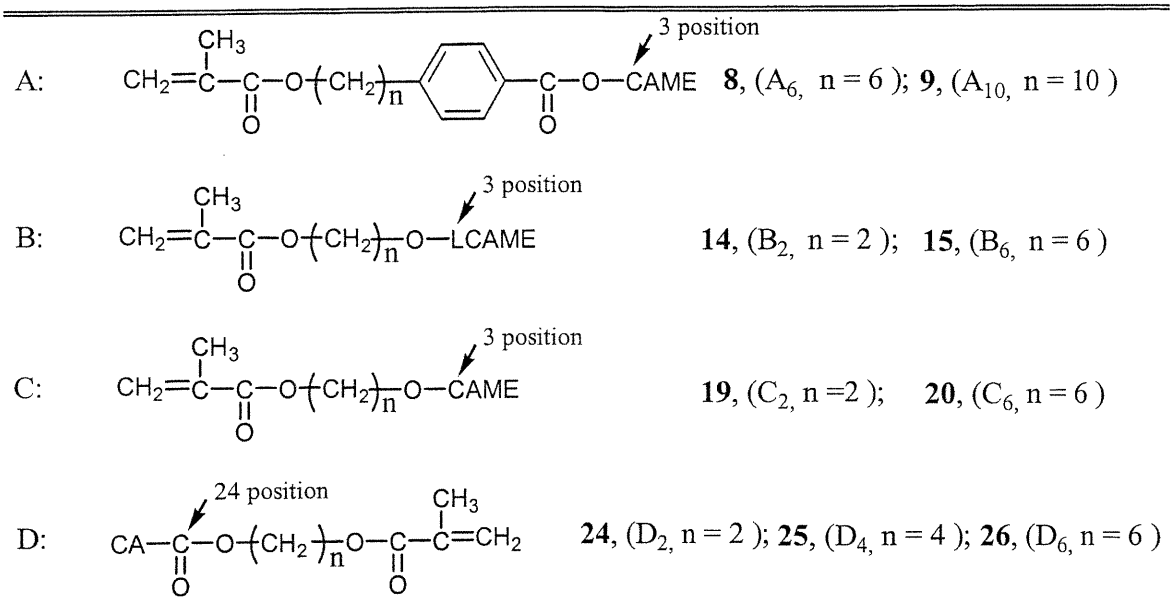

Figure 2.1 The structure of the monomers to be synthesized.

Monomers A

The syntheses route of the mesogenic methacrylate monomers A is outlined in Figure 2.2.

1: 4-(6-hydroxyhexyloxy)benzoic acid (**1** , n = 6)

In a 250 mL three-neck flask with a magnetic stir and condenser, the *p*-hydroxybenzoic acid (0.05 mol) and KOH (0.11 mol) are dissolved in 80 mL ethanol and 40 mL distilled water, with a trace amount of KI added as a catalyst. The solution is refluxed for 1 hour before slow addition of 6-chloro-1-hexanol or 10-chloro-1-decanol (0.06 mol). Subsequently, the reaction mixture is refluxed for an additional 12 hours then cooled down to room temperature. The ethanol is removed by rotary evaporation and the

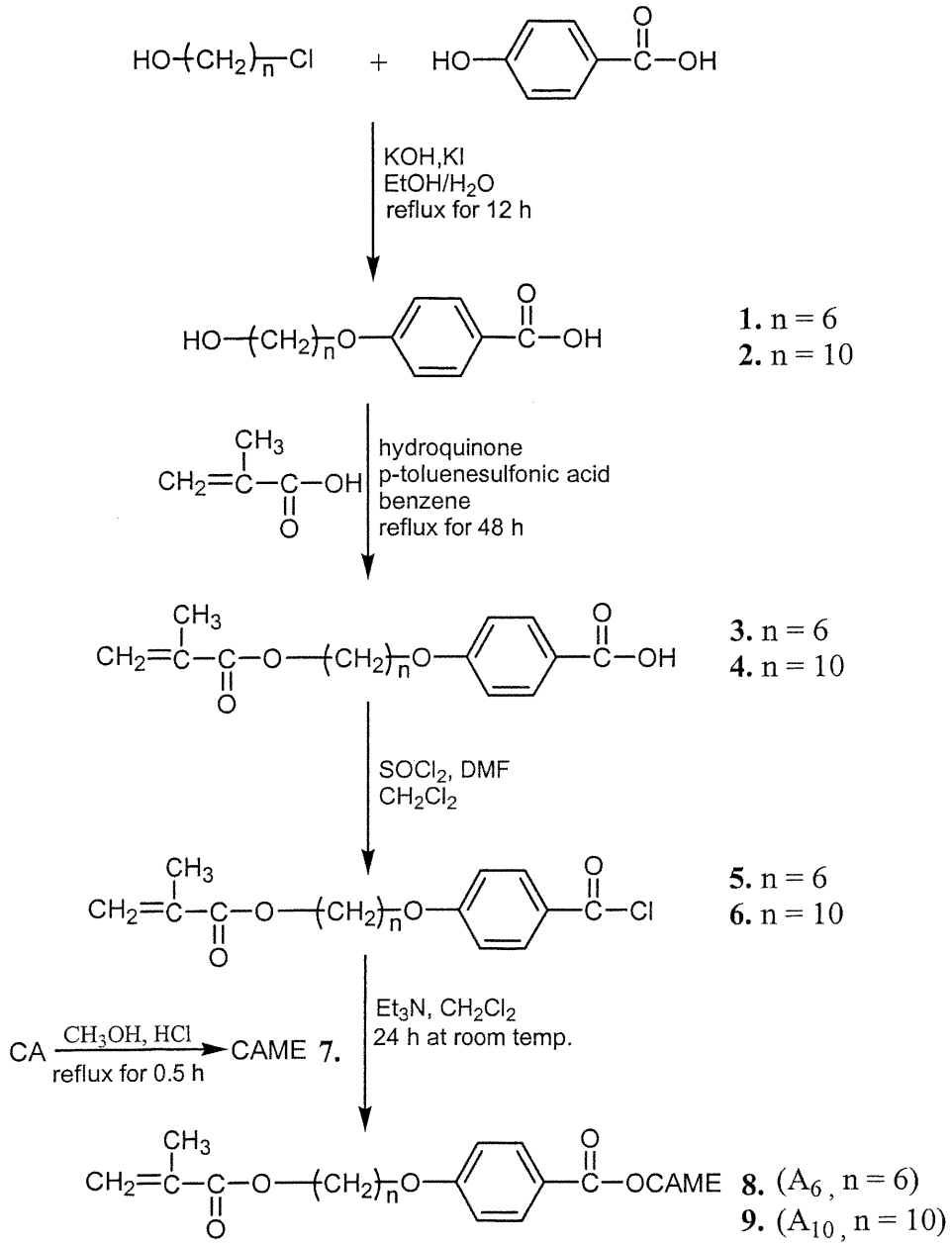

Figure 2.2 The syntheses of methacrylate monomers A with CAME. (n = 6, 10 CA: cholic acid, CAME: cholic acid methyl ester).

resulting mixture with white solid particles is diluted with 100 mL of distilled water. The resulting solution is washed several times with 60 mL diethyl ether to remove unreacted 6-chloro-1-hexanol and acidified with 1mL HCl. The white precipitate is collected and washed several times with distilled water. The crude product is dried in a vacuum oven and is purified by recrystallization in ethanol. The product consists of white crystals with a melting point of 144°C. The yield is about 75%.

^{1}H NMR in deuterated methanol (CD_3OD) chemical shift: 1.4-1.8 (m, 8 secondary H, -CH_2-), 3.4 (t, 2 secondary H, -O-CH_2-), 4.2(t, 2 secondary H, -CH_2-O-Ar), 6.9 and 7.9 (2d, 4 aromatic H).

4-(10-hydroxydecyloxy)benzoic acid (**2**, n = 10): yield: 72%, m.p.: 112°C. ^{1}H NMR in CD_3OD chemical shift: 1.4-1.8 (m, 16 secondary H, -CH_2-), 4.1 (t, 2 secondary H, -O-CH_2-), 4.2 (t, 2 secondary H, -CH_2-O-Ar), 6.9 and 8.0 (2d, 4 aromatic H).

2: 4-(6-(methacryloyloxy)hexyloxy)benzoic acid (**3**, n = 6)

A mixture of compound **1** (12 mmol), 0.4 g p-toluene sulfonic acid, 0.2 g hydroquinone and methacrylic acid (0.12 mol) is refluxed in 30 mL benzene for 48 hours in a Dean-Stark apparatus until 12 mmol water is collected. The cooling reaction mixture is mixed thoroughly with a 3 to 4 fold quantity of diethyl ether. The diethyl ether layer is separated and then extensively washed with warm distilled water to remove the methacrylic acid residue completely. The diethyl ether is distilled off in a rotavapor, giving a white sticky solid. The solid product is dissolved in acetone and precipitated in distilled water. The white precipitate is dried in a vacuum oven and recrystallized in ethanol.

The yield for product **3** (n = 6) is about 82%. m.p.: 86°C. ^{1}H NMR (in $CDCl_3$) chemical shift: 1.5-1.8 (m, 8 secondary H, -CH_2-). 1.9 (s, 3 primary H, =(C-)-CH_3), 4.0 (t, 2 secondary H, -CH_2-O-Ar), 4.2 (t, 2 secondary H), 6.9 and 8.0 (2d, 4 aromatic H).

4-(10-(methacryloyloxy)decyloxy)benzoic acid (**4**, n = 10): white crystals, yield: 78 % m.p.: 77°C. ^{1}H NMR (in $CDCl_3$) chemical shift: 1.4-1.8 (m, 16 secondary H, -CH_2-). 1.9 (s, 3 primary H, =(C-)-CH_3), 4.0 (t, 2 secondary H, -CH_2-O-Ar), 4.2 (t, 2 secondary H), 6.9 and 8.0 (2d, 4 aromatic H).

3: The acyl chloride (**5**, n = 6; **6**, n = 10)

It is obtained by dissolving 6 mmol of **3** or **4** in 25 mL dried dichloromethane. Excess thionyl chloride (0.05 mol) and 2 drops of N,N-dimethylformamide (DMF) as catalyst are added to the solution. The mixture is stirred under nitrogen at room temperature for 2 hours. The solvent and extra thionyl chloride are completely evaporated under vacuum to obtain the liquid acyl chloride. This liquid product is kept in nitrogen purge before using.

4: Cholic acid methyl ester (CAME: **7**)

In a 100 mL flask with stirrer and condenser, the mixture of 15 mmol cholic acid with 1 mL HCl and 50 mL methanol is heated until reflux and reacted for 30 minutes. It is then cooled down to room temperature. The crystals are collected and dried in a vacuum oven. White needle crystals are obtained with a yield of about 90% and the m.p. is 154-155°C[53].

^{1}H NMR (in $CDCl_3$) chemical shift: 0.69 (s, three primary H, C18-CH_3), 0.89 (s, three primary H, C19-CH_3), 0.98 (d, three primary H, C21-CH_3), 3.46 (m, one secondary H in C3), 3.66 (s, three H in OCH_3), 3.85 (s, 1H, C7), 3.98 (s, 1H, C12). 1.0-2.5 (various ring CH_2)

5: The methacrylate monomer, **8** (A_6, n = 6), 4-(6-(methacryloyloxy)hexyloxy)benzoate cholic acid methyl ester; **9** (A_{10}, n = 10), 4-(10-(methacryloyloxy)decyloxy)benzoate cholic acid methyl ester)

In a 150 mL three-neck flask with magnetic stirrer, acyl chloride (6 mmol) is dissolved in 20 mL dried dichloromethane and added to a mixture of 5 mL triethylamine and 6 mmol CAME in 75 mL dichloromethane at 0°C (ice bath) under a nitrogen purge. After the addition of acyl chloride, the temperature is slowly raised to room temperature and the mixture is left to react for a further 24 hours. The solvent is removed in the rotary evaporator. The crude product is dissolved in ethyl acetate and washed several times with distilled water, then dried over anhydrous Na_2SO_4. The solvent is distilled off and the crude product is purified by column chromatography on silica gels with an eluent mixture of acetone and petroleum ether (volume ratio = 1:2).

The TLC revealed many points close to one another indicating that the monomer is not very pure and the yield is very low. This may be due to the steric hindrance of CAME and acyl chloride, since both of them are large units. The product we are seeking is obtained in a too small quantity and cannot be isolated.

Monomers B: The syntheses route is shown in Figure 2.3.

The first step is the synthesis of methacryloyl chloride which has been described by Stempel *et al.*[54]. In a 50 mL flask equipped with magnetic stirrer and condenser, 10.4 mL (0.03 mol) methacrylic acid and an excess quantity of 28 mL benzoyl chloride (0.06 mol) are added and heated until reflux for 1 hour. The mixture is then distilled. The product is in the fraction collected between 90-95°C.

1: Lithocholic acid methyl ester (**10**)

In a 100 mL flask with magnetic stirrer and condenser, 50 mL methanol and 5.65 g lithocholic acid (15 mmol) are acidified with 1 mL HCl and heated to reflux for 30 minutes. The solution is cooled until the appearance of the methyl ester crystals. They are collected and dried in a vacuum oven for 1 day. The yield is about 92%, the m.p.: 120-121°C[53].

^{1}H NMR (in $CDCl_3$) chemical shift: 0.64 (s, 3H, C18-CH_3), 0.90 (s, 3H, C19-CH_3), 0.92 (d, 3H, C21-CH_3), 3.51 (m, 1H in C3-CH), 3.65 (s, 3H in OCH_3). 1.0-2.5 (various ring CH_2)

2: Tosylate of lithocholic acid methyl ester (**11**)

In a 50 mL flask, 1.98 g (5 mmol) of **10** is dissolved in 15 mL dried pyridine in nitrogen atmosphere and cooled to 0°C in an ice bath. A solution of *p*-toluenesulfonyl chloride 1.05 g (5.5 mol) in 5 mL pyridine is added drop by drop during 30 minutes. Then the solution is slowly warmed to room temperature and left to react for further 24 hours. The white pyridine salt particles are filtered and the solvent is distilled off. The crude product is purified by column chromatography on silica gel with a mixture of ethyl acetate and petroleum ether (volume ratio = 1:4) with R_f = 0.45. The collected liquid is left overnight when the colorless hexagonal-shaped crystals of **11** appear. The yield is about 82%. m.p.: 114-115°C[56].

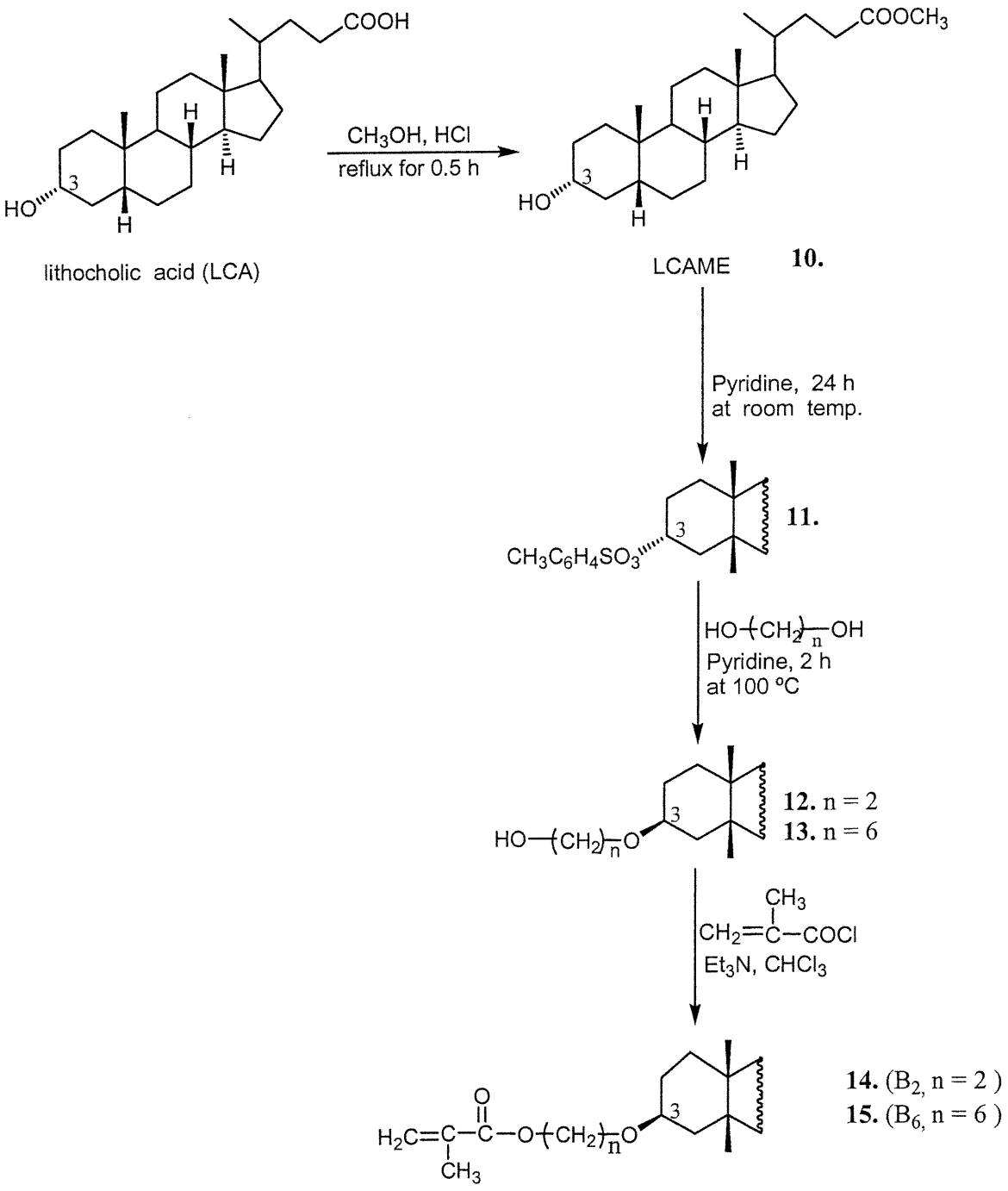

Figure 2.3 The syntheses of methacrylate monomers B with LCAME (B_2, B_6).

(LCA: lithocholic acid, LCAME: lithocholic acid methyl ester)

^{1}H NMR (in $CDCl_3$) chemical shift: 0.65 (s, 3H, C18-CH_3), 0.88 (s, 3H, C19-CH_3), 0.93 (d, 3H, C21-CH_3), 2.42 (s, 3H, tosyl, CH_3), 3.66 (s, 3H, OCH_3), 4.44 (m, 1H, C3-CH), 7.32 (d, 2H, aromatic CH), 7.76 (d, 2H, aromatic CH) 1.0-2.5 (various ring CH_2).

3: Intermediate of methyl 3β-(2-hydroxyethoxy)-5β-lithocholan-24-ate (**12**, n = 2) and methyl 3β-(6-hydroxyhexaneoxy)-5β-lithocholan-24-ate (**13**, n = 6)

In a 100 mL flask, a solution of compound **11** (2 mmol) and 1,2-ethylene glycol, 20 mL, with pyridine, 5 mL is heated to 100 °C under a nitrogen stream for 2 hours. The solution is cooled to room temperature and the pyridine is evaporated. The product is dissolved in 20 mL ethyl acetate and transferred into a separatory funnel. It is washed 4 times with 60 mL distilled water. The excess 1,2-ethylene glycol and salt of pyridine is washed off. The organic phase is collected and dried with anhydrous Na_2SO_4. The crude product is then purified by column chromatography on silica gels with ethyl acetate and petroleum ether (volume ratio = 1:1) as eluent. The yield is 40%.

^{1}H NMR (in $CDCl_3$) chemical shift: 0.71 (s, 3H, C18-CH_3), 0.87 (s, 3H, C19-CH_3), 0.95 (d, 3H, C21-CH_3), 3.48 and 3.72 (s, 2H, CH_2 in ethylene), 3.65 (s, 1H, 3β-CH), 3.67 (s, 3H, OCH_3). 1.0-2.5 (various ring CH_2)

For **13** (n = 6), the same process described above for the synthesis of **12** (n = 2) is followed. However, there is a competition between the elimination and substitution reactions[55-60], so the yield in the case of the longer spacer is very low.

Monomers C:

The synthesis procedure for monomers C is the same as for monomers B. The only difference between them is that monomers B are made from lithocholic acid and monomers C are from cholic acid. The difference between the two acids, it is that cholic acid has three hydroxyl groups, while cholic acid has just one hydroxyl group at the 3 position. The preparation scheme was shown in Figure 2.4.

1. Cholic acid methyl ester (CAME)

In a 250 mL flask equipped with a magnetic stirrer and condenser, 125 mL methanol and 27.37 g cholic acid (67 mmol) are acidified with 1 mL HCl and heated to

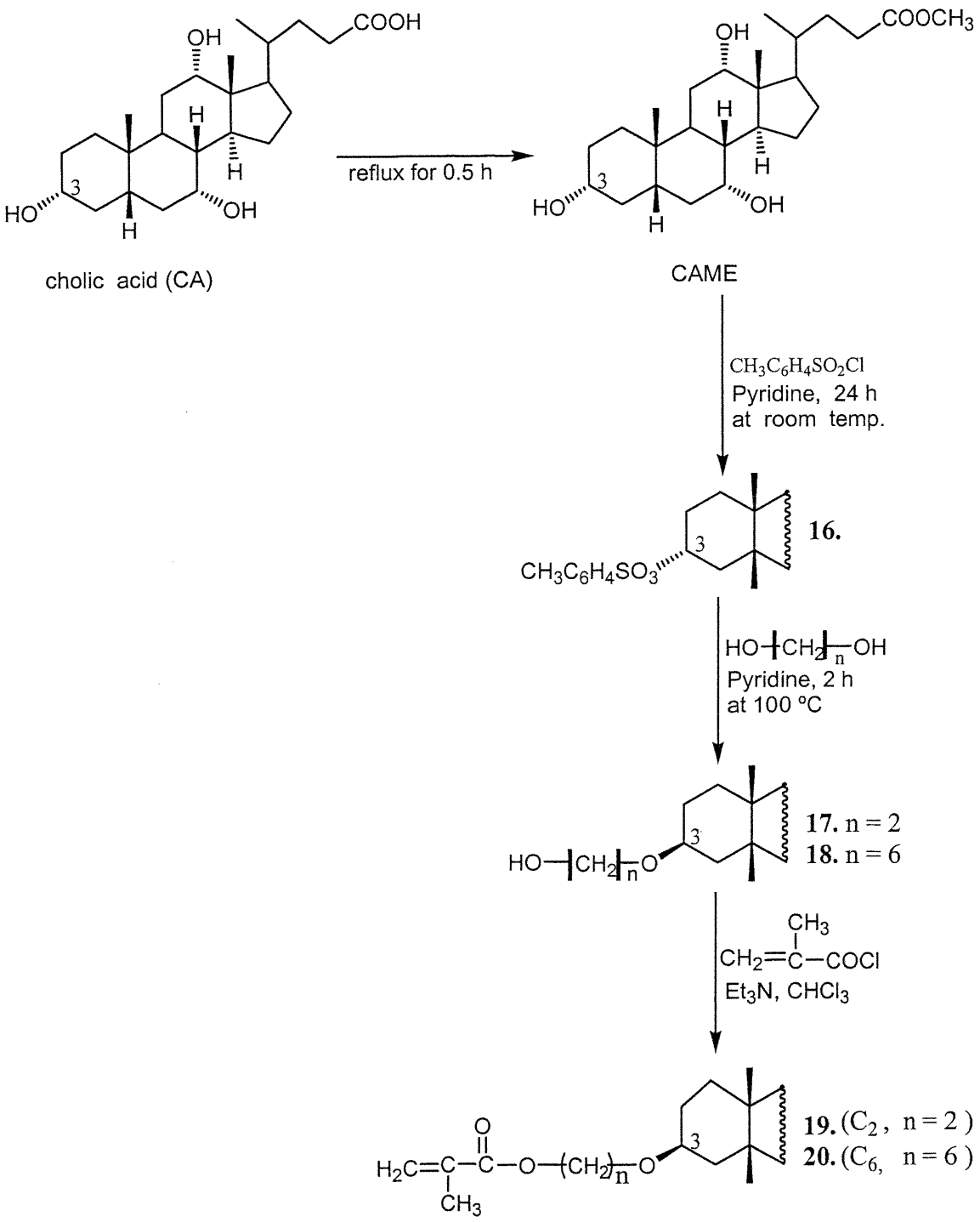

Figure 2.4 The syntheses of methacrylate monomers C with CAME (C_2, C_6).

reflux for 30 minutes. The solution is cooled down until the solid methyl ester appears in the solution. The crystals are collected and dried in a vacuum oven for 1 day. The yield is about 90%. m.p.: 153-154°C[53].

^{1}H NMR (in $CDCl_3$) chemical shift: 0.69 (s, three primary H, C18-CH_3), 0.89 (s, three primary H, C19-CH_3), 0.98 (d, three primary H, C21-CH_3), 3.46 (m, one secondary H in C3), 3.66 (s, three H in OCH_3), 3.85 (s, 1H, C7), 3.98 (s,1H, C12). 1.0-2.5 (various ring CH_2)

2. Tosylate of CAME (**16**)

In a 100 mL flask with a magnetic stirrer, 4.22 g (10 mmol) of compound CAME is dissolved in 35 mL dried pyridine with a nitrogen purge and cooled to 0 °C in an ice bath. A solution of *p*-toluenesulfonyl chloride 2.29 g (12.0 mol) in 10 mL pyridine is added dropwise during 30 minutes. Then the temperature of the mixture is slowly raised to room temperature and allowed to react for a further 24 hours. After that, the pyridine salt is filtered and the solvent is evaporated. The crude product is purified by column chromatography on silica gel with the eluent mixture of ethyl acetate and petroleum ether (volume ratio = 1:4) with $R_f = 0.42$. The collected liquid is evaporated and a sticky liquid is obtained. It is dried under vacuum. At last, a white solid amorphous foam is obtained. The yield is about 86%. m.p.: 159°C.

^{1}H NMR (in $CDCl_3$) chemical shift: 0.69 (s, 3H, C18-CH_3), 0.89 (s, 3H, C19-CH_3), 0.99 (d, 3H, C21-CH_3), 2.42 (s, 3H, tosyl, CH_3), 3.66 (s, 3H, OCH_3), 3.85 (s, 1H, C7-CH), 3.98 (s, 1H, C12-CH), 4.44 (m, 1H, C3-CH), 7.32 (d, 2H, aromatic CH), 7.76 (d, 2H, aromatic CH). 1.0-2.5 (various ring CH_2)

3. Intermediate methyl 3β-(2-hydroxyethoxy)-5β-cholan-24-ate (**17**) and 3β-(2-hydroxyhexanoxy)-5β-cholan-24-ate (**18**)

The synthetic procedure is the same as that followed for **12** methyl 3β-(2-hydroxyethoxy)-5β-cholan-24-ate. We attempted to react the 1,6-hexanediol with the tosylate of CAME in order to get the substitution product **18**. However, only a very small amount of the desired intermediate product was obtained. This method does not allow for the synthesis of monomers C with a longer spacer (n = 6 or more), although it works well for a shorter spacer $n \leq 4$. The longer the spacer, the lower the yield [55-60].

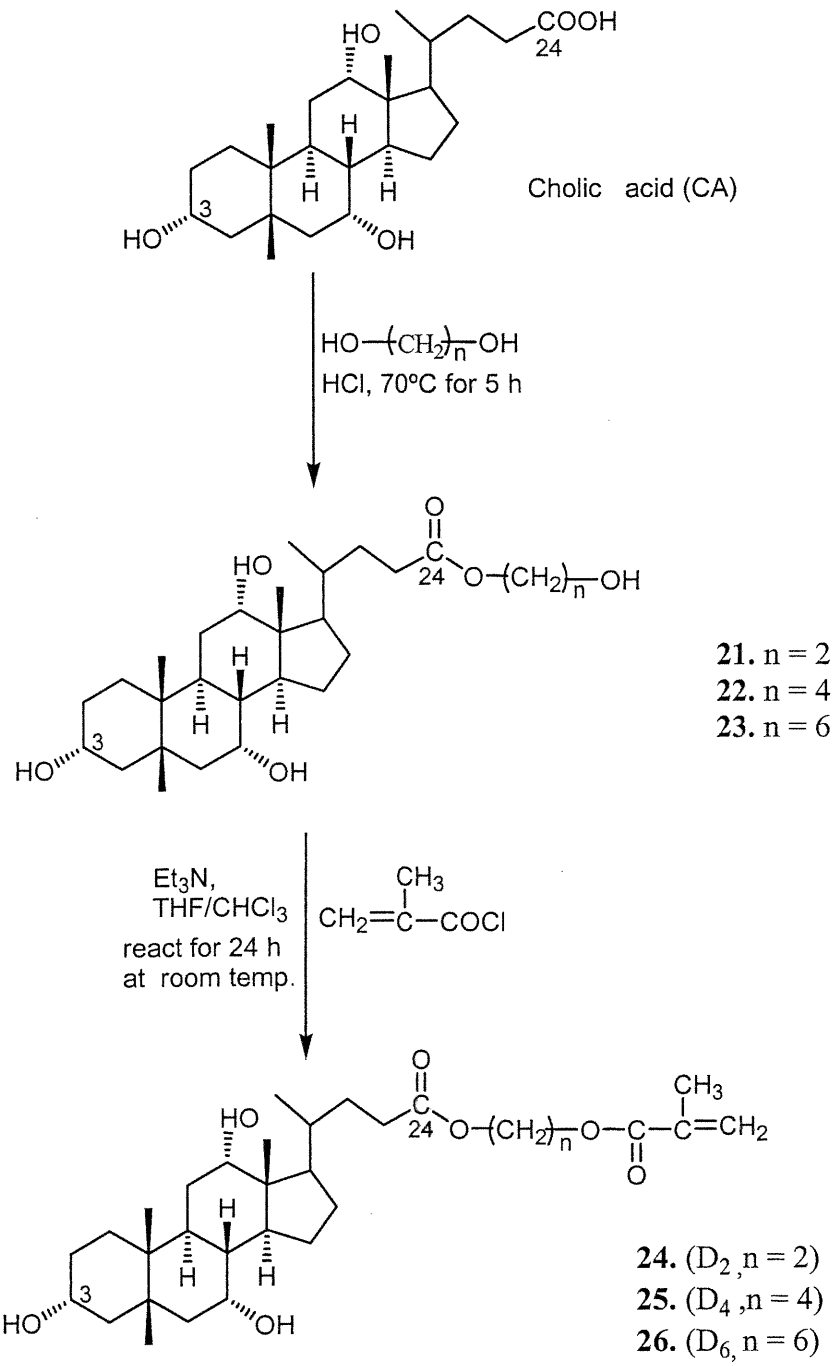

Figure 2.5 The synthesis of methacrylate monomers **24**, **25**, **26** with cholic acid.

Monomers D:

The synthesis procedure is outlined in Figure 2.5.

1: Synthesis of (2-hydroxyethoxy) 3α,7α,12α-trihydroxy-5β-cholan-24 ate (**21** , n = 2)

The ethylene glycol ester of cholic acid is produced with the help of a catalyst, in this case, a small amount of hydrochloric acid. In a 50 mL flask with magnetic stirrer and condenser, 3.1 g (50 mmol) ethylene glycol and 2.046 g cholic acid (5 mmol) are added and 2 drops of HCl are introduced. The mixture is heated to 70°C for 5 hours, then cooled to room temperature. It is dissolved in 30 mL ethyl acetate and transferred to a separatory funnel. It is washed with 150 mL distilled water in order to eliminate the excess ethylene glycol. The organic phase is collected and dried with anhydrous Na_2SO_4. The solvent is evaporated by a rotavapor until a very sticky yellow liquid appears. It is dried again under vacuum for 8 hours until a foam fills the flask. The foam is scratched from the flask and a light yellowish product is obtained. The crude product is recrystallized in chloroform and gives small white crystals in a yield of about 89%. m.p.: 126°C. The product is identified by ^{1}H NMR.

^{1}H NMR(in $CDCl_3$) chemical shift: 0.69 (s, 3H, C18-CH_3), 0.89 (s, 3H, C19-CH_3), 0.99 (d, 3H, C21-CH_3), 3.45 (m, 1H, C3-CH), 3.85 (s, 1H, C7-CH), 3.83 (t, 2H, -O-CH_2), 4.00 (s, 1H, C12-CH), 4.22 (t, 2H, -CH_2-O). 1.0-2.5 (various ring CH_2)

For the (4-hydroxybutyloxy) 3α,7α,12α-trihydroxy-5β-cholan-24-ate (**22**, n = 4), the synthesis route is the same as the above procedure. The crude product is also recrystallized by chloroform and gives a yield of about 88%, m.p.: 83°C. The product is identified by ^{1}H NMR.

^{1}H NMR (in $CDCl_3$) chemical shift: 0.69 (s, 3H, C18-CH_3), 0.89 (s, 3H, C19-CH_3), 0.99 (d, 3H, C21-CH_3), 1.6-1.8 (m, 4H, -CH_2-CH_2-), 3.45 (m, 1H, C3-CH), 3.85 (s, 1H, C7-CH), 3.69 (t, 2H, -O-CH_2), 3.98 (s, 1H, C12-CH), 4.11 (t, 2H, -CH_2-O). 1.0-2.5 (various ring CH_2).

The procedure described above is followed to synthesize the (6-hydroxyhexyloxy) 3α,7α,12α-trihydroxy-5β-cholan-24-ate (**23**, n = 6). The yield is about 91%. m.p.: 64°C.

^{1}H NMR (in $CDCl_3$) chemical shift: 0.69 (s, 3H, C18-CH_3), 0.90 (s, 3H, C19-CH_3), 0.99 (d, 3H, C21-CH_3), 1.40 (m, 8H, -(CH_2-)$_4$), 3.46 (m, 1H, C3-CH), 3.85 (s, 1H,

C7-CH), 3.64 (t, 2H, -O-CH_2), 3.98 (s,1H, C12-CH), 4.07 (t, 2H, -CH_2-O), 1.40 (m, 8H, -(CH_2-)$_4$). 1.0-2.5 (various ring CH_2)

2: The synthesis of final methacrylate monomers: (**24**: methacryloyloxy-ethoxy 3α, 7α, 12α-trihydroxy-5β-cholan-24-ate, n = 2).

In a 100 mL three neck flask with magnetic stirrer, the ethylene glycol ester of cholic acid (3.57 g, 7 mmol) is dissolved in a solvent mixture containing 20 mL THF and 17 mL chloroform. Then, 1.27 g (12.6 mmol) triethylamine is added. The tight system is purged with nitrogen and the temperature lowered to 0°C with an ice bath. Then 3 mL chloroform solution of 1.317 g (12.6 mmol) methacryloyl chloride in an addition funnel is added dropwise in 30 minutes. The reaction mixture is slowly warmed to room temperature and kept at this temperature for a further 24 hours. The mixture is added to ice/water containing 1 mL hydrochloric acid then transferred to a separatory funnel. The organic phase is washed again with distilled water for several times until it is neutral. It is dried over anhydrous Na_2SO_4 overnight and the solvent is evaporated by rotavapor. The crude product is purified by column chromatography on silica gels with pure ethyl acetate (R_f = 0.22). The solution is collected and the solvent evaporated. A sticky product is obtained. It is dissolved again in a small amount acetone and is precipitated in 100 mL petroleum ether. The precipitate is dried in a vacuum oven for 24 hours at room temperature. The yield about 40%. m.p.: 109°C. The final monomer **24** is identified by ^{1}H NMR.

^{1}H NMR (in $CDCl_3$) chemical shift: 0.69 (s, 3H, C18-CH_3), 0.89 (s, 3H, C19-CH_3), 0.99(d, 3H, C21-CH_3), 1.92 (s, 3H, methacrylate-CH_3) 3.45 (m, 1H, C3-CH), 3.89 (s, 1H, C7), 4.01(s, 1H, C12) 4.34(s, 4H, -O-CH_2-CH_2-O), 5.57 and 6.11 (m, each of 1H, vinyl). 1.0-2.5 (various ring CH_2)

For the final monomer **25**: methacryloyloxy-butyloxy 3α,7α,12α-trihydroxy-5β-cholan-24-ate (D_4, n = 4), the synthesis procedure is the same as the above. The same eluent is used to purify the product by column chromatography and R_f = 0.23. The yield is about 38%. m.p.: 94°C.

^{1}H NMR (in $CDCl_3$) chemical shift: 0.69 (s, 3H, C18-CH_3), 0.90 (s, 3H, C19-CH_3), 1.00 (d, 3H, C21-CH_3), 1.78 (m, 4H, -CH_2-CH_2-), 1.94 (s, 3H, methacrylate-CH_3)

3.45 (m, 1H, C3-CH), 3.84 (s, 1H, C7), 3.97 (s, 1H, C12), 4.10 (t, 2H, -O-CH_2-), 4.19 (t, 2H, -CH_2-O), 5.57 and 6.10 (m, each of 1H, vinyl). 1.0-2.5 (various ring CH_2)

For the final monomer **26**: methacryloyloxy-hexyloxy 3α,7α,12α-trihydroxy-5β-cholan-24-ate (D_6, n = 6), the synthesis procedure is also the same as the above. The same eluent is used and R_f = 0.25. The yield is about 43%. This monomer can be recrystallized. It takes two to three weeks to grow crystals from a very dilute mixture of acetone and petroleum ether (volume ratio = 1: 40). The crystals appear as white needles with m.p.: 87°C.

^{1}H NMR (in $CDCl_3$) chemical shift: 0.69 (s, 3H, C18-CH_3), 0.90 (s, 3H, C19-CH_3), 1.00 (d, 3H, C21-CH_3), 1.39 (m, 4H, -CH_2-CH_2-), 1.75 (m, 4H, -CH_2, CH_2-), 1.95 (s, 3H, methacrylate-CH_3), 3.45 (m, 1H, C3-CH), 3.84 (s, 1H, C7), 3.97 (s, 1H, C12), 4.07 (t, 2H, -O-CH_2-), 4.15 (t, 2H, -CH_2-O), 5.56 and 6.10 (m, each of 1H, vinyl).

2.4 Structure of model compounds determined by X-ray diffraction

2.4.1. Tosylate of lithocholic acid methyl ester, 11 ($C_{32}H_{48}O_5S$)

A good crystal of the tosylate of lithocholic acid methyl ester was glued to a thin glass fiber and installed on a goniometer head. Then the assembly was mounted on a Bruker Platform diffractometer equipped with a Bruker SMART 2K CCD area detector using the SMART and normal focus sealed tube source graphite monochromatized CuKα radiation. The crystal-to-detector distance was 4.908 cm and the data collection was carried out in 512 × 512 pixel mode, utilizing 4 × 4 pixel binning. The initial unit-cell dimensions were determined by a least-squares fit to the angular settings of strong reflections, collected by a 9.0 degree scan in 30 frames over four different parts of the reciprocal space. One complete sphere of data was collected to better than 0.8 Å resolution. Upon completion of the data collection, the first 101 frames were recollected in order to improve the decay correction analysis. The very large unit cell volume, V = 18426.2 (2) Å^3, contains 24 molecules. Since in the $P2_12_12_1$ orthorhombic space group the order of the general position is 4, there are 6 independent molecules per asymmetric unit. This translates into 6 × 38 = 228 atoms to be located. The structure was eventually solved by Michel Simard of the lab of X-ray diffraction in University of Montreal. The crystal data and the structure refinement indicators are given in Table 2.2[61-70].

Table 2.2 Crystal data and structure refinement for $C_{32}H_{48}O_5S$

Empirical formula	$C_{32}H_{48}O_5S$
Formula weight	544.79
Temperature	293 (2) K
Wavelength	1.54178 Å
Crystal system	Orthorhombic
Space group	$P2_12_12_1$
Unit cell dimensions	a = 11.6982 (1) Å $\alpha = 90°$
	b = 22.1349 (1) Å $\beta = 90°$
	c = 71.1604 (1) Å $\gamma = 90°$
Volume	18426.17(19) $Å^3$
Z	24
Density (calculated, experimental value)	1.178, 1.203 g/cm^3
Absorption coefficient	1.224 mm^{-1}
F (000)	7104.0
Crystal size	0.52 × 0.42 × 0.33 mm
Theta range for data collection	1.24 to 73.00°
Index range	$-14 \le h \le 14$
	$-23 \le k \le 26$
	$-87 \le l \le 86$
Reflection collected	223508
Independent reflections	36421 [R (int) = 0.0848]
Absorption correction	Multi-scan
Max. and min. transmission	0.7580 and 0.2950
Refinement method	Full matrix least-square on F^2
Data / restraint / parameters	36421/ 3237/ 2120
Goodness-of-fit on F^2	1.227
Final R indices [I > 2 sigma (I)]	$R_1 = 0.1425$, $wR_2 = 0.3189$
R indices (all data)	$R_1 = 0.1693$, $wR_2 = 0.3467$
Absolute structure parameter	0.03 (2)
Extinction coefficient	0.0058 (3)
Largest diff. peak and hole	1.553 and -0.729e. $Å^{-3}$

Table 2.3 Crystal data and structure refinement for $C_{34}H_{56}O_7.H_2O$

Empirical formula	$C_{34}H_{58}O_8$
Formula weight	594.80
Temperature	293 (2) K
Wavelength	1.54178 Å
Crystal system	Monoclinic
Space group	$P2_1$
Unit cell dimensions	a = 11.5401 (1) Å
	b = 7.8751 (1) Å
	c = 18.5539 (3) Å
	β = 103.400 (4)°
Volume	1640.3(2) Å^3
Z	2
Density (calculated, experimental value)	1.204, 1.234 g/cm^3
Absorption coefficient	0.674 mm^{-1}
Crystal size	0.43 × 0.06 × 0.05 mm
Theta range for data collection	2.45 to 65.74°
Index range	$-14 \leq h \leq 14$
	$-9 \leq k \leq 7$
	$-22 \leq l \leq 22$
Reflection collected	19872
Independent reflections	5311 [R (int) = 0.1707]
Standard reflections	122
Absorption correction	Multi-scan SADABS (Sheldrick, 1996)
Max. and min. transmission	0.9700 and 0.8700
Refinement method	Full matrix least-square on F^2
Data / restraint / parameters	5311 / 2264 / 458
Goodness-of-fit on F^2	1.224
Final R indices [I > 2 sigma (I)]	R_1 = 0.1127, wR_2 = 0.2633
R indices (all data)	R_1 = 0.1891, wR_2 = 0.3107
Absolute structure	Flack (1983)
Flack parameter	-0.3 (7)
Extinction coefficient	0.0013 (9)
Largest diff. peak and hole	0.405 and -0.552e. Å^{-3}

2.4.2 Final monomer of methacrylate of cholic acid, 26 ($C_{34}H_{56}O_7.H_2O$)

The needle crystal was cut into a small piece with size of 0.43 × 0.06 × 0.05mm and glued to a very thin glass fiber. It was then installed on a goniometer head. The X-ray data were collected on the Bruker SMART 2K CCD diffractometer as for the above compound. One complete sphere of data was collected to better than 0.8 Å resolution. resolution. Upon completion of the data collection, the first 101 frames were recollected in order to improve the decay correction analysis. The unit cell volume is V = 1640.3 (2) $Å^3$, contains 2 molecules. Since in the $P2_1$ monoclinic space group the order of the general position is 2, there is just one independent molecule per asymmetric unit. It was found that the cholic acid part of the molecule is rigid and its atoms are well behaved. However, many atoms of the flexible spacer were found to be disordered over two distinct orientations. Moreover, one water molecule was found to be H-bonded to the OH at the 7 position. The crystal data and the structure refinement indicators are given in Table 2.3[61-71]. The final refined fractional coordinated and the anisotropic temperatures for the semi-heavy atoms for both compounds are placed in Appendix A1.

2.5 Syntheses of polymers

All the polymers were synthesized by radical polymerisation in dried THF solution using 2,2'-azo-bis(isobutyronitrile), AIBN, as initiator. The AIBN was purified by recrystallization in chloroform[72] or ethanol[73] and dried in vacuum oven.

2.5.1 Homopolymers

The homopolymers were synthesized as shown as Figure 2.6.

Synthesis of poly-CA2 (**HP2**)

In a 25 mL flask with magnetic stirrer and condenser, 0.5130 g (0.9865 mmol) of monomer **23** (D_2, n = 2) and 0.0048 g (0.0295 mmol) AIBN were introduced and the tight system was purged by the stream of nitrogen gas for 30 minutes. Then 10 mL THF was added and the system was heated to 70°C for 2 hours (2°C/min) to make sure the polymerisation reaction occurred gradually. The temperature was maintained for 60 hours. After the disappearance of double bonds, as checked by ^1H NMR, the solution was cooled down to room temperature and the THF solvent was evaporated. The sticky

polymer was redissolved in a small amount of THF and precipitated in 200 mL of ethyl acetate. The white precipitate was filtered off and dried at 50°C for 24 hours in vacuum oven The yield was about 70%. The molecular weight, as determined by SEC, is: M_w = 9753, M_n = 5552, M_w/M_n = 1.76

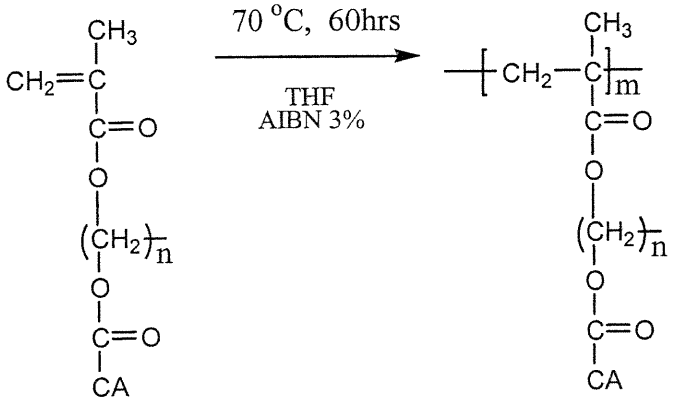

Figure 2.6 The syntheses of different homopolymers with n = 2, 4, 6, respectively.

Synthesis of poly-CA4 (**HP4**)

This polymer was also synthesized by the same method as the above polymer with monomer **25** (D_4, n = 4) and gave a yield of about 76%. The molecular weight, as determined by SEC, is: M_w = 7557, M_n = 4617, M_w/M_n = 1.64.

Synthesis of polyCA-6 (**HP6**)

It was synthesized in the same method with monomer **26** (D_6, n = 6) and a white polymer with yield of about 73% was obtained. The molecular weight, determined by SEC, is: M_w = 9763, M_n = 5490, M_w/M_n = 1.78.

2.5.2 Syntheses of copolymers

The copolymers were synthesized are shown in Figure 2.7.

A series of copolymers with different molar ratio of spacer length were made according to the following tables. The copolymers made from monomer **24** with spacer

length n = 2 and monomer **25** with n = 4, are identified as CP24; while those made from monomer **24** with spacer length n = 2 and monomer **26** with n = 6 are identified as CP26, while copolymers with monomer **25** (n = 4) and **26** (n = 6) are named as CP46. The detailed copolymers names and their molecular weights obtained by SEC are given in the Tables 2.4, 2.5 and 2.6.

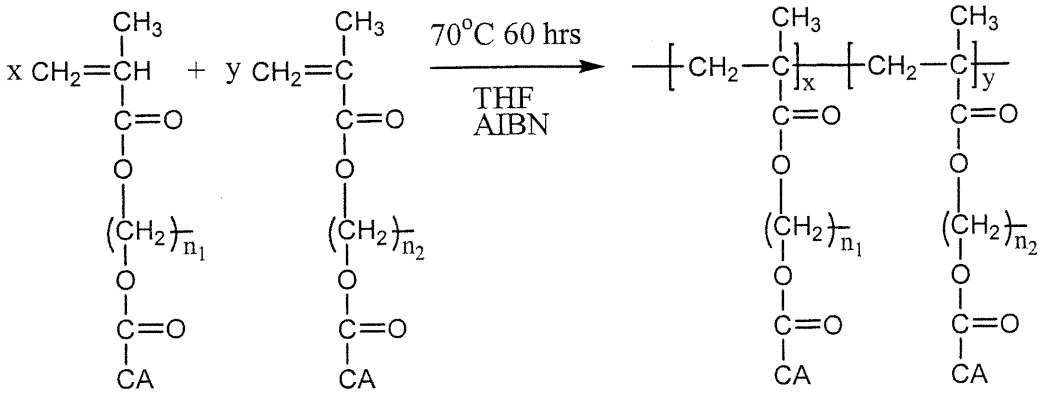

Figure 2.7 The syntheses of copolymers.

Table 2.4 The molecular weight of copolymers CP26 with **24** ($n_1 = 2$) and **26** ($n_2 = 6$)

Copolymers	x : y	M_w	M_n	M_w / M_n
CP26-28	2 : 8	10488	6500	1.61
CP26-46	4 : 6	10902	6774	1.61
CP26-64	6 : 4	10579	6597	1.60
CP26-82	8 : 2	11978	6822	1.76

Table 2.5 The molecular weight of copolymers CP24 with **24** ($n_1 = 2$) and **25** ($n_2 = 4$)

Copolymers	x : y	M_w	M_n	M_w / M_n
CP24-28	2 : 8	11127	7050	1.58
CP24-46	4 : 6	9057	4837	1.87
CP24-64	6 : 4	10242	5204	1.97
CP24-82	8 : 2	10997	5396	2.03

Table 2.6 The molecular weight of copolymers CP46 with **25** ($n_1 = 4$) and **26** ($n_2 = 6$)

Copolymers	x : y	M_w	M_n	M_w / M_n
CP46-28	2 : 8	9038	6591	1.37
CP46-46	4 : 6	19353	8651	2.24
CP46-64	6 : 4	13784	7447	1.85
CP46-82	8 : 2	11703	6652	1.76

Copolymer CP24-82 is made by monomer **24** (D_2, n = 2) and monomer **25** (D_4, n = 4) with molar composition 80% and 20% respectively. First, 0.4079 g (0.7844 mmol) monomer (n = 2), 0.1075 g (0.1961 mol) monomer (n = 4) and 0.0048 g (0.0293 mmol) AIBN were added in the 25mL flask with magnetic stirrer and condenser. The air-tight system was purged with nitrogen for 30 minutes. After that, 10 mL THF are introduced with a syringe. The system was then heated to 70°C and kept at this temperature for 60 hours until the disappearance of the double bonds, as established by ^{1}H NMR. The mixture was cooled down to room temperature and the THF solvent was evaporated. The polymer was redissolved in a small amount of THF. It is precipitated in stirred ethyl acetate solvent. The precipitate is filtered and dried in a vacuum oven for 24 hours. Finally, a white solid product is obtained with a yield about 78%.

The copolymers CP26 and CP46 are also made following the method described above. Their detailed compositions are given in Tables 2.4 and 2.6.

2.6 X-ray diffraction of polymers

Polymer films were made with high concentration solution (20% weight) of polymers on glass plates. The solution was coated homogenously five times and dried at room temperature slowly. It was found the films were very fragile. The main reason is probably due to the fact that molecular weight of polymers is not very high. One small film was scraped off the glass plate, then it was glued to a thin glass fiber and installed on a goniometer head. The SMART and normal focus sealed tube source graphite monochromatized CuKα radiation was used. X-ray diffraction patterns of the polymers are shown in Chapter 3.

CHAPTER 3

RESULTS AND DISCUSSIONS

In the first part of this chapter, the syntheses and the crystal structure determinations of the monomers will be discussed. The discussion on the syntheses and physical properties of the homo and copolymers will follow.

3.1 Preparation of the monomers

A series of monomers were synthesized according to our molecular design. The common feature is that they all are methacrylates containing a double bond at one end and a flexible spacer of n methylene groups inserted between the bile acid and the double bond. During this work I attempted to synthesize four monomers whose structures are illustrated in Figure 2.1.

3.1.1 Syntheses of monomers A (8, 9)

The traditional synthetic route for a typical mesogenic side chain polymers with spacer was already illustrated in Figure 2.2. The longer spacers (n = 6, 10) are first attached to the hydroxybenzoic acid to form products **1** and **2**, respectively. The yield of this reaction can be as high as 90%. The following process, that of the introduction of the double bond, is not difficult either. The addition of a small amount of hydroquinone is very important in order to prevent the polymerization of the double bond since methacrylic acid and products **3** and **4** may easily polymerize at a higher temperature. Once this step is completed, the carboxyl group is converted into the acyl chloride. This compound will react with the hydroxyl group of the methyl ester of the cholic acid (CAME). All the steps before arriving at the final monomers **8** and **9** were completed successfully. However, the reaction leading to the final monomers could not be achieved. This was surprising at first since many monomers were reported to have been synthesized by this method. However, all the reported monomers[74-78] contained much smaller

molecules than the bile acid units. Thus, it could be that the bile acid derivatives are too large for the reaction to succeed. The steric factors of the huge acyl chloride and bile acid units decrease greatly their reactivity and the probability of contact required in order to arrive at the desired products.

3.1.2 Syntheses of monomers B (11, 14, 15)

For monomers B (the synthesis procedure is illustrated in Figure 2.3), the carboxyl group of lithocholic acid (LCA) is first converted into the methyl ester (LCAME) with HCl as catalyst. This reaction was completed with a high yield in just 30 minutes. The reason for converting LCA into LCAME is that the later has a much higher solubility in organic solvent than LCA. The methyl ester group protects the carboxylic acid group thus preventing side reactions during the synthesis of the monomers. In the B monomers, the spacer and the bile acid are linked by an ether bond. Para-toluenesulfonyl chloride was reacted with LCAME since the ether bond cannot be easily formed directly. A tosylate of LCAME, which is a good leaving group, was obtained with a high yield. The tosylate was then purified by column chromatography with an eluent mixture of petroleum ether and ethyl acetate in a 1:4 volume ratio. The experiment revealed that column chromatography is indispensable for the purification of the tosylate. Recrystallization is not enough to purify the tosylate because a small amount of pyridine salt is always present. When the column chromatography process is completed, the collected liquid is left overnight and "hexagonal" crystals **11** are obtained by the next day. These good quality crystals of compound **11** were used for an X-ray diffraction analysis (see section 3.3.1).

The next step, the substitution reaction by the tosylate and diols, occurred with a typical S_{N2} mechanism[56, 79]. The substitution is accompanied by an elimination process probably as the result of steric hindrance at position C_3 on the steroid backbone of **11**[56 - 59]. The longer the spacer, the lower the yield of the substitution products. For n = 2, the yield of **12** is about 50%. And it decreases to 40% when 1, 4-butanediol (n = 4) was used as reactant[54]. When n is 6, the yield of **13** is so small that there is practically no pure substitution product. The final step of this synthesis could only be achieved for n = 2 and n = 4.

3.1.3 Syntheses of monomers C (19, 20)

The procedure, shown in Figure 2.4, was similar to that used in the synthesis of the monomers B. However, in the process to make monomer C, we could not obtain the tosylate of cholic acid methyl ester (CAME) in a crystalline form. The product is always obtained as an amorphous white solid although different recrystallization solvents were tried. Some publications reported that the tosylate of CAME is amorphous[57]. The two tosylates have similar chemical structures but the reason as to why one does form crystals and the other does not is not known.

In the next step, the substitution reaction of tosylate by diols, there is a competition between the substitution and the elimination reactions. Furthermore, we observe here, as in reference[54, 60], that the longer the spacer, the lower the yield.

Dry solvents were required for the syntheses of the above monomers. Otherwise, the yield would decrease significantly. For example, pyridine, the most often used solvent in these experiments, must be dried overnight with potassium hydroxide, and then refluxed for 3-4 hours before distillation, and stored with 4A molecular sieves.

The use of fresh methacryloyl chloride was also very important for the syntheses of the final monomers. It must be used when freshly prepared from methacrylic acid and benzoyl chloride. The product must be kept in a refrigerator and for no more than two weeks. Otherwise, it becomes gradually yellowish and slowly polymerizes.

3.1.4 Syntheses of monomers D (24, 25, 26)

The first step of the syntheses of the D monomers, the diol esters of cholic acid **21**, **22**, **23**, was easily performed (see Figure 2.5). Moreover, this reaction may be performed without a solvent. The liquid ethylene glycol, 1,4-butanediol, and solid 1,6-hexanediol act as both reactants and solvents since they all are liquids at the temperature of 70°C. All diols are used in large excess in order to avoid the formation of dimers. Normally the ratio of diols to cholic acid is 10:1. The cholic acid will gradually react with the diols using HCl as a catalyst. After 3 hours, the cholic acid was completely dissolved. The reactants were left to react for a further 2 hours to complete the process. When a higher temperature, 100°C for 2 hours, was tried, some minor superfluous peaks appeared in the NMR spectrum, revealing the presence of byproducts.

The crude product was obtained as a yellowish and extremely viscous liquid. As it was dried under vacuum, the product expanded into foam. The solid foam was scraped from the flask and was recrystallized using chloroform, ethyl acetate or other organic solvents.

The process of recrystallization is unusual. The solution was kept for 1-2 days, but the crystals did not form even when the solution was completely evaporated. It was only when the solution was constantly stirred with magnetic stirrer that the crystals appeared. A nucleus is needed to initiate the crystallization and the stirring accelerates its formation. Once a nucleus is formed, the crystals will appear quickly. The friction and scratching between the stirring magnetic bar and the glass flask produced tiny grit just as the nucleus of the crystals. Another reason to hasten the formation of crystals during agitation is that the polar hydroxyl groups in cholic acid cannot be easily dissolved in the non-polar chloroform solvent, especially the end hydroxyl group in the obstructive long flexible alkyl chain. It was easier to recrystallize when the solution was agitated. The crystals are not very soluble in most organic solvents. We had to choose a mixture of chloroform and THF (volume ratio of 1:1) in order to synthesize the final monomers. Several experiments proved that the synthesis reaction is more efficient in a mixture of solvents than in any single solvent.

The four hydroxyl groups in the diol ester of cholic acid are of different reactivities. One hydroxyl is at the end of the alkyl group, the other three are in the cholic acid moiety. The primary alcohol group is more accessible than the other three and has a higher reactivity. Both types of hydroxyl groups can react with methacryloyl chloride when it is present in excess. The other two hydroxyl groups at the 7 and 12 positions have a lower reactivity because they are more sterically hindered and less accessible. Experiments were performed in order to find the optimum ratio of ester to acyl chloride. The best yield was found for a ratio of 1:1.8. Once the reaction was completed, the monomers were purified by column chromatography with ethyl acetate as eluent. The solvent was then evaporated and a very sticky liquid was obtained. It was dried under vacuum to form foam. The foam collapsed and contracted gradually into a transparent glass-like product with high viscosity. Recrystallization was not successful. The product could only be recrystallized when a poor solvent such as petroleum ether was used. The

upper layer of the turbid suspension solution was left to crystallize slowly. This solution was very dilute since the product's solubility in petroleum ether was very low. It took 2-3 weeks to grow crystals. Once the crystals appeared, the turbid solution became clear. For **26** (D_6, n = 6), the crystals are needle like. While crystals of **24** (D_2, n = 2) always appear irregular shape like flowers. X-diffraction indicates that the crystals of **24** are always twinned. Thus, they are not suitable for a crystal structure determination. No crystals of **25** (D_4, n = 4) could be obtained, although many solvent and approaches were used. Only monomer **26** is suitable for an X-ray diffraction analysis.

3.2 Characterization of monomers

The monomers' structure and composition were characterized by elemental analysis, mass spectrometry, FTIR, NMR and X-ray diffraction.

3.2.1 Elemental analysis

The chemical compositions of the monomers were established by elemental analysis. The products were dried fully at 30°C for 48 hrs in a vacuum oven before elemental analysis. The experimental and calculated values are compared in Table 3.1.

Table 3.1 Comparison of theoretical and experimental elemental analysis results

Name	Formula	Molecular weight	Theoretical value (%)		Experimental value (%)	
			C	H	C	H
24	$C_{30}H_{48}O_7$	520.7	69.23	9.23	68.90	9.86
25	$C_{32}H_{52}O_7$	548.8	70.07	9.49	69.69	10.39
26	$C_{34}H_{56}O_7$	576.8	70.83	9.72	70.35	10.68

The comparison indicates the results are reasonable. From the elemental analysis, we can say the composition and structure of **24**, **25**, **26** are correct.

3.2.2 MS characterization

Mass spectrometry provides us with information about the molecular weight of a molecule, but also about the mass of a series of molecular fragments which reflect the fine structure and composition of the compound. This technique plays a very important role in structure elucidation studies. The mass spectrometer performs three essential functions: First, molecules are converted into ions by the bombardment of high-energy electrons and accelerated in an electrical field. Then the accelerated ions are separated according to their mass-to-charge ratio (*m/e*). Finally, the ions with a particular mass-to-charge ratio are measured by a detector. The mass spectrum (MS) is shown as a plot of ion abundance versus the *m/e* ratio. The beam of electrons in the ionization chamber converts some of the sample molecules into positive ions. The simple removal of an electron from a molecule yields an ion whose weight is the actual molecular weight of the original molecule. The beam may have enough energy to shatter some molecules and thus produces a series of fragments. A fragment ion is often the most abundant ion rather than the parent molecule ion.

Another way fragment ions are produced is when the unstable molecular ion decomposes before it arrives at the ionization chamber. Lifetimes which are less than 10^{-6} second are typical in this type of fragmentation. Figures 3.1, 3.2 and 3.3 show the mass spectra of the final monomers with spacer lengths of n = 2, 4, 6, respectively. The most abundant ion formed gives rise to the highest peak in the mass spectrum, the base peak. We can see from the MS that the base peaks for the three monomers are at *m/e* = 153.2, 68.4 and 55.0, respectively. In the three MS spectra obtained, the smaller fragment ions are always higher than the original molecular ion. We observed for **26**, the most abundant peak at 55.0 is 100%, while the parent molecular ion at 577.5 is only about 25%.

One of the most important developments in MS in the last few years has been the introduction of fast atom bombardment (FAB) ionization. In this research, our monomers were studied by FAB MS technique. Its importance stems from the ability to ionize many of the polar, charged, biologically relevant molecules of high molecular weight such as the bile acids derivatives. Despite the use of a high-energy ionizing atom beam, the

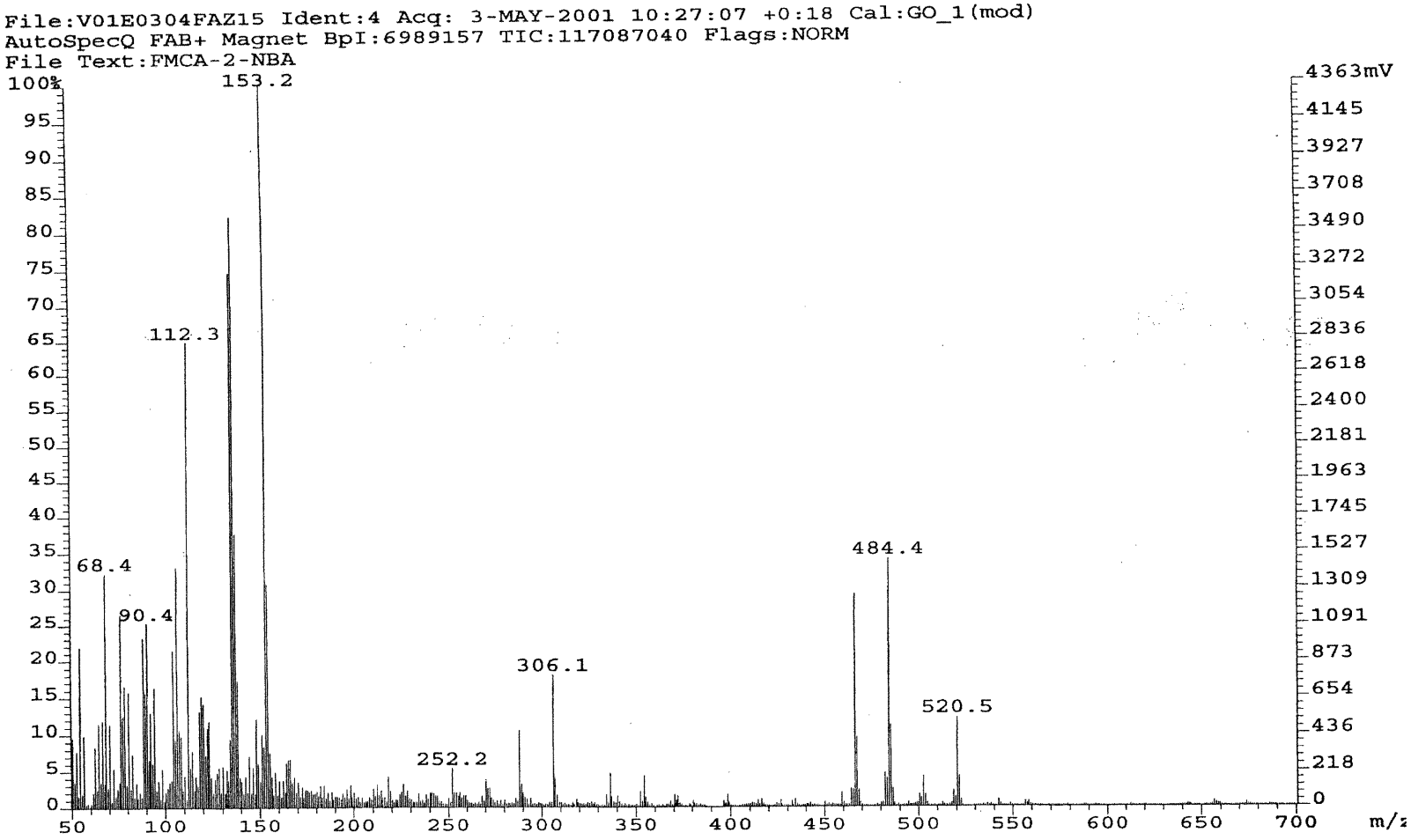

Figure 3.1 The mass spectrum of monomer **24** (n = 2).

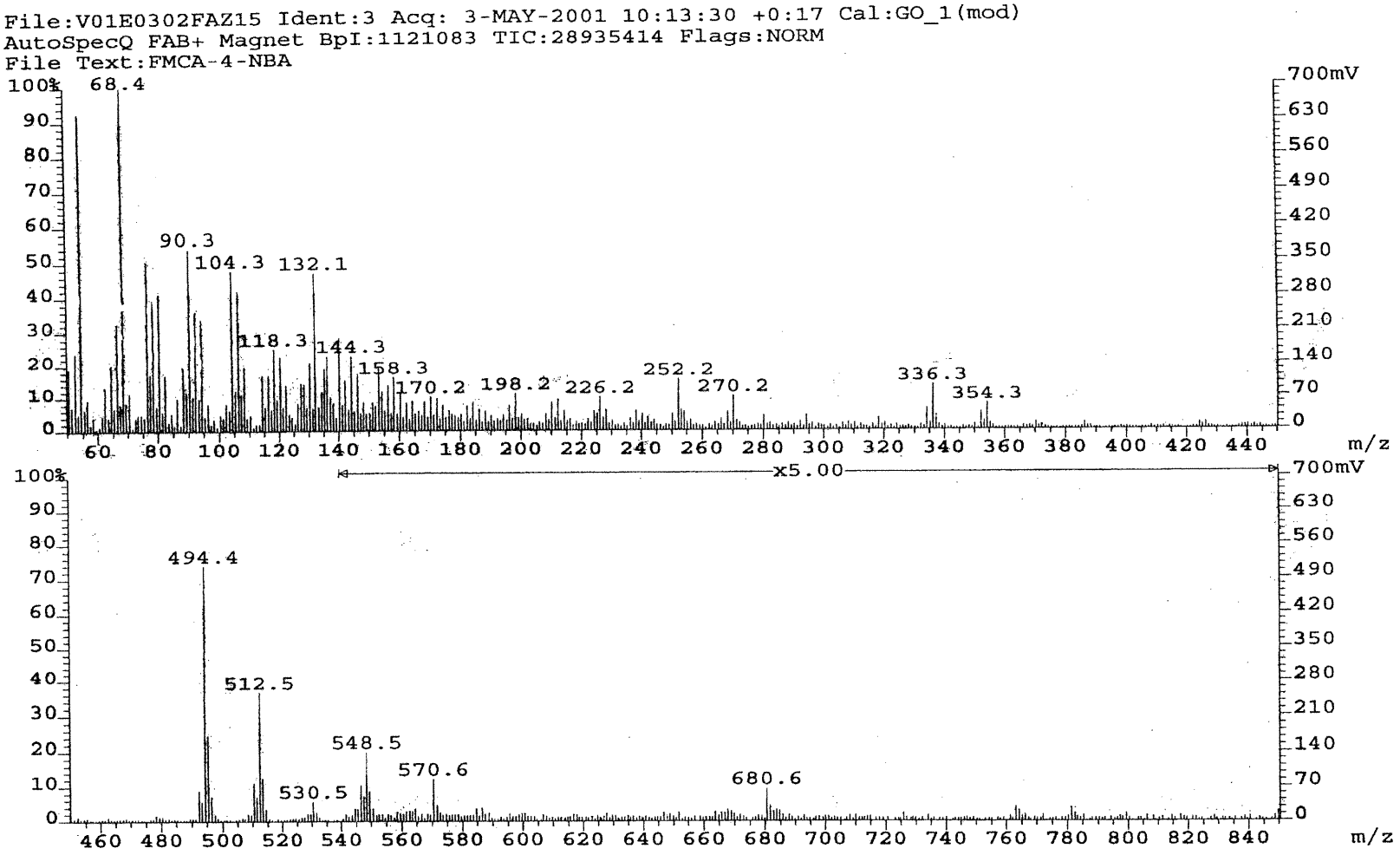

Figure 3.2 The mass spectrum of monomer **25** (n = 4).

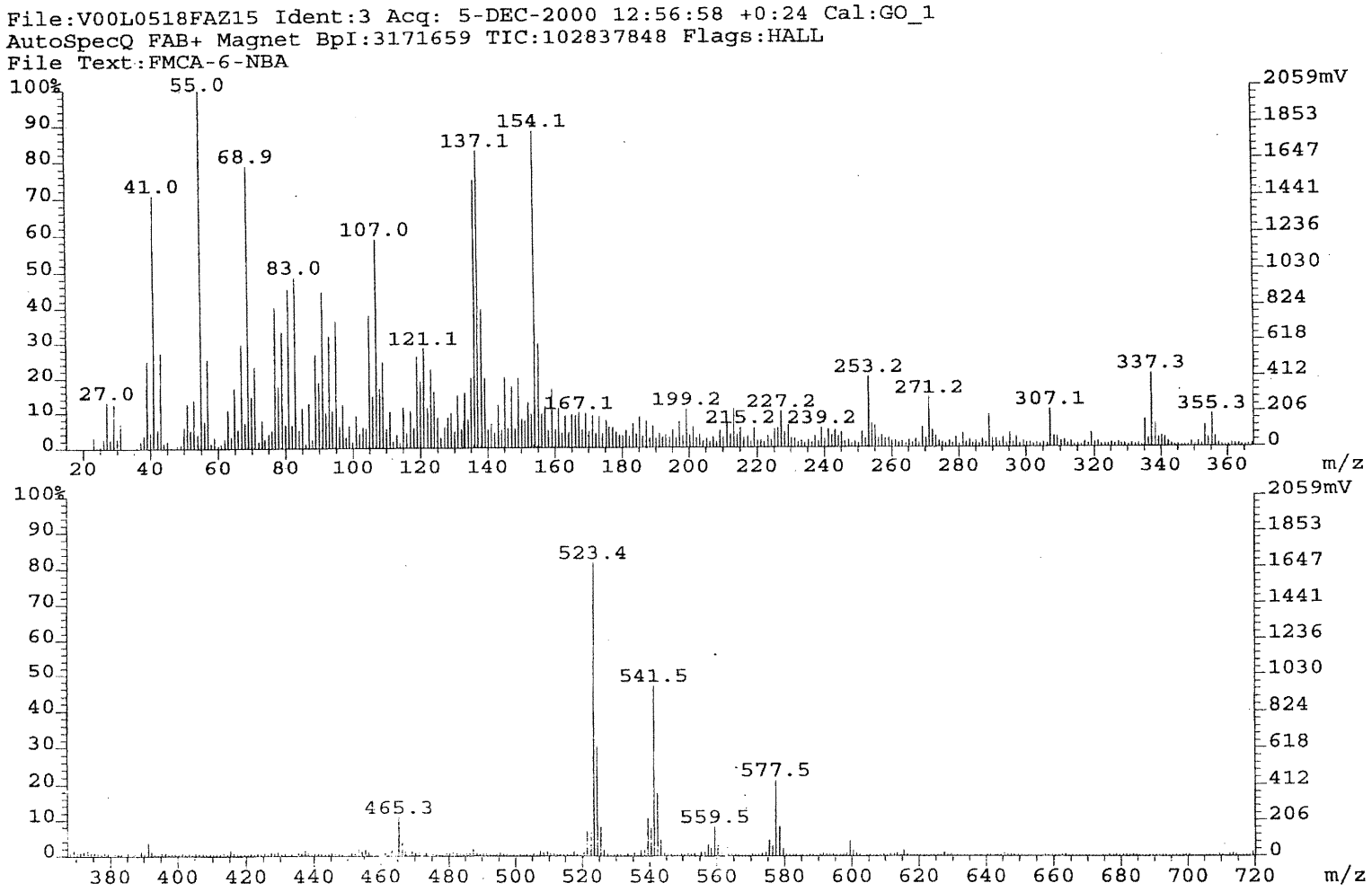

Figure 3.3 The mass spectrum of monomer **26** (n = 6).

quasimolecular ions (molecular ion species) are almost always produced. Both positive and negative ions, such as $[M+H]^+$ and $[M-H]^-$ can be produced by FAB. Sometimes, a small amount of intact molecules associated with low molecular weight ions to constitute an ionic cluster.

The highest peak, corresponding to the molecular ion at 577.5, is observed for **26** (Figure 3.3), while the calculated molecular weight is 576.8. When one hydroxyl group and one methine hydrogen are lost, a second peak appears at 559.5 (577.5-17-1 = 559.5). In a similar way, the third and fourth peaks were also present at 541.5 and 523.5 (541.5-17-1 = 523.5). The three peaks indicate that the molecular ion became relatively stable when all three hydroxyl groups were lost since the peak at 523.4 is one of the highest peaks and has a relatively high abundance. In Figure 3.3 the peak at 55.0 is the highest and indicates that there is plenty of alkyl ions $(CH_3CH_2CH_2CH_2)^-$ issued from the spacer.

The spectra of **24** and **25** in Figures 3.1 and 3.2 may be explained similarly. Two very small additional peaks at 680.6 and 570.6 are observed for **25** (they are enlarged by a factor of 5 on the figure). They correspond to the sum of the parent molecular ion and the lower molecular weight ion (548.5 + 132.1 = 680.6) or the sum of several ion peaks (90.3 + 144.0 + 336.3 = 570.6). It is quite likely that some cluster ions were produced by combining the above ions[80]. The calculated and experimental values of the molecular weight are almost identical (see Table 3.2), thus confirming the identity of the monomers.

Table 3.2 The comparison of the theoretical and experimental molecular weight of the three monomers

Monomers	Theoretical molecular weight	Experimental mass spectrometry value
24 (D_2, n = 2)	520.7	520.5
25 (D_4, n = 4)	548.8	548.5
26 (D_6, n = 6)	576.8	577.5

3.2.3 FTIR of the monomers (24, 25, 26)

An infrared recording yields many structural information about a molecule since every type of bond has a different vibrational frequency and absorption. By comparing the infrared spectra of various compounds, one can determine whether they are identical or similar in structure, or comparable in their features.

The FTIR spectra of the final monomers, **24**, **25**, **26** are shown in Figure 3.4. The spectra all have strong absorptions at 2928 and 2863 cm^{-1}, which are attributed to the C-H asymmetric and symmetric stretching vibrations of the methyl groups respectively. The broad absorption band in the 3300-3600 cm^{-1} region is characteristic of an H-bond involving the hydroxyl groups in the cholic acid. Another large peak appears at about 1720 cm^{-1}; it is attributed to C=O stretching vibration of the carbonyl group in the monomers. For **26**, this peak is split into two peaks which lie at 1718 and 1733 cm^{-1}. The peak is still clearly split for **25** while a shoulder can be detected for **24**. The reason is that the two C=O groups have slightly different environments, as they are separated by relatively a long spacer. As the spacer length becomes shorter, the two distinct peaks begin to merge together from n = 6 to n = 2. This trend is reflected in other peaks as well. The peak at 1250 cm^{-1} represent the C-O stretching vibration. It is also split into two small peaks for **26**. And there is small shoulder for **25** and **24**. A small peak at 1650 cm^{-1} is assigned to the C=C double bond present in all three monomers. The peak at 1100 cm^{-1}, can be regarded as stretching absorption of the C-OH bonds between cholic acid and its hydroxyl groups. The CH_2 methylene groups, have a characteristic absorption at approximately 1450 cm^{-1}. The other smaller peaks, C-C stretching vibrations, are not very useful for a structure determination.

3.2.4 NMR characterization

^1H NMR spectroscopy is a very important spectroscopic technique to study the fine structure of molecules. The NMR spectra not only provide us with the information about the number of each type of hydrogen atoms but also information regarding the nature of the immediate environment of each of these atoms. The structure of a molecule can be almost determined from its NMR spectrum. The structure of bile acids have been studied by NMR in the 1960s[81].

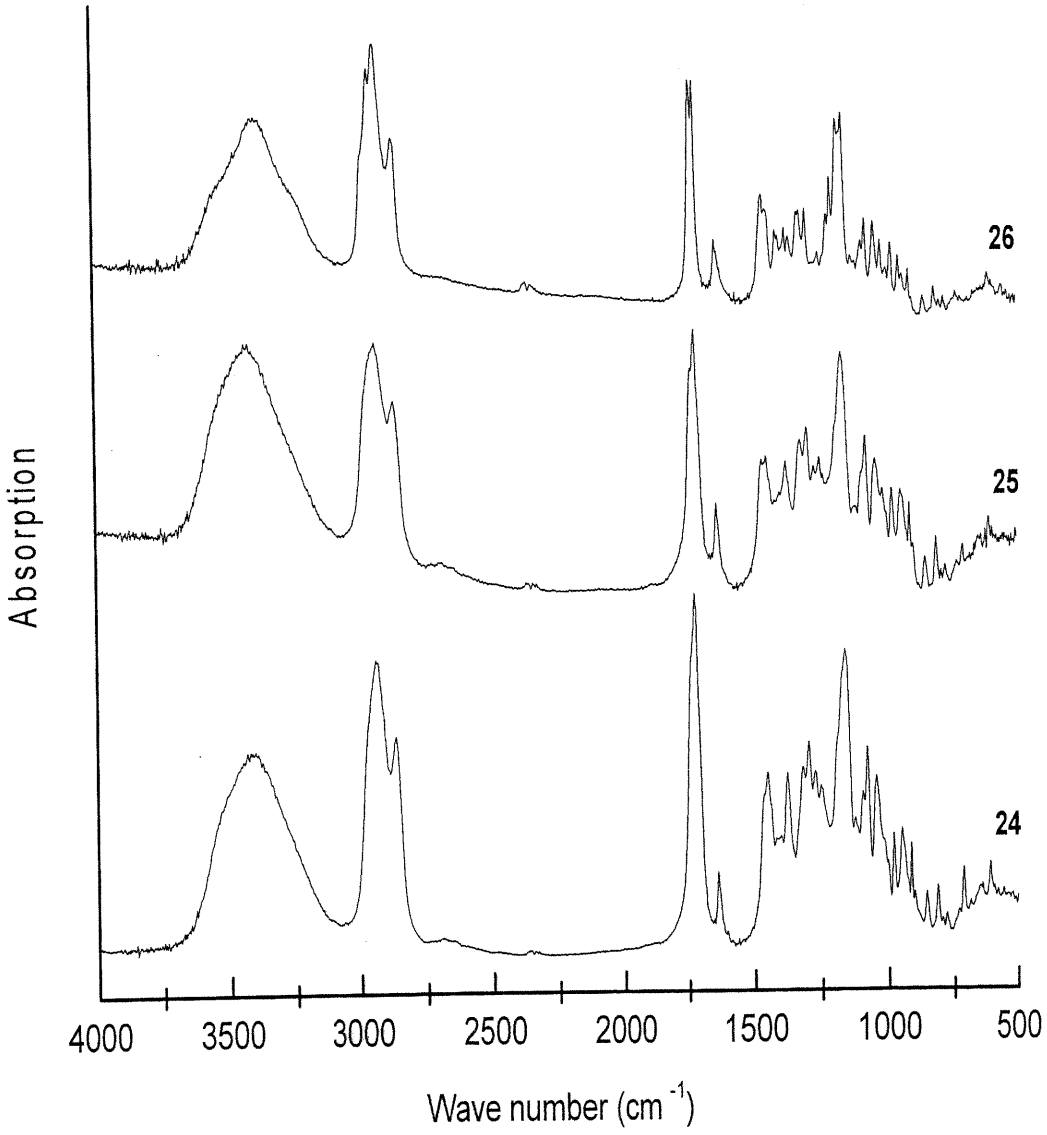

Figure 3.4 The IR spectra of the final monomers **24**, **25**, **26**.

The distinguishing features of the ^1H NMR spectrum of cholic acid and lithocholic acid are clearly visible in Figure 3.5. For lithocholic acid, the $CDCl_3$ peak is not in the range shown in the Figure 3.5 (B). For cholic acid, the solvent is CD_3OD, because its solubility in chloroform is very low. The CD_3OD solvent has two peaks which lie at 3.3 ppm and 4.8 ppm (due to trace water in CD_3OD) respectively. Most of the peaks are comparable, except for those at 3.78 and 3.89 ppm, which are attributed to the OH groups at the C7 and C12 positions of cholic acid. Lithocholic acid does not have hydroxyl groups at these positions. Both acids have a peak, 3.35 ppm for cholic acid and 3.65 ppm for lithocholic acid, which can be attributed to the hydroxyl group at C3. This peak splits into a quintet by the four hydrogen atoms on the neighboring carbons. That is correct according to the (n + 1) rule and Pascal's Triangle.

Singlet				1				
Doublet			1		1			
Triplet		1		2		1		
Quartet	1		3		3		1	
Quintet	1		4		6		4	1

The multiplicity arises from spin coupling between neighboring protons. It is likely to be observed between protons that are nonequivalent, in the sense that they resonate at different frequencies. In such a case, the multiplicity of a signal is given by the (n + 1) rule: if proton H_A "senses" a number n of equivalent protons H_B on the next bonded carbon, the resonance peak is split into (n + 1) peaks. The effect is transmitted through bonds and results in a characteristic resonance pattern with intensities following Pascal's Triangle.

The methyl peaks of the bile acids are visible in the NMR spectrum shown in Fig. 3.5. The two singlets at 0.69 ppm and 0.89 ppm are assigned to the methyl groups at the 18 and 19 positions. There is also a doublet at 0.99-1.02 ppm associated to the methyl group at the 21 position as there is only one neighboring hydrogen. The overlapping resonance peaks in the 1.02 ppm to 2.60 ppm region are attributed to all other CH_2 and CH protons.

The magnitude of spin coupling expressed by the coupling constant J, in hertz (Hz), is another useful parameter. Coupling constants are independent of the applied

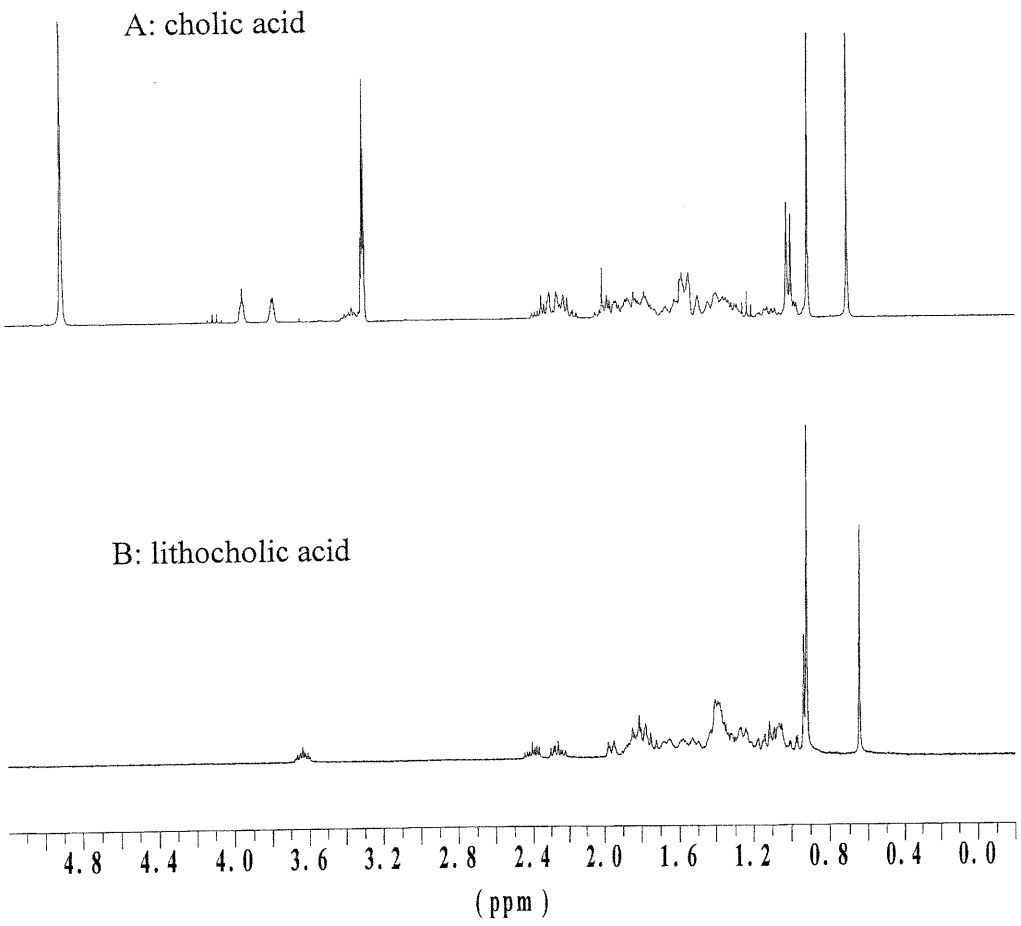

Figure 3.5 ^{1}H NMR spectra of cholic acid (A) in CD_3OD and lithocholic acid (B) in $CDCl_3$.

magnetic field, being a property of the molecule itself. The value of J is an important indicator of the conformation in relatively rigid molecules. However, more important for structural studies of cholic acid is the multiplicity and the width of the signal due to methine proton geminal to a hydroxyl group (=CH-OH), as a result of coupling to as many as four vicinal protons on the ring system.

According to Karplus[82] , the numerical value of the coupling constant J between two vicinal protons in a molecule is related to the torsion angle (ω) between the two C-H bonds, as viewed in projection along the C-C axis. The value of J varies approximately as the square of cosine (ω), that is:

$$J = k \cos^2 \omega \qquad \text{Karplus equation}$$

The proportionality ''constant'' k is not a true constant, it depends on surrounding of the protons involved. For ω in the range 0-90°, k typically has a value of 10, whereas for ω in the range 90-180°, k is likely to be 14. The torsion angles between vicinal pairs of C-H bonds depend on their respective conformation (ax = axial; eq = equatorial):

$$\omega_{ax/ax} \cong 180°, \ \omega_{ax/eq} \cong \omega_{eq/eq} \cong 60°$$

So $J_{ax/ax} \cong 14$ Hz and $J_{ax/eq} \cong J_{eq/eq} \cong 2.5$ Hz. The total width of a signal due to a methine proton with several vicinal neighbors is the sum of the relevant J values. In the structure of cholic acid (Figure 3.6), it is evident that there are axial/axial couplings between the 3β-proton and each of the 2α and 4α protons. Axial/equatorial couplings between the 3β-proton and each of the 2β and 4β protons also exist. So the total signal width calculated is 33 Hz (14 + 14 + 2.5 + 2.5 = 33) for 3α-hydroxyl-bile acid and 10 Hz (2.5 x 4 = 10) for 3β bile acid. This value can be used to judge whether the bile acid derivatives is α or β connection in C3 position. In a similar way, for 7α-H and 12α-H in bile acids, the signal widths are 7.5 Hz and 5 Hz respectively. The experimental values obtained from the NMR spectra (the J values for 3-H, 7-H and 12-H in Figure 3.7 are 33, 7.5 and 5 Hz) are the same as the theoretical interpretation and that justify the theoretical interpretation.

When bile acids are converted into methyl esters, the apparent change in the ^{1}H NMR spectrum is illustrated in Figure 3.7. There is one sharp singlet at 3.65 ppm caused by the ester group of the C24 position. This is a distinctive feature of the methyl protons of the bile acid methyl ester.

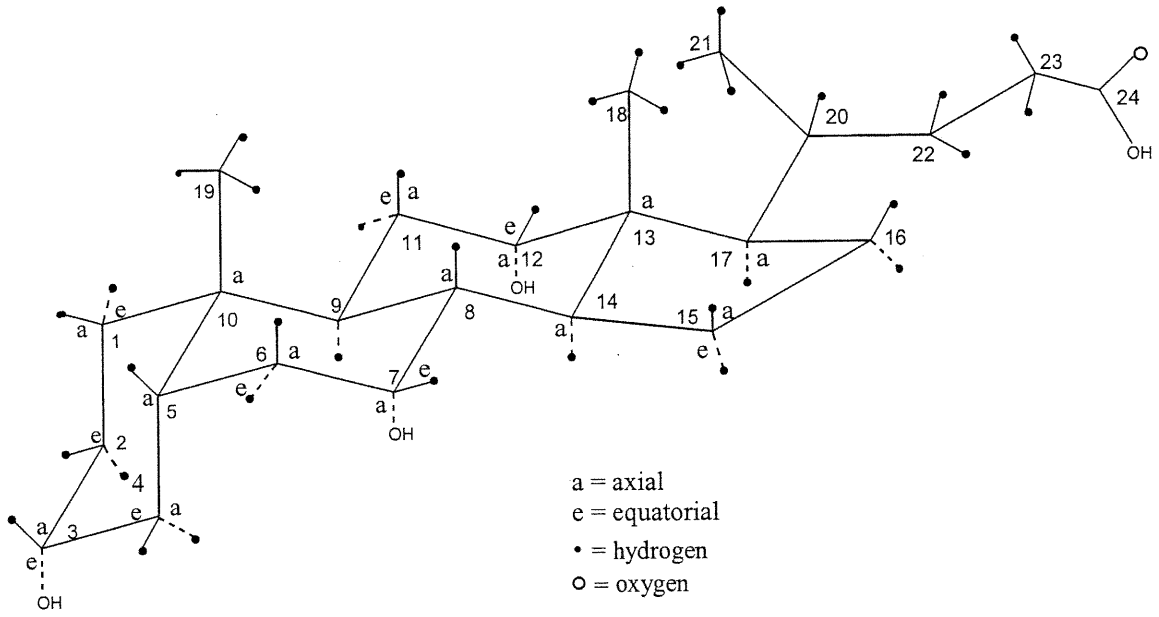

Figure 3.6 Perspective drawing of the cholic acid molecule. The orientation of the side chain, carbons from 20 to 24, is arbitrary. Ring protons are equatorial (e) or axial (a).

The NMR spectra in Figure 3.8 confirm the successful obtaining of the intermediates **1** and **2**. The peaks at 1.4-1.8 ppm are due to the central (n – 2) methylene groups in the spacer.

For compound **1**, we can see the integration in this region is smaller than in the case of **2**. The two triplet peaks at 4.2 ppm and 3.4 ppm are due to the two end methylene groups attached to the phenoxy and hydroxyl groups, respectively. The peak at 3.4 ppm is broader than that at 4.2 ppm. This is due to the fact that the triplet peak is overlapped with a water peak. The two doublets at 6.9 ppm and 7.8 ppm are assigned to the 4 protons of the phenyl group.

The spectra of methacryloyl chloride and intermediates **3** and **4** with double bonds are shown in Figure 3.9. We note the presence of two peaks at 6.1 ppm and 5.6 ppm which confirm that the double bonds in molecules **1** and **2** are present. The sharp singlet at 1.9 ppm is attributed to the methyl group of the methacrylate. The peaks of the terminal methylene group are shifted from 3.4 to 4.2 ppm because the hydroxyl group was replaced by an ester. Thus, it is established that the longer spacer and the methacrylate double bonds were introduced into the molecular structure.

In the syntheses of monomers B and C, the intermediate tosylates **16** and **11** from the CAME and LCAME can be observed in the spectra in Figure 3.10 (A and B). Because the hydroxyl group was replaced by a tosylate at position 3, the methine chemical shift changed from 3.4 to 4.4 ppm. The phenyl ring in the tosylate is responsible for the appearance of two doublets at 7.3 and 7.8 ppm.

Diols were used to react with the tosylate to yield an ether bond between the bile acids and a longer spacer. However, we found that the longer the spacer is, the more elimination products were obtained. When the spacer length n increased from 2 to 6, there was less and less of the substitution product. The structure of the substitution product and the NMR spectrum are shown in Figures 3.12 (A) and 3.11 (A). The elimination products with double bonds are schematically illustrated in Figures 3.12 B, C, D and E. The most obvious feature of these products is the double bond between the carbons at positions 2 and 3 or positions 3 and 4. The characteristic peaks of these double bonds lie in 5.3-5.8 ppm region of the NMR spectra in Figure 3.11 (B and C).

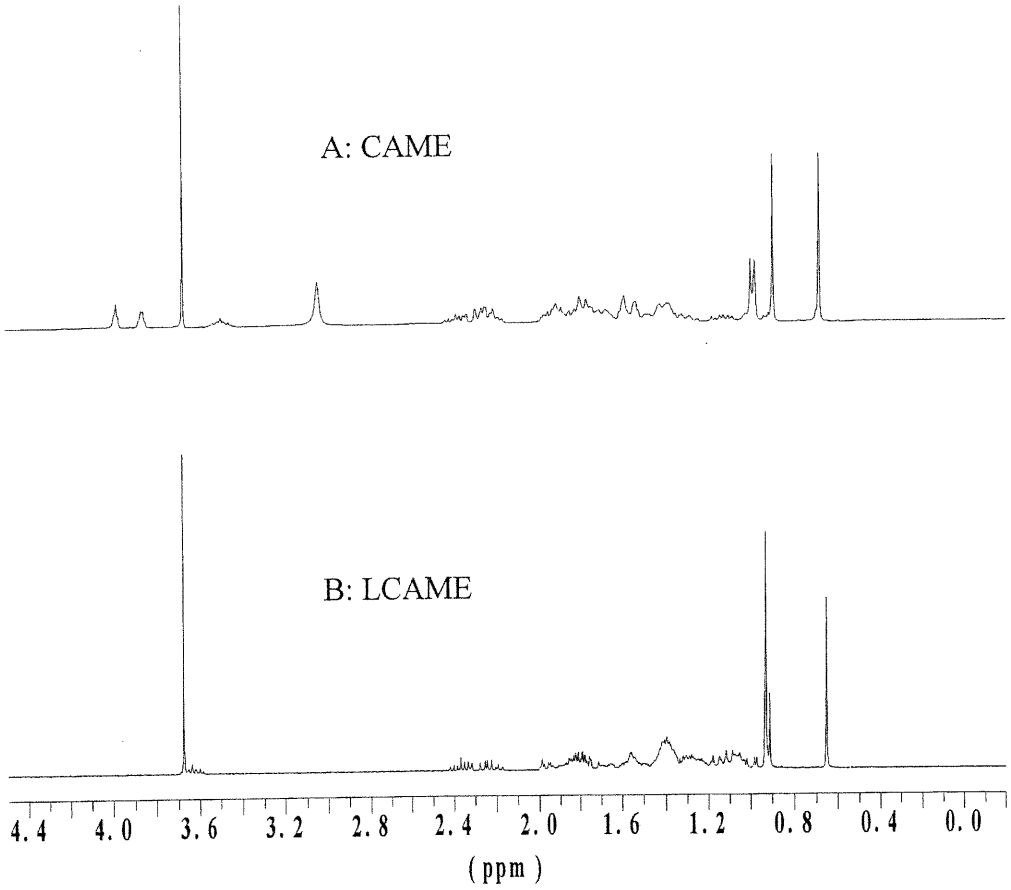

Figure 3.7 ^{1}H NMR spectra of **7**: CAME (A) in $CDCl_3$ and **10**: LCAME (B) in $CDCl_3$.

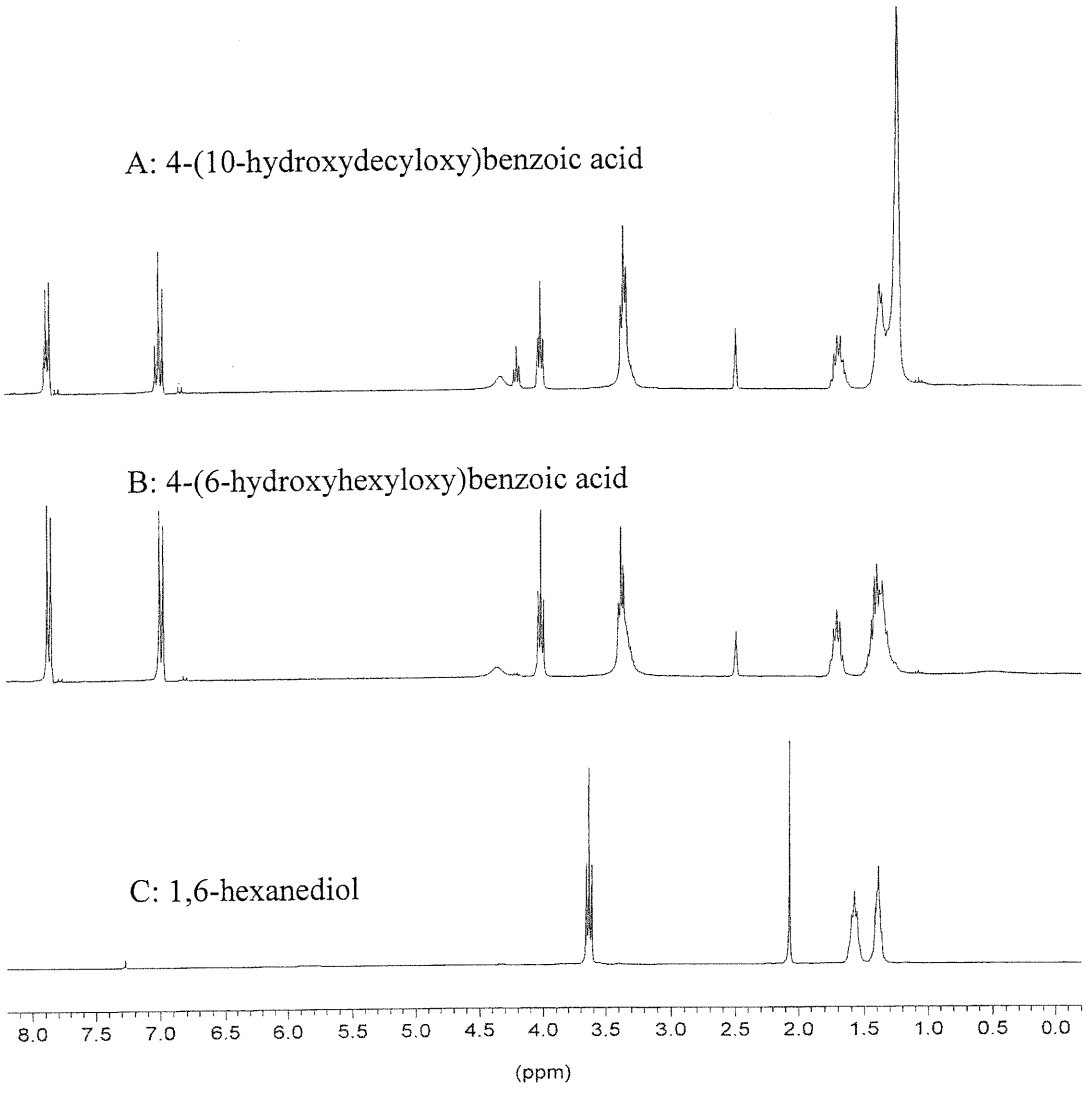

Figure 3.8 ^{1}H NMR spectra of **2**: 4-(10-hydroxydecyloxy) benzoic acid (A) in DMSO, **1**: 4-(6-hydroxyhexyloxy)benzoic acid (B) in DMSO and 1, 6-hexanediol (C) in $CDCl_3$.

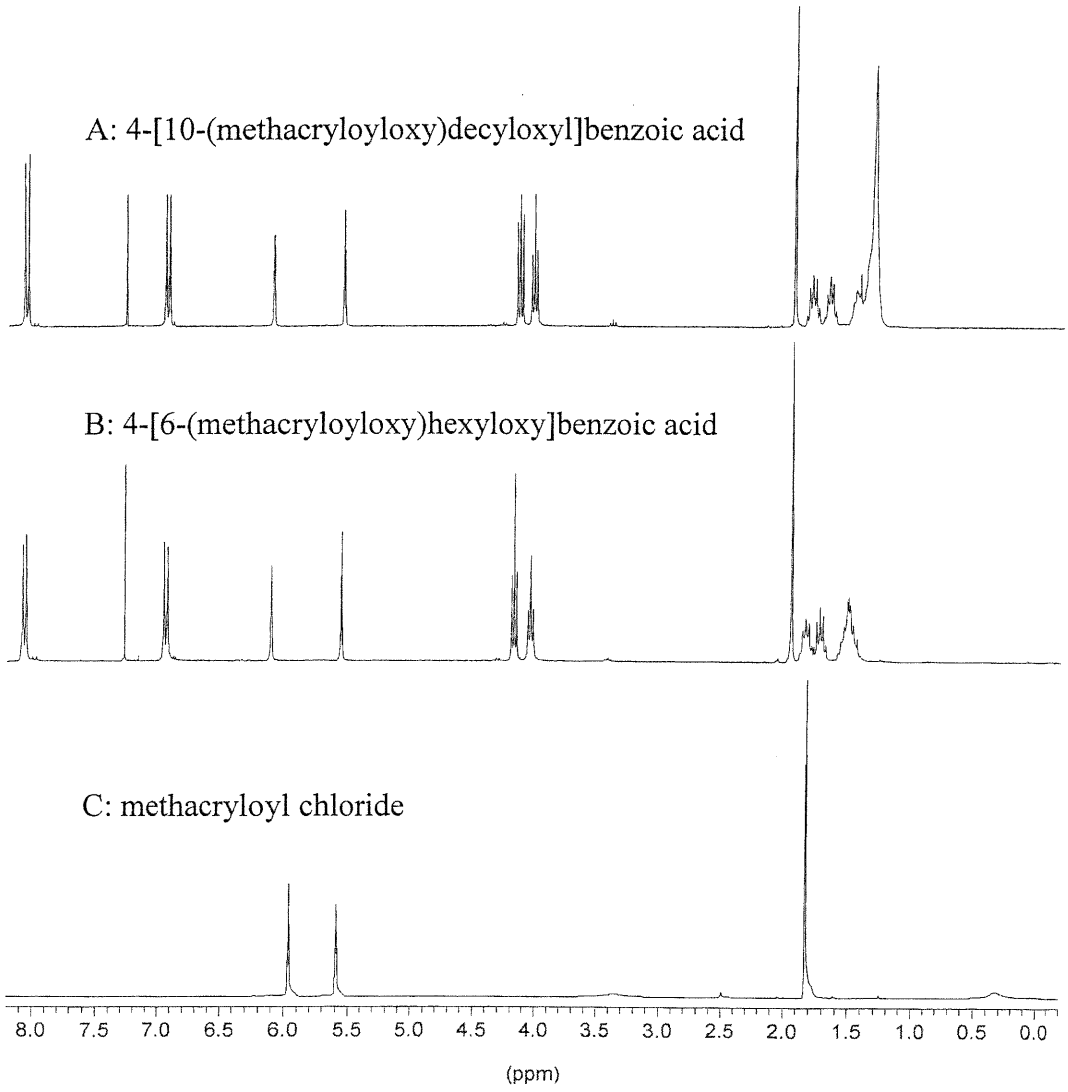

Figure 3.9 ^{1}H NMR spectra of **4**: 4-[10-methacryloyloxy)decyloxy]benzoic acid (A) in $CDCl_3$, **3**: 4-[6-(methacryloyloxy)hexyloxy]benzoic acid (B) in $CDCl_3$ and methacryloyl chloride (C) in $CDCl_3$.

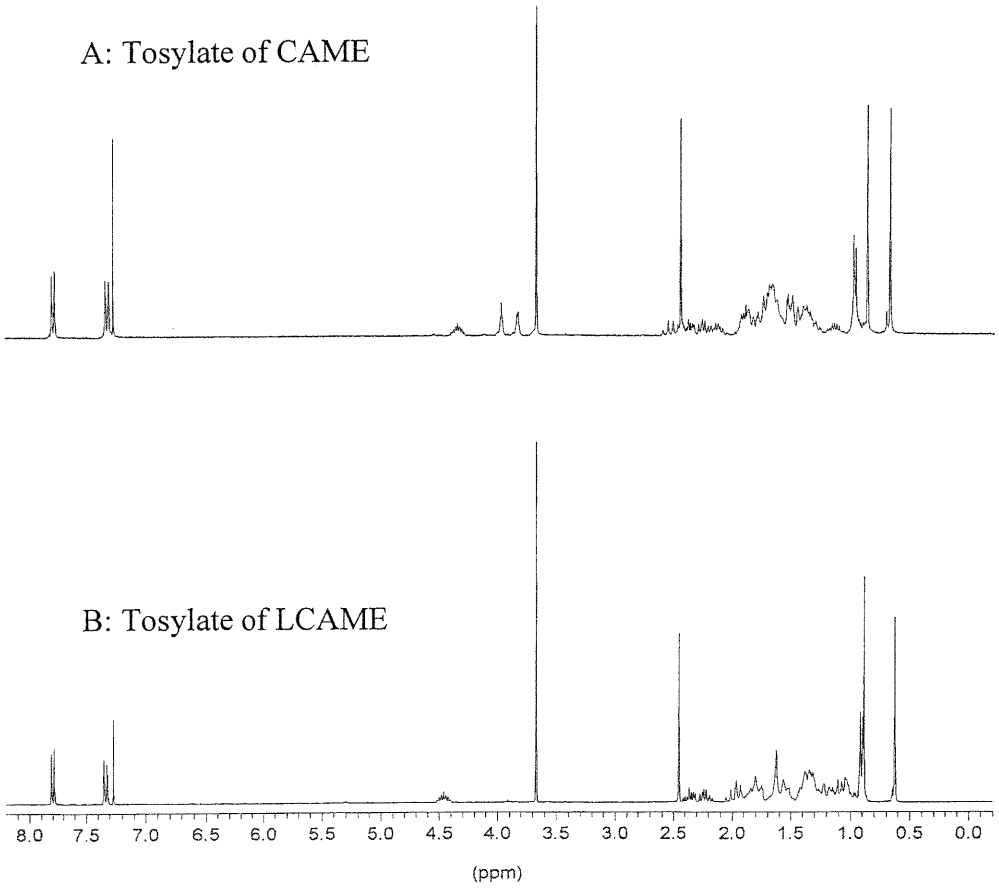

Figure 3.10 ^{1}H NMR spectra of **16**: tosylate of CAME (A) in $CDCl_3$ and **11**: tosylate of LCAME (B) in $CDCl_3$.

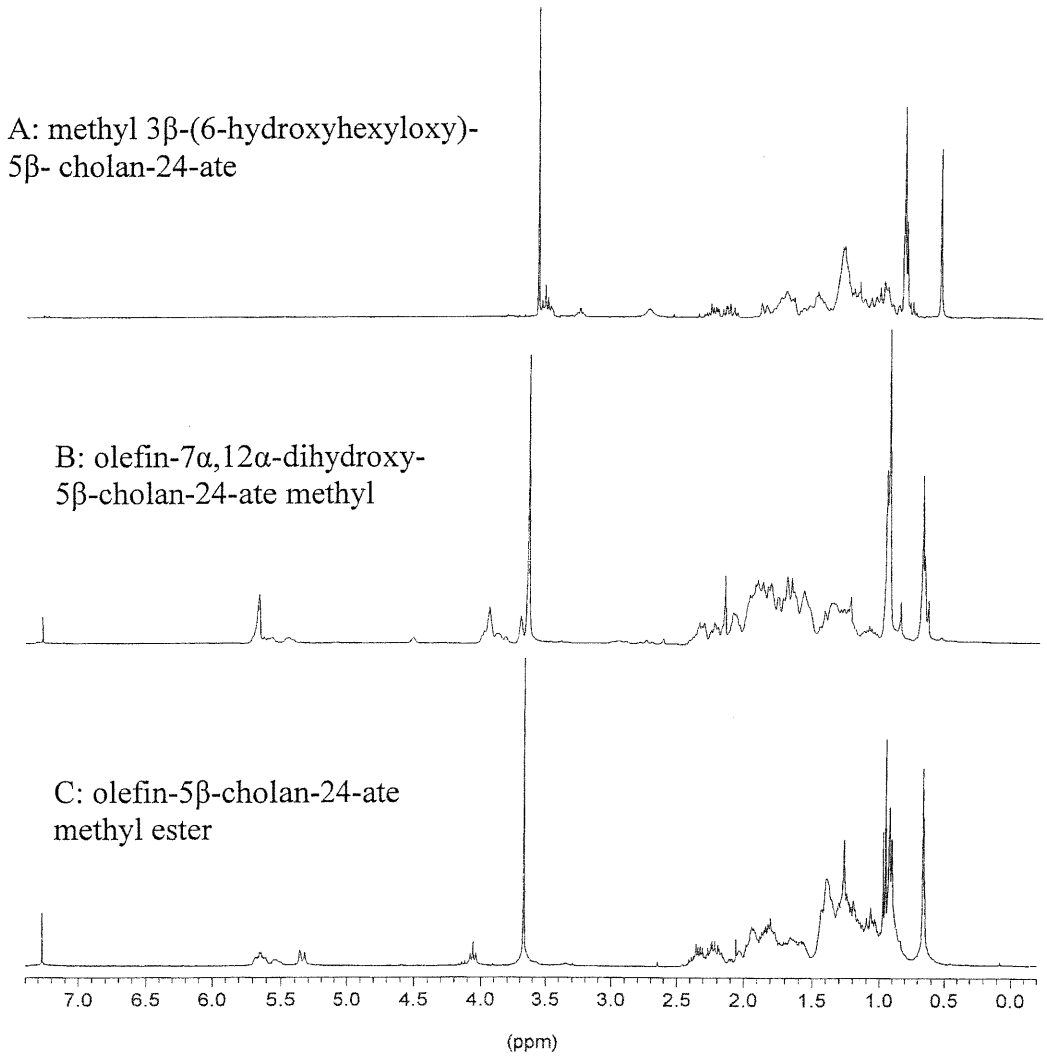

Figure 3.11 ^{1}H NMR spectra of **13**: Methyl 3β-(6-hydroxyhexyloxy)-5β-cholan-24-ate (A) in $CDCl_3$ and olefin-7α,12α-dihydroxy-5β-cholan-24-ate methyl ester (B) in $CDCl_3$, olefin-5β-cholan-24-ate methyl ester (C) in $CDCl_3$.

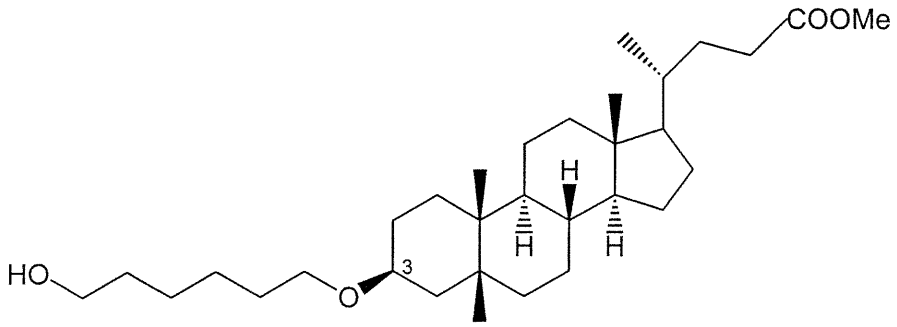

A: methyl 3ß-(6-hydroxyhexyloxy)-5ß-cholan-24-ate **13**

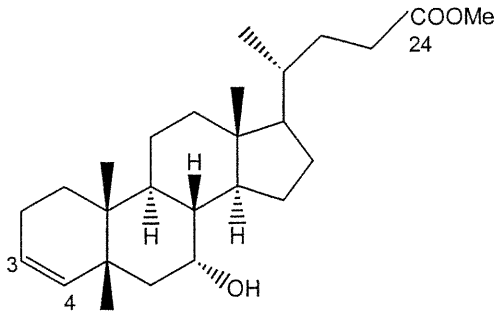

B: 3-olefin-5ß-cholan-24-ate methyl ester

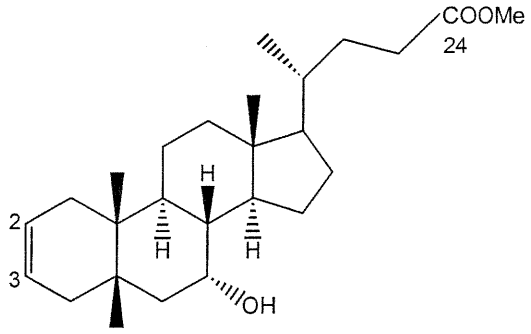

C: 2-olefin-5ß-cholan-24-ate methyl ester

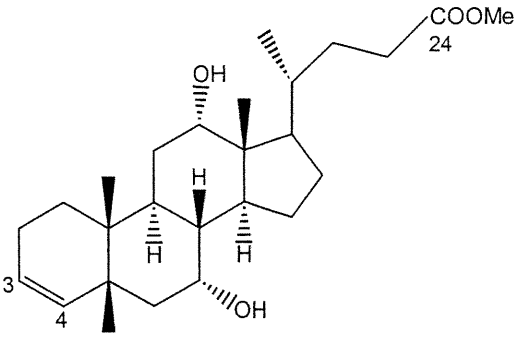

D: 3- olefin-7a,12a-dihydroxy-5ß-cholan-24-ate methyl ester

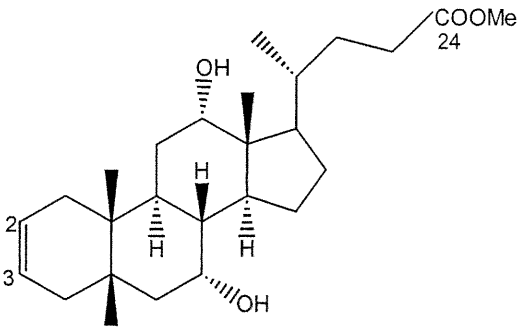

E: 2-olefin-7a,12a-dihydroxy-5ß-cholan-24-ate methyl ester

Figure 3.12 The chemical structures of **13**: methyl 3β-(6-hydroxyhexyloxy)-5β-cholan-24-ate (A), olefin-7α,12α-dihydroxy-5β-cholan-24-ate methyl ester (B, C) and olefin-5β-cholan-24-ate methyl ester (D, E).

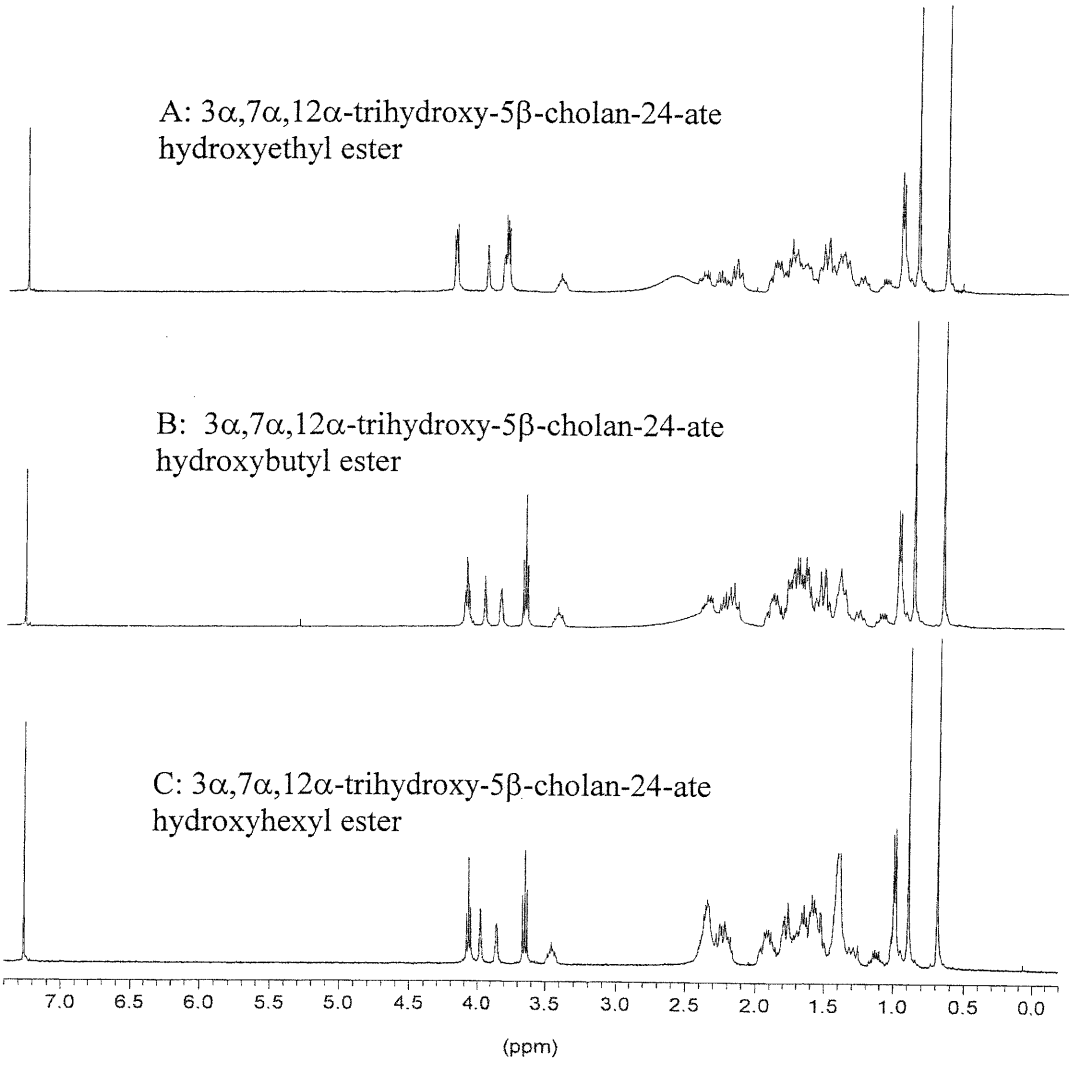

Figure 3. 13 ^{1}H NMR spectra of intermediate **21**: 3α,7α,12α-trihydroxy-5β-cholan -24-ate hydroxyethyl ester (A) in $CDCl_3$, **22**: 3α,7α,12α-tri-hydroxy-5β-cholan-24-ate hydroxybutyl ester (B) in $CDCl_3$ and **23**: 3α,7α,12α-trihydroxy-5β-cholan-24-ate hydroxyhexyl ester (C) in $CDCl_3$.

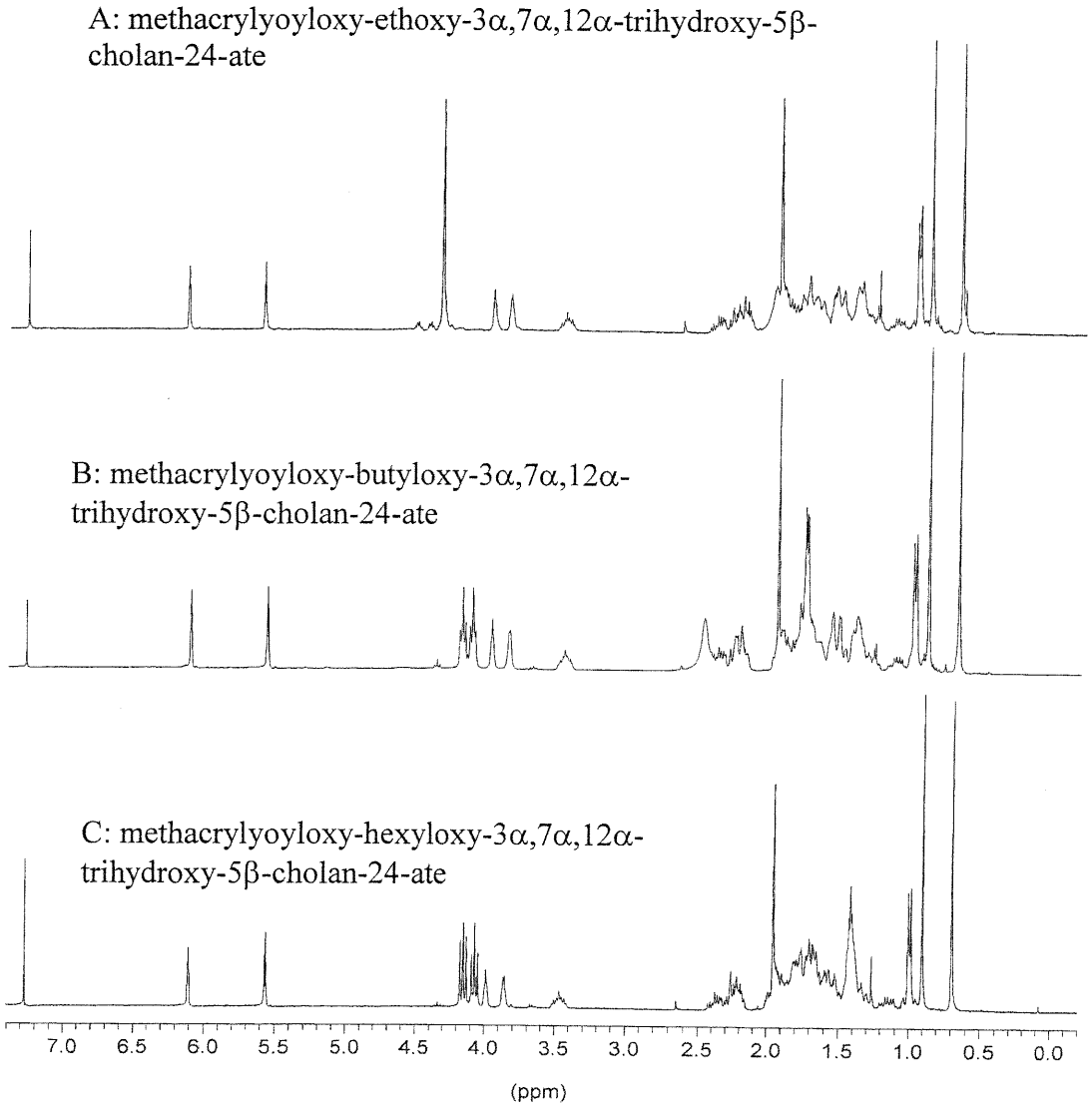

Figure 3.14 ^{1}H NMR spectra of final monomers **24** : methacrylyoyloxy-ethoxy-3α,7α,12α-trihydroxy-5β-cholan-24-ate (A) in $CDCl_3$, **25** : methacrylyoyloxy-butyloxy-3α,7α,12α-trihydroxy-5β-cholan-24-ate (B) in $CDCl_3$ and **26** : methacrylyoyloxy-hexyloxy-3α,7α,12α-trihydroxy-5β-cholan-24-ate (C) in $CDCl_3$.

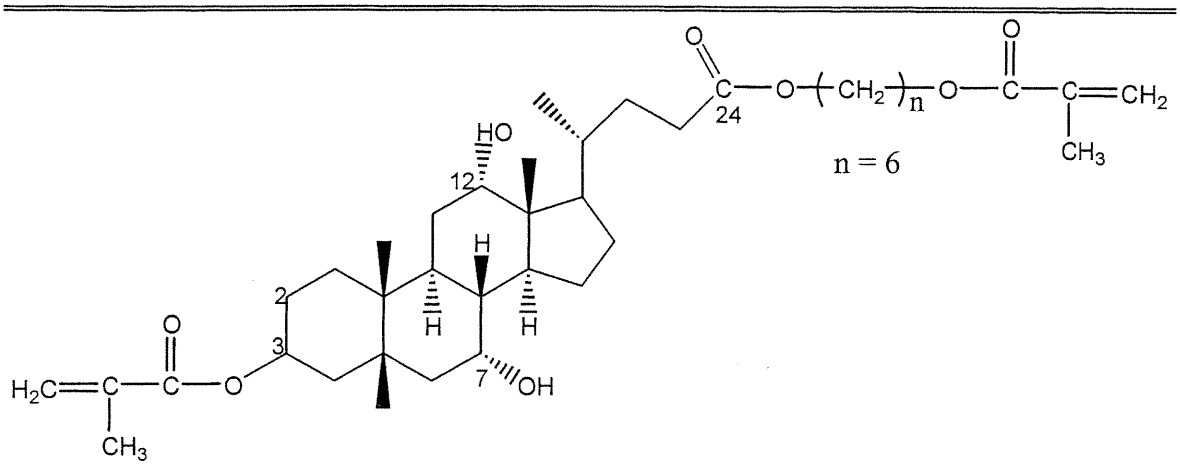

methacryloyloxy-ethoxy-3α(methacryloyloxy)-7α,12α-dihydroxy-5β-cholan-24 ate

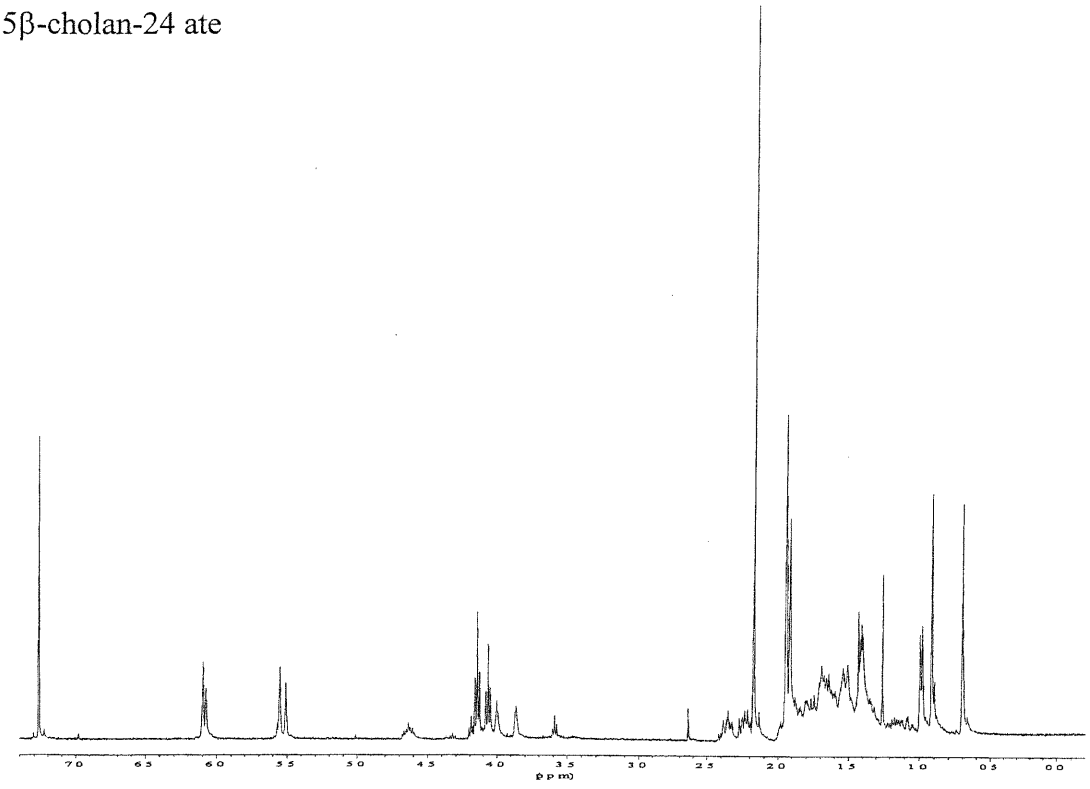

Figure 3.15 The chemical structure and ^{1}H NMR spectrum of byproduct: methacrylyoyloxy- ethoxy-3α(methyacrylyoyloxy)-7α, 12α-dihydroxy-5β-cholan -24-ate (two double bonds at two ends of cholic acid) in $CDCl_3$.

The esterification of cholic acid with diols in the preparation of the D intermediates **21**, **22**, **23** can be seen in NMR spectra (Figure 3.13 A, B, C). For **23** (n = 6), the triplets at 4.1 ppm and 3.6 ppm are due to the protons bound to the ester group and the hydroxyl group, respectively. However, when 1,4-butanediol and ethylene glycol are used to prepare **22** and **21**, the peaks are slightly shifted to higher field. In Figure 3.13 A, the triplet of the methylene attached to the end hydroxyl group in **21** is partly overlapped with the singlet of methine bound to the hydroxyl group of the 7 position of cholic acid.

The final monomers **24** (D_2, n = 2), **25** (D_4, n = 4), **26** (D_6, n = 6) were identified by their NMR spectra, shown in Figure 3.14 A, B and C, respectively. The spectra display three main features. The first one is the cholic acid skeleton which can be reflected by the three methyl peaks (singlets at 0.69 and 0.89 ppm are attributed to the methyl groups at positions 18 and 19 respectively; the doublet peak at 0.91 ppm is due to the methyl group at position 21) and the three methine groups bound to the hydroxyl groups (multiplet at 3.4 ppm from the proton at position 3; singlets at 3.9 and 4.0 ppm are assigned to the protons at positions 7 and 12. The second feature is that the methylene and methine groups of the cholic acid and the alkyl spacer show up in the region of the 1.2-1.5 ppm. The longer the spacer is, the higher the peaks are in this region. The third feature is the methacrylate group (at 2.0 ppm due to the methyl group and the other two peaks at 5.6 and 6.1 ppm which are associated to the vicinal hydrogens in the double bond). The integration of the various protons is as expected. It can be concluded that, according to the NMR spectra, the chemical structures of the monomers are those expected. The detailed values of the ^{1}H NMR chemical shifts of the final monomers **24**, **25**, **26** and their intermediates **21**, **22**, **23** are listed in Table 3.3.

Due to the relatively higher chemical reactivity of the OH group at position 3 of cholic acid and the excess amount of methacryloyl chloride, it is very possible to obtain a product with two methacrylate double bonds during the final reaction (the structure is shown in Figure 3.15). That is also why the yield of the desired monomer is not as high as expected (actual yield is 40%). The yield depends on the ratio of methacryloyl chloride and cholic acid. The NMR spectrum shown in Figure 3.15 is that of a by-product. The two characteristic double bonds can be seen at 5.5 and 6.1 ppm. The two methyl groups in methacrylate appear at 1.9 ppm. The highest peak at 2.1 ppm and the peak at 1.2 ppm

are those of acetone and ethyl acetate solvents residue. Other peaks can be attributed to the cholic acid skeleton.

It is concluded from the above experiments that the monomers synthesized have the expected structures. The monomers are pure enough to carry out the polymerization reaction.

Table 3.3 NMR Chemical shifts (ppm) of final monomers and intermediates dissolved in $CDCl_3$

Protons	Intermediate			Final Monomers		
Spacer length	n = 2,	n = 4,	n =6	n = 2,	n = 4,	n = 6
Name	**21**	**22**	**23**	**24**	**25**	**26**
3-CH	3.45	3.45	3.46	3.45	3.45	3.47
7-CH	3.85	3.85	3.85	3.89	3.88	3.86
12-CH	4.00	3.98	3.98	4.01	4.00	3.98
18-CH_3	0.69	0.69	0.69	0.69	0.69	0.69
19-CH_3	0.89	0.89	0.90	0.89	0.90	0.90
21-CH_3	0.99	0.99	1.00	0.99	1.00	1.00
Methacrylate						
Methyl -CH_3	No			1.92	1.94	1.95
C=CH_2	No			5.57	5.57	5.56
				6.11	6.10	6.10
Methylene $(CH_2)_n$	-----	1.76	1.32	-----	1.78	1.39
-OCH_2	3.83	3.69	3.64	4.34	4.10	4.07
-OCH_2	4.22	4.11	4.07	4.34	4.19	4.15

3.3 X-ray structure determination of monomers 11 and 26

3.3.1 Tosylate of lithocholic acid methyl ester (11)

The compound crystallizes with a very large unit cell volume, V = 18426.2(2) $Å^3$, which contains 24 molecules. Since in the $P2_12_12_1$ orthorhombic space group the order of the general position is 4, there are 6 independent molecules in the asymmetric unit. The large number of atomic coordinates to be established is not a trivial problem. In fact, when the structure was solved, the problem was further complicated since in each of the six independent molecules, the *para*-toluenesulfonyl side chain was distributed over two positions in the 57:43, 51:49, 63:37, 52:48, 51:49 and 53:47 ratios for the six molecules A, B, C, D, E and F, respectively. It can be seen the common ratio is about 50:50. However, there are two molecules which have the ratio out of this value, but they don't have too much difference. In order to pack themselves into the asymmetric unit, the six molecules will have to coordinate and try to adopt the different conformation. The similar conformation ratio is not necessary from the experimental value. Restraints were applied to the phenyl groups of atoms to keep them with the proper geometry (the C-C distance is 1.395 Å, the bond angle is 120°). Furthermore, compounding the already complicated situation, it appeared that the crystal was probably twinned. However, the twinning law could not be established. Consequently, although the crystal structure was solved, it could not be refined to the usual standard of reliability. Considering the number of observed reflections, 36421, only the coordinates and the anisotropic temperature factors of the S, O and C atoms were refined for a total of 2120 adjustable parameters. The H atoms were kept at fixed, calculated positions.

3.3.1.1 Description of the structure

The bond distance, bond angle and torsion angles are listed in Tables 3.4, 3.5 and 3.6 respectively. A view of one of the six molecules is shown in Figure 3.16. The packing of the molecules is illustrated by the *bc*-projection in Figure 3.17 and the a*c*-projection in Figure 3.18.

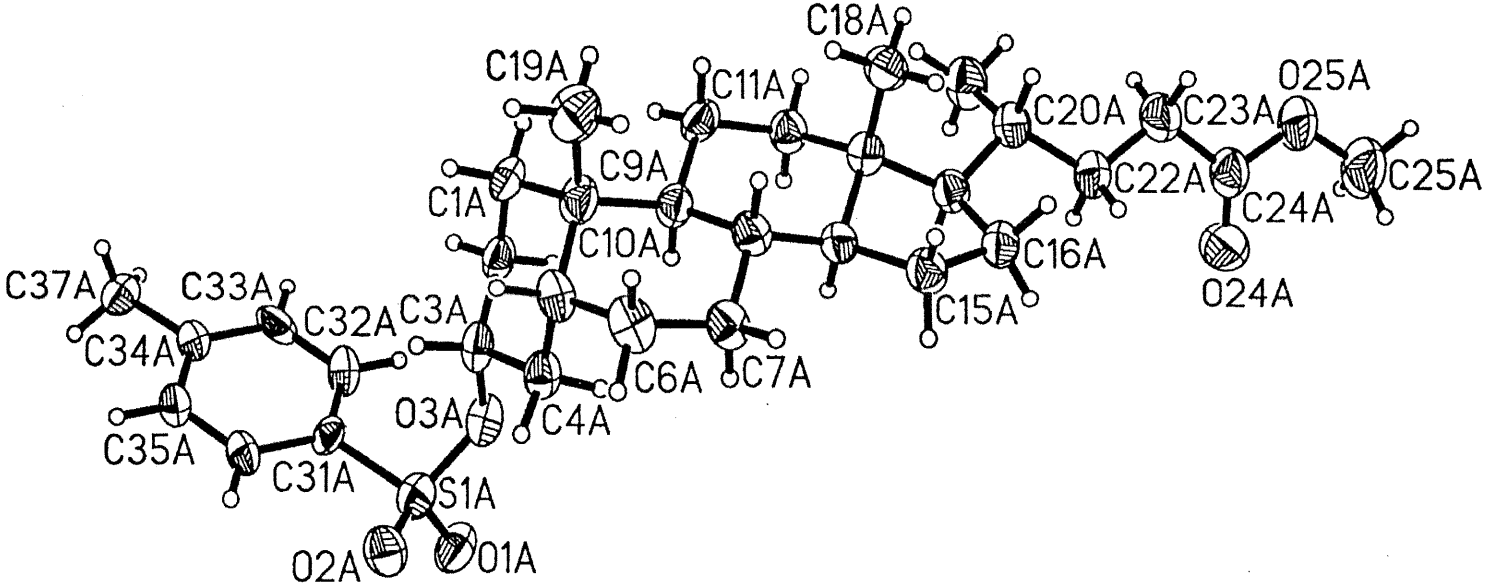

Figure 3.16 ORTEP view of one of the six molecules of $C_{32}H_{48}O_5S$ **(11)** in the asymmetric unit, and with the numbering scheme adopted. Ellipsoids drawn at 30% probability level. The hydrogen atoms are represented by sphere of arbitrary size.

Table 3.4 Comparison of the bond distances, Å, in the six independent molecules of lithocholic acid tosylate (monomer **11**)

Distance	A	B	C	D	E	F
O24-C24	1.166(7)	1.188(8)	1.187(8)	1.170(8)	1.191(7)	1.179(8)
O25-C24	1.328(6)	1.326(7)	1.313(7)	1.317(7)	1.311(7)	1.330(7)
O25-C25	1.434(8)	1.432(8)	1.429(8)	1.446(9)	1.439(9)	1.449(9)
C1-C2	1.528(7)	1.505(9)	1.490(6)	1.515(8)	1.501(7)	1.517(6)
C1-C10	1.532(7)	1.526(7)	1.524(7)	1.549(7)	1.527(6)	1.539(7)
C2-C3	1.505(6)	1.514(9)	1.521(6)	1.498(8)	1.489(8)	1.494(9)
C3-O3	1.469(8)	1.489(10)	1.455(8)	1.456(10)	1.462(10)	1.454(9)
C3-O3	1.482(10)	1.458(10)	1.463(11)	1.505(10)	1.475(10)	1.486(9)
C3-C4	1.500(5)	1.455(8)	1.500(6)	1.486(8)	1.503(8)	1.485(8)
C4-C5	1.521(6)	1.529(6)	1.536(6)	1.530(6)	1.511(8)	1.536(7)
C5-C6	1.536(6)	1.515(7)	1.515(7)	1.529(7)	1.521(7)	1.527(8)
C5-C10	1.545(7)	1.537(7)	1.542(7)	1.546(6)	1.549(7)	1.539(7)
C6-C7	1.512(6)	1.519(7)	1.523(7)	1.520(7)	1.527(7)	1.514(7)
C7-C8	1.514(6)	1.506(6)	1.515(6)	1.525(6)	1.526(7)	1.515(7)
C8-C9	1.554(6)	1.541(6)	1.543(6)	1.537(6)	1.543(6)	1.546(6)
C8-C14	1.511(6)	1.513(6)	1.511(6)	1.527(6)	1.528(6)	1.521(6)
C9-C10	1.552(5)	1.554(6)	1.571(6)	1.562(6)	1.554(6)	1.561(6)
C9-C11	1.532(6)	1.530(6)	1.527(6)	1.546(6)	1.542(6)	1.527(7)
C10-C19	1.556(7)	1.545(7)	1.552(7)	1.525(7)	1.526(7)	1.536(6)
C11-C12	1.522(6)	1.520(7)	1.536(7)	1.536(7)	1.531(7)	1.520(7)
C12-C13	1.558(5)	1.524(6)	1.535(6)	1.544(6)	1.516(6)	1.530(6)
C13-C14	1.555(6)	1.541(6)	1.561(6)	1.543(6)	1.560(6)	1.541(6)
C13-C17	1.564(6)	1.557(6)	1.546(6)	1.557(6)	1.547(6)	1.560(6)
C13-C18	1.518(6)	1.555(6)	1.544(6)	1.518(6)	1.537(6)	1.546(6)
C14-C15	1.518(6)	1.527(6)	1.528(6)	1.511(6)	1.509(6)	1.516(6)
C15-C16	1.533(6)	1.546(7)	1.558(7)	1.532(7)	1.529(8)	1.562(7)
C16-C17	1.549(6)	1.526(7)	1.531(7)	1.546(7)	1.543(7)	1.548(7)
C17-C20	1.547(6)	1.542(6)	1.543(6)	1.545(6)	1.529(7)	1.548(6)
C20-C21	1.504(7)	1.503(8)	1.502(8)	1.504(7)	1.522(8)	1.493(8)
C20-C22	1.518(6)	1.527(7)	1.532(7)	1.527(7)	1.528(7)	1.526(8)
C22-C23	1.509(7)	1.533(7)	1.520(7)	1.506(7)	1.516(7)	1.529(7)
C23-C24	1.529(7)	1.491(8)	1.500(8)	1.511(8)	1.500(8)	1.507(9)
S1-O1	1.423(11)	1.483(8)	1.463(10)	1.427(8)	1.431(7)	1.438(9)
S1-O1	1.435(9)	1.433(8)	1.437(5)	1.434(7)	1.439(7)	1.455(9)
S1-O2	1.426(8)	1.415(6)	1.413(7)	1.433(9)	1.407(8)	1.415(7)
S1-O2	1.412(10)	1.435(6)	1.380(11)	1.423(11)	1.451(8)	1.435(7)
S1-O3	1.556(8)	1.610(9)	1.581(7)	1.600(9)	1.613(10)	1.550(9)
S1-O3	1.585(11)	1.616(9)	1.571(10)	1.554(10)	1.606(9)	1.598(9)
S1-C31	1.738(9)	1.745(6)	1.759(8)	1.746(7)	1.767(5)	1.754(5)
S1-C31	1.741(7)	1.808(6)	1.772(5)	1.740(6)	1.758(5)	1.748(6)

Table 3.5 Comparison of the bond angles, degree, in the six independent molecules of lithocholic acid tosylate (monomer **11**)

Bond angle	A	B	C	D	E	F
C(24)-O(25)-C(25)	114.9(6)	116.1(6)	116.7(7)	116.3(6)	115.6(6)	115.6(6)
O(24)-C(24)-C(23)	127.2(5)	125.0(6)	126.1(6)	125.9(6)	125.4(6)	126.9(6)
C(22)-C(23)-C(24)	111.9(5)	114.3(5)	114.1(6)	112.7(5)	113.1(5)	113.2(6)
C(21)-C(20)-C(22)	109.8(5)	109.8(5)	109.7(5)	109.7(5)	108.5(5)	109.8(6)
C(20)-C(17)-C(13)	120.0(4)	119.7(4)	119.2(4)	120.5(4)	119.9(4)	118.2(4)
C(22)-C(20)-C(17)	110.1(4)	109.5(4)	109.7(4)	109.5(5)	109.5(5)	109.8(4)
O(25)-C(24)-C(23)	110.0(5)	111.9(6)	113.7(6)	110.3(6)	111.3(6)	111.8(6)
O(24)-C(24)-O(25)	122.8(6)	123.0(6)	120.2(7)	123.7(6)	123.2(6)	121.3(7)
C(23)-C(22)-C(20)	115.9(5)	113.8(5)	113.9(5)	116.3(5)	116.1(5)	113.9(6)
C(21)-C(20)-C(17)	112.9(4)	113.0(5)	114.9(5)	113.2(4)	113.5(4)	115.0(5)
C(20)-C(17)-C(16)	113.3(3)	111.3(4)	111.8(4)	114.7(4)	112.9(4)	111.4(4)
C(16)-C(17)-C(13)	102.8(4)	104.0(4)	105.0(4)	102.4(4)	103.4(4)	104.5(4)
C(14)-C(15)-C(16)	105.0(4)	103.9(4)	103.6(4)	103.6(4)	104.5(4)	103.5(4)
C(15)-C(16)-C(17)	106.4(4)	107.6(4)	107.2(4)	108.0(4)	107.1(4)	106.2(4)
C(15)-C(14)-C(13)	102.9(3)	103.2(4)	103.6(4)	104.2(4)	103.7(4)	104.1(4)
C(8)-C(14)-C(15)	119.2(4)	119.2(4)	119.4(4)	118.6(4)	118.8(4)	118.3(4)
C(14)-C(13)-C(17)	98.9(3)	101.4(4)	100.6(4)	100.0(3)	99.3(4)	99.8(4)
C(14)-C(13)-C(12)	107.0(3)	106.4(4)	106.2(4)	106.7(3)	106.6(4)	106.4(4)
C(18)-C(13)-C(14)	113.4(4)	111.1(4)	110.8(4)	112.2(4)	110.9(5)	110.6(4)
C(18)-C(13)-C(12)	110.0(4)	111.1(4)	111.5(4)	110.3(4)	110.5(4)	111.9(4)
C(18)-C(13)-C(17)	110.2(4)	109.4(4)	109.8(4)	110.4(4)	110.1(4)	110.6(4)
C(12)-C(13)-C(17)	117.0(4)	117.0(4)	117.2(4)	116.9(4)	118.7(4)	116.7(4)
C(8)-C(14)-C(13)	114.7(4)	115.1(4)	114.5(4)	114.8(3)	114.9(4)	114.3(4)
C(11)-C(12)-C(13)	111.3(4)	111.6(4)	111.6(4)	111.6(4)	112.9(4)	111.9(4)
C(12)-C(11)-C(9)	114.0(4)	114.8(4)	114.5(4)	112.9(4)	113.2(4)	115.1(4)
C(5)-C(10)-C(19)	111.0(5)	107.6(5)	108.9(5)	108.8(5)	109.9(5)	108.2(5)
C(31)-C(32)-C(33)	120.0	120.0	120.0	120.0	120.0	120.0

(Continuation)

Bond angle	A	B	C	D	E	F
C(9)-C(10)-C(19)	109.4(4)	110.4(4)	110.4(4)	111.8(4)	111.1(4)	111.4(4)
C(5)-C(10)-C(9)	109.5(4)	110.7(4)	110.5(4)	110.3(4)	108.6(3)	110.3(4)
C(1)-C(10)-C(19)	106.5(4)	107.7(5)	106.5(5)	107.8(5)	107.2(5)	107.3(4)
C(1)-C(10)-C(9)	111.7(4)	112.1(4)	111.6(4)	111.1(4)	112.2(4)	111.2(4)
C(1)-C(10)-C(5)	108.8(4)	108.1(5)	109.4(4)	106.8(4)	107.7(4)	108.3(4)
C(11)-C(9)-C(18)	111.1(3)	110.9(4)	110.9(4)	111.2(3)	110.7(4)	111.0(4)
C(7)-C(8)-C(9)	110.5(3)	110.9(4)	111.5(4)	110.8(4)	110.4(4)	111.2(4)
C(14)-C(8)-C(7)	111.1(4)	113.1(4)	111.6(4)	111.5(4)	110.7(4)	112.4(4)
C(7)-C(6)-C(5)	112.5(4)	112.5(4)	113.3(4)	113.1(4)	111.6(5)	113.4(5)
C(4)-C(5)-C(10)	112.6(4)	111.5(4)	111.2(4)	112.2(4)	112.7(4)	112.2(5)
C(3)-C(4)-C(5)	113.1(4)	114.5(5)	114.0(4)	112.7(5)	113.1(4)	115.1(5)
C(10)-C(9)-C(8)	112.5(4)	112.4(4)	112.3(4)	112.4(4)	112.4(4)	112.0(4)
C(11)-C(9)-C(10)	115.4(4)	114.8(4)	114.5(4)	114.4(4)	114.3(4)	115.1(4)
C(14)-C(8)-C(9)	109.1(3)	108.4(4)	108.6(4)	108.8(3)	108.7(4)	109.3(4)
C(6)-C(7)-C(8)	113.3(4)	113.2(5)	111.3(5)	113.1(4)	112.4(5)	112.2(5)
C(6)-C(5)-C(10)	110.8(4)	112.7(4)	112.3(4)	111.5(4)	112.9(5)	111.8(4)
C(4)-C(5)-C(6)	111.1(4)	110.7(5)	111.0(5)	108.5(4)	109.5(5)	110.9(5)
C(4)-C(3)-C(2)	112.6(4)	112.9(5)	111.6(4)	111.4(4)	112.3(5)	110.9(5)
O(3)-C(3)-C(2)	108.6(5)	104.8(7)	108.2(5)	107.2(7)	110.0(7)	112.1(7)
O(3)-C(3)-C(4)	106.2(6)	110.1(7)	108.1(5)	103.9(7)	102.0(7)	105.9(7)
C(2)-C(1)-C(10)	112.8(4)	116.0(6)	115.6(4)	114.1(5)	114.1(4)	114.4(4)
C(3)-C(2)-C(1)	111.0(4)	108.2(5)	108.9(4)	109.6(5)	110.7(5)	110.2(5)
O(2)-S(1)-O(1)	116.1(9)	121.1(6)	119.4(5)	121.7(8)	121.9(6)	115.2(6)
O(1)-S(1)-O(3)	103.8(8)	118.3(6)	113.0(5)	108.8(6)	101.9(5)	103.6(7)
O(1)-S(1)-C(31)	109.6(9)	109.3(5)	110.0(5)	111.8(6)	107.3(5)	112.5(6)
C(3)-O(3)-S(1)	125.4(8)	114.9(8)	119.4(7)	121.8(9)	114.4(8)	121.2(9)
C(32)-C(31)-S(1)	119.4(4)	121.0(4)	122.4(4)	121.4(5)	118.9(4)	116.5(4)

Table 3.6 (a) Comparison of the torsion angles (degrees), of the methyl ester terminal, in the six independent molecules of lithocholic acid tosylate (monomer **11**)

	A	B	C	D	E	F	average values
Methyl ester terminal							
C13-C17-C20-C21	-61.8(6)	-54.6(7)	-54.2(8)	-58.8(7)	-59.6(7)	-55.0(8)	-57.3(3.0)
C16-C17-C20-C21	176.4(5)	-176.0(6)	-177.0(6)	178.2(6)	178.2(6)	-175.9(6)	177.0(1.2)
C13-C17-C20-C22	175.1(4)	-177.3(5)	-178.2(5)	178.4(5)	178.8(4)	-179.4(5)	177,9(1.5)
C16-C17-C20-C22	53.3(6)	61.2(6)	58.9(6)	55.4(7)	56.6(6)	59.7(7)	57.5(4.0)
C17-C20-C22-C23	-170.5(5)	-158.3(5)	-157.7(6)	-167.3(6)	-168.5(5)	-156.4(6)	163.1(7.5)
C20-C22-C23-C24	-172.2(5)	-158.5(6)	-160.6(6)	-171.4(6)	-173.1(6)	-160.7(6)	166.1(10.0)
C21-C20-C22-C23	64.6(7)	77.0(7)	75.3(7)	67.9(8)	67.0(7)	76.3(8)	71.3(6.0)
C22-C23-C24-O24	16.4(11)	13.9(12)	14.7(13)	14.9(12)	12.4(11)	10.6(13)	13.8(3.0)
C22-C23-C24-O25-	163.5(6)	-166.8(6)	-166.3(7)	-168.6(7)	-166.3(6)	-169.4(7)	166.8(2.4)
C23-C24-O25-C25	-178.8(7)	-174.6(7)	-175.2(8)	-178.1(8)	-178.1(8)	-174.9(7)	176.6(2.0)
O24-C24-O25-C25	1.3(11)	4.7(12)	3.8(13)	-1.5(13)	3.2(12)	5.2(13)	3.3(2.0)

Lithocholic acid moiety (LA)

The bond distances, bond angles and molecular conformation of the six independent molecules in the unit cell (A, B, C, D, E, F) are all the same within experimental errors. The structure determination confirms that the *para*-toluenesulfonyl group is indeed connected at the C3 position. The molecules consist of a rigid steroid nucleus, a flexible methyl ester tail extending out from C17 of the five-membered ring, while the *para*-toluenesulfonyl group is attached at C3. The fused ring system that makes up the steroid nucleus has methyl groups C18 and C19, at C13 and C10, respectively. These substitutions along with the ring junctions provide torsion barriers. Consequently, it is likely that when the molecules aggregate or pack in a crystal lattice, the entropic considerations will favor the lowest energy steroid structure. That is, for

Table 3.6 (b) Torsion angle in the *para*-toluenesulfonyl terminal (molecule **11**)

Molecule	A		B		C		D		E		F	
Occupancy (%)	57	43	51	49	63	37	52	48	51	49	53	47
C2-C3-O3-S1	-131.6(8)	-134.4(9)	-98.0(9)	-122.6(1)	-95.7(7)	-110.3(11)	-130.4(9)	-112.3(1)	-134.9(8)	-105.8(1)	-115.4(9)	98.4(11)
C4-C3-O3-S1	107.1(9)	104.8(10)	140.3(7)	116.6(10)	143.3(6)	129.8(10)	111.6(9)	127.7(9)	105.8(8)	132.3(11)	123.4(9)	142.2(9)
C3-O3-S1-O1	-177.3(11)	-175.7(1)	29.7(12)	57.3(13)	41.3(10)	54.2(16)	-170.2(9)	171.1(11)	-172.3(9)	170.2(12)	59.6(12)	22.8(14)
C3-O3-S1-O2	-50.0(12)	- 46.1(13)	164.3(9)	-176.5(1)	172.0(6)	177.4(11)	-38.3(13)	-70.8(13)	-34.9(12)	-64.9(14)	179.8(10)	161.6(10)
C3-O3-S1-C31	67.7(10)	65.6(11)	-85.7(9)	-54.9(13)	-76.1(7)	-54.2(14)	73.9(10)	51.8(13)	79.4(9)	47.7(14)	-63.7(12)	-84.9(11)
O1-S1-C31-C32	-62.4 (9)	-46.0(13)	-9.2(6)	17.1(6)	11.9(6)	-14.6(11)	-33.0(7)	-40.5(7)	-28.2(5)	-60.7(6)	-18.2(6)	-9.7(7)
O2-S1-C31-C32	170.3(5)	178.4(7)	-143.1(5)	-116.0(5)	-120.2(5)	-143.4(11)	-170.6(6)	-168.4(7)	-162.8(5)	168.2(6)	-146.2(5)	-147.4(6)
O3-S1-C31-C32	48.4(6)	68.1(8)	113.4(5)	122.6(6)	131.4(5)	94.5(9)	80.6(6)	72.0(8)	75.1(5)	60.6(7)	100.2(6)	100.1(6)
O1-S1-C31-C36	117.6(9)	133.8(13)	169.9(5)	-164.8(6)	-168.8(6)	164.6(10)	146.4(6)	142.3(6)	150.2(5)	116.3(5)	163.9(5)	170.2(6)
O2-S1-C31-C36	-9.7(6)	-1.7(8)	36.1(6)	62.1(6)	59.2(5)	35.9(10)	8.7(7)	14.4(8)	15.6(6)	-14.8(6)	36.0(6)	32.5(7)
O3-S1-C31-C36	-131.1(6)	-112.0(8)	-67.5(5)	-59.4(7)	-49.2(5)	-86.2(9)	-100.0(6)	-105.2(7)	-106.5(5)	-122.4(6)	-77.6(7)	-80.0(6)

three six-membered rings, the lowest energy structures adopt approximate chair conformation; while the five-membered ring is in an approximate envelope conformation.

The methyl ester terminal (ME)

Although the torsional angles of the ME terminal of the six distinct molecules fluctuate significantly as shown in Table 3.6(a), it remains that they all adopt the same conformation. Surprisingly, the largest fluctuations are for the torsion angles around the C17-C20, C20-C22 and C22-C23 bonds. The average conformation is given in the last column of Table 3.6(a). Thus the sequence C13-C17-C20-C22-C23-C24-O25-C25 is nearly in the fully extended conformation, from C13 to C25. The average deviation from $t = trans \sim 180^{\circ}$ is only $\pm 10^{\circ}$.

The para-toluenelsulfonyl terminal (MS)

The *para*-toluenesulfonyl terminal of the molecule is very disordered. For each of the six molecules there is an approximate 50:50 disorder, hence, twelve orientations. The individual torsion angles are compared in Table 3.6(b). Taking into account the quoted standard deviations, the twelve orientations, shown in the Appendix, may be regrouped in two distinct groups whose conformations are illustrated in Figure 3.17.

The A, D and E molecules are similar and they belong to one group. The B, C, F molecules resemble one another; they constitute the other group. Both of them have similarity in that the same torsion angles difference of 180° between O1-S1-C31-C32 and O1-S1-C31-C36, O2-S1-C31-C32 and O2-S1-C31-C36 (170.3-(-9.7) = 180, 117.6-(-62.4) = 180). However, in the part of sulfonyl and lithocholic acid, the torsion angle differences are not same. In A, D and E molecules, the larger torsion angle differences of 157.1° lie in C4-C3-O3-S1 and C3-O3-S1-O2 (107.1- (-50.0) = 157.1); the smaller torsion angle differences of 70.4° lie in C3-O3-S1-O1 and C3-O3-S1-C31 (67.7 + (180-177.3) = 70.4). In B, C, F molecules, the larger torsion angle differences 157.1° lie in C4-C3-O3-S1 and C3-O3-S1-C31 (107.1 + 50.0) = 157.1); the smaller torsion angle differences 123.2° lie in C3-O3-S1-O1 and C3-O3-S1-O2 (177.4-54.2 = 123.2). Although the torsion angle differences are not the same in the six molecules (actually 12

conformations), they try to adopt the most stable conformation by arranging themselves in the $P2_12_12_1$ orthorhombic space group.

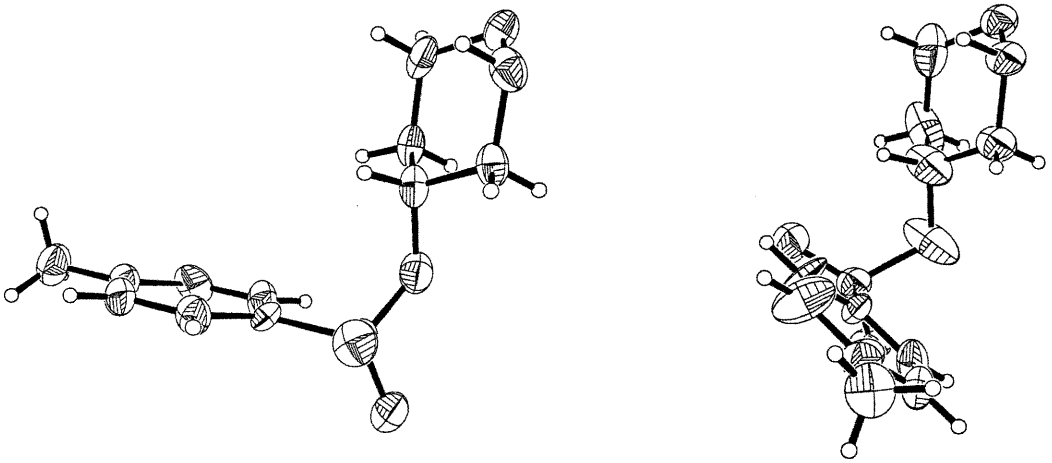

Figure 3.17 The two distinct groups of conformations in the six molecules of compound **11**.

3.3.1.2 Structural organization of the molecules

The packing of the molecules, shown in Figures 3.18 and 3.19, has a number of interesting characteristics. Although the molecules in the unit cell have important conformational fluctuations, the rigid lithocholic acid moieties (LA) are nearly parallel to one another and inclined by 30° with respect to the *bc*-face of the unit cell. They constitute layers parallel to the *ab*-face. This disposition of the molecules resembles that of the liquid crystal phase of the smectic Sc-type.

The methyl ester groups (ME) are located between two consecutive layers while the *para*-methylphenylsulfonyl terminals (MS) occupy the space between the next layers and so on. Four such layers are observed in the unit cell, perpendicular to the *c*-axis. The packing sequence along the *c*-direction is: ME-LA-MS MS-LA-ME ME-LA-MS MS-LA-ME, etc.

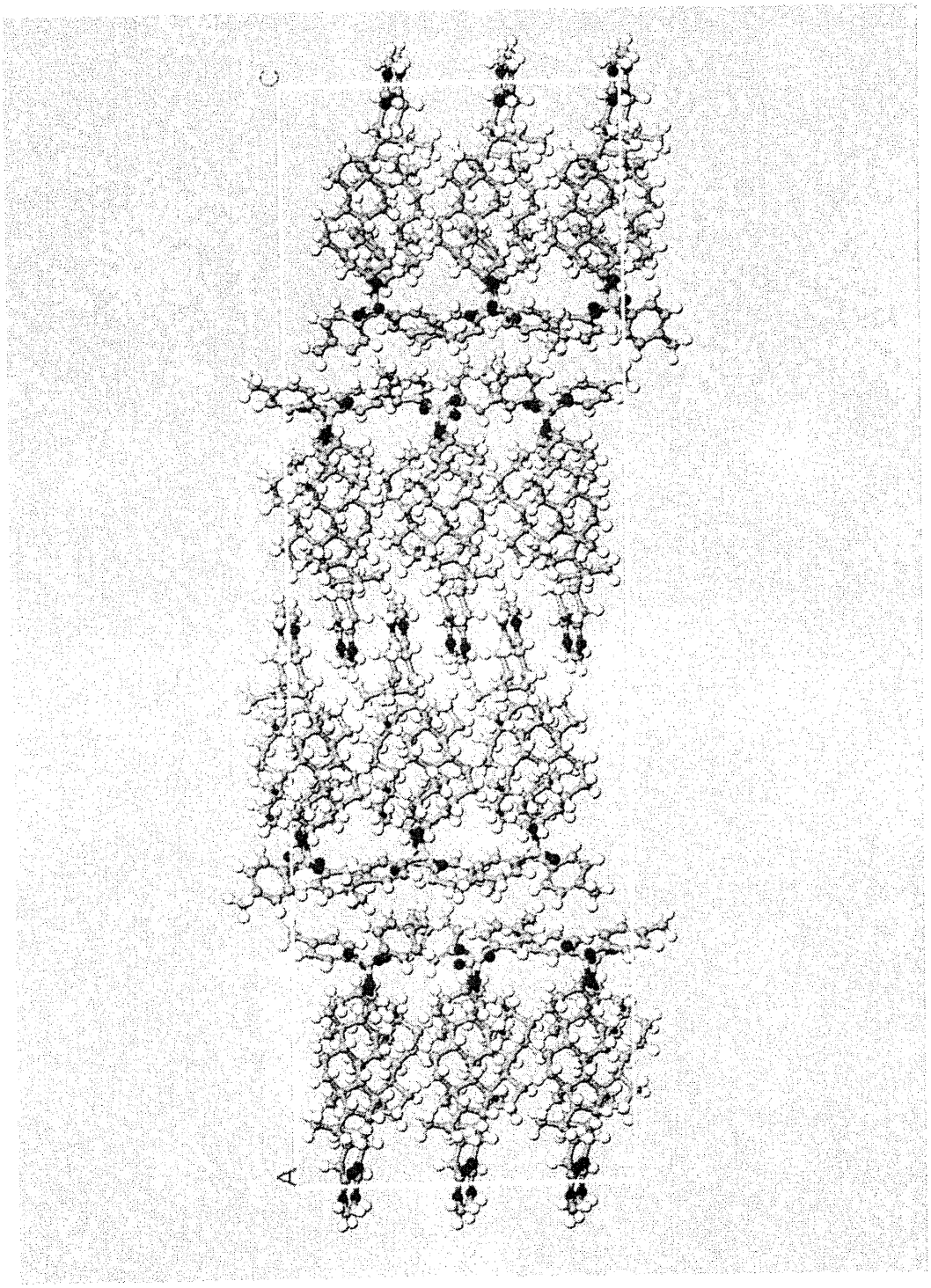

Figure 3. 18 Packing of the substituted lithocholic acid molecules **11** projected on the *bc*-plane. The *c*-axis is vertical while the *b*-axis goes from left to right. The four layers of molecules are clearly visible.

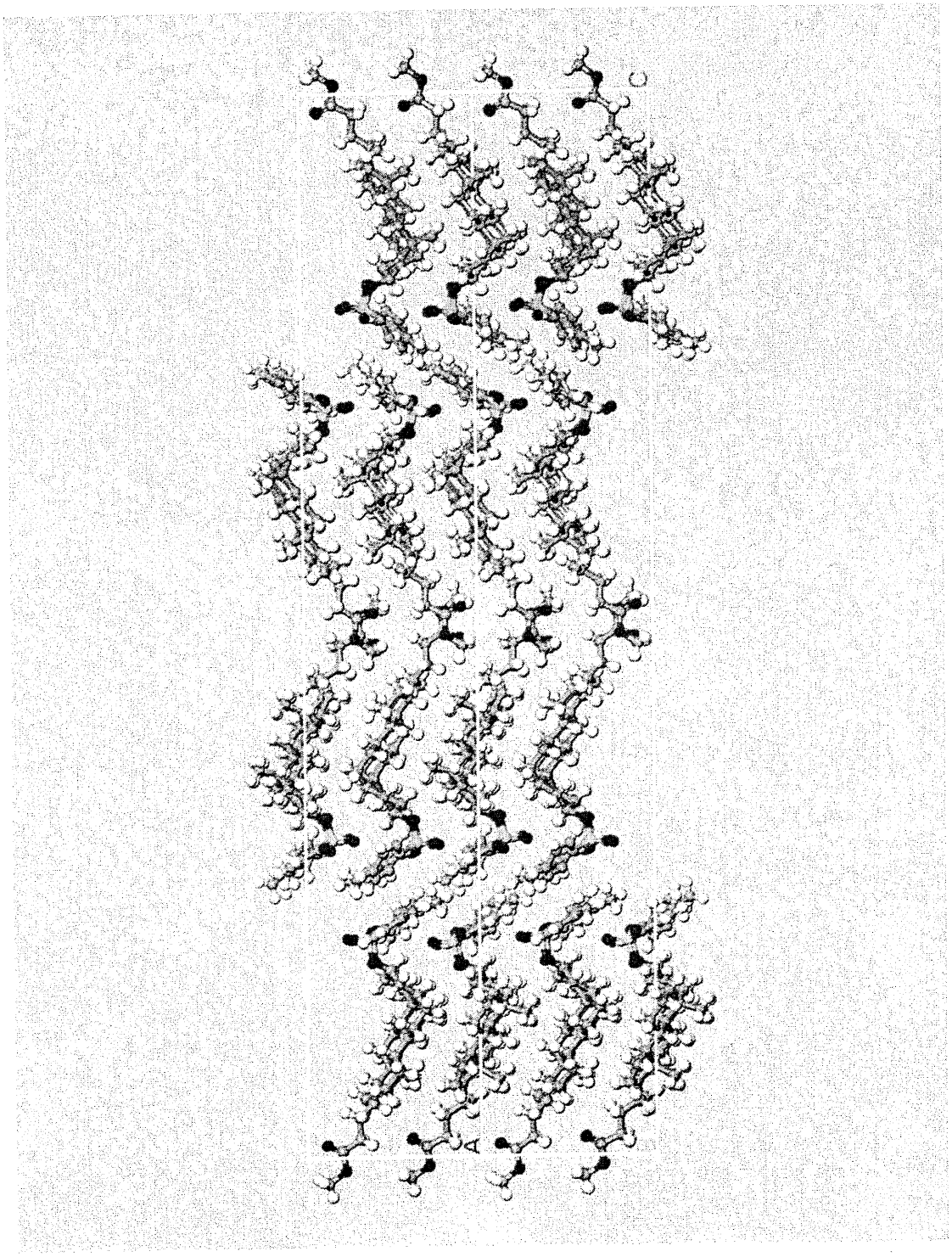

Figure 3.19 Packing of the substituted lithocholic acid molecules **11** projected on the *ac*-plane. The *c*-axis is vertical while the *a*-axis goes from left to right. Two unit cells are shown side by side

3.3.2 Methacrylyoyloxy-hexyloxy-3α,7α,12α-trihydroxy-5β-cholan-24- ate. H_2O (26)

3.3.2.1 Description of the structure

The crystal structure determination reveals the presence of a water molecule as part of the structure. The experimental density is in agreement with the presence of one water molecule per cholic acid derivative. This water is H-bonded to O1 and O7. The characteristics of the hydrogen bond are given in Table 3.8.

The bond distances, bond angles and torsion angles are listed in Tables 3.7, 3.9 and 3.10 respectively. The structure determination indicates that there is only one independent molecule in the monoclinic unit cell. The bond distances and angles are similar to those in the tosylate of lithocholic acid methyl ester **11**. However, there is a 53:47 disorder at the end of the long terminal, from C31 to C35. The aliphatic segment from C23 to C32 does not adopt the fully extended conformation (i.e., not all-*trans*). The sequence of torsion angles is schematically described as $t\ t\ g\ t\ t\ t\ g\ t\ g^-$, where t = *trans* ~ 180°, g = *gauche* ~ 60° and g^- = *gauche*$^-$ ~ - 60°. The average deviation from t, g or g^- is ± 5° for the torsion angles from C13 to C30. The deviations are much larger, up to ± 24°, in the disordered group of atoms.

The structure of molecule **26** is shown in Figure 3.20 A, B and C. The B and C show the disorder in the C24-C34 segments. The cholic acid skeleton is the same as in **11**, although the end of the flexible spacer part is disordered. The bond angles and torsion angles also reveals that there are many nearly coplanar groups of atoms in the molecule such as C3-C4-C5-C6, C1-C2-C3-O3 and C7-C8-C14-C13 atoms. However, as for molecule **11**, the whole molecule is not planar. The three six-membered rings are in the chair conformation, while the five-membered ring adopts an approximate envelope conformation.

3.3.2.2 Structural organization of the molecules

The monoclinic unit cell of **26** contains only 2 molecules crystallographically related by a 2_1 helicoidal axis. The disposition of the molecules in the unit cell is shown

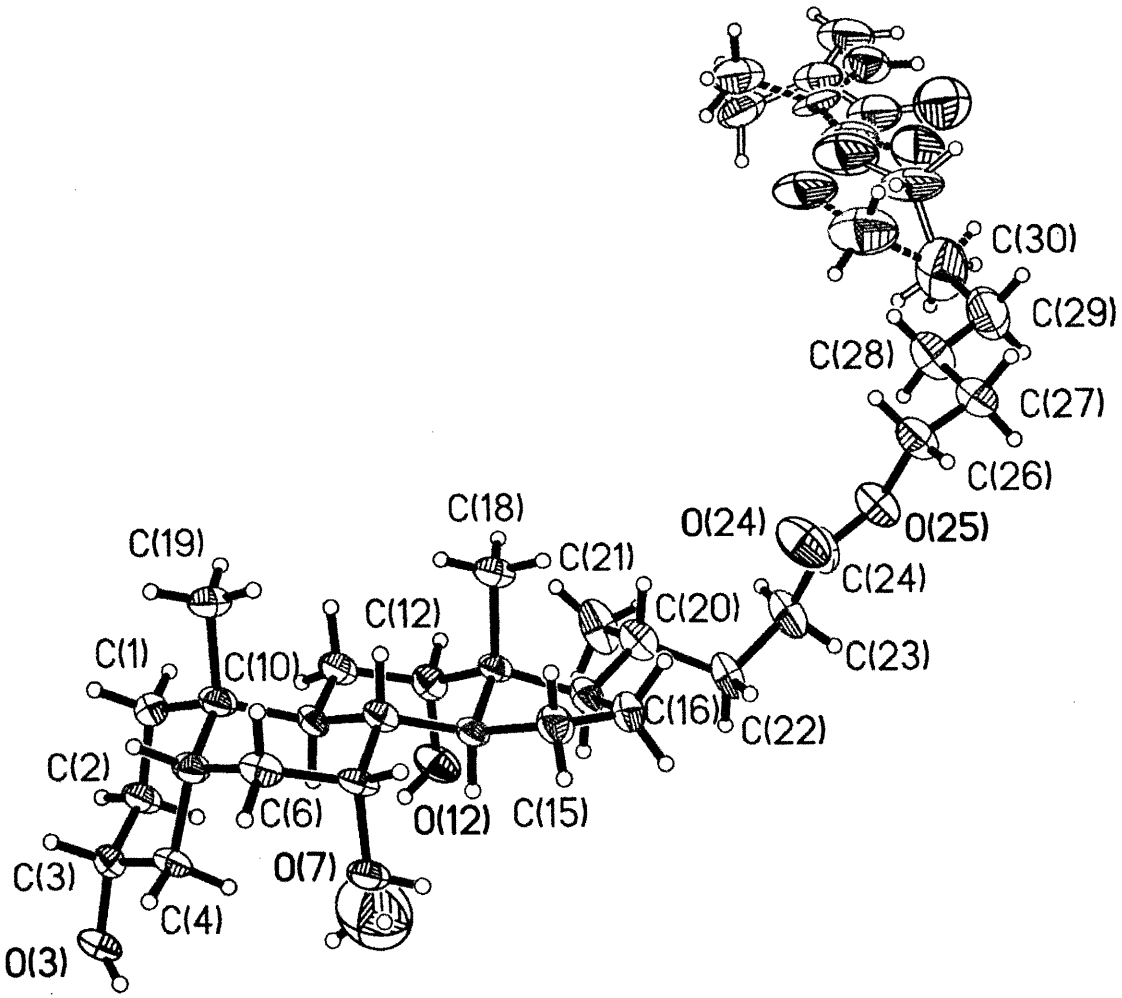

Figure 3.20 (A) An ORTEP view of molecule $C_{34}H_{56}O_7.H_2O$ (**26**) including the atomic numbering. Elipsoids are drawn at 30% probability. The A drawing contains both orientations of the flexible groups from C30-C34. They are illustrated separately in B and C.

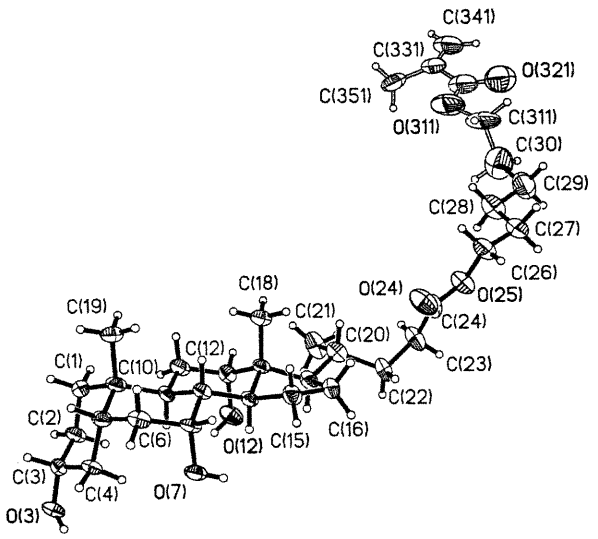

Figure 3.20 (B) Some selected structural configuration of monomer **26** showing the disorder in the C24-C34 segments.

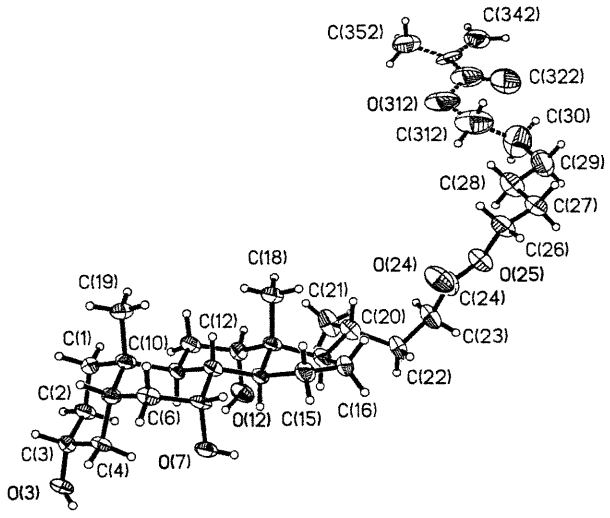

Figure 3.20 (C) Some selected structural configuration of monomer **26** showing the disorder in the C24-C34 segments.

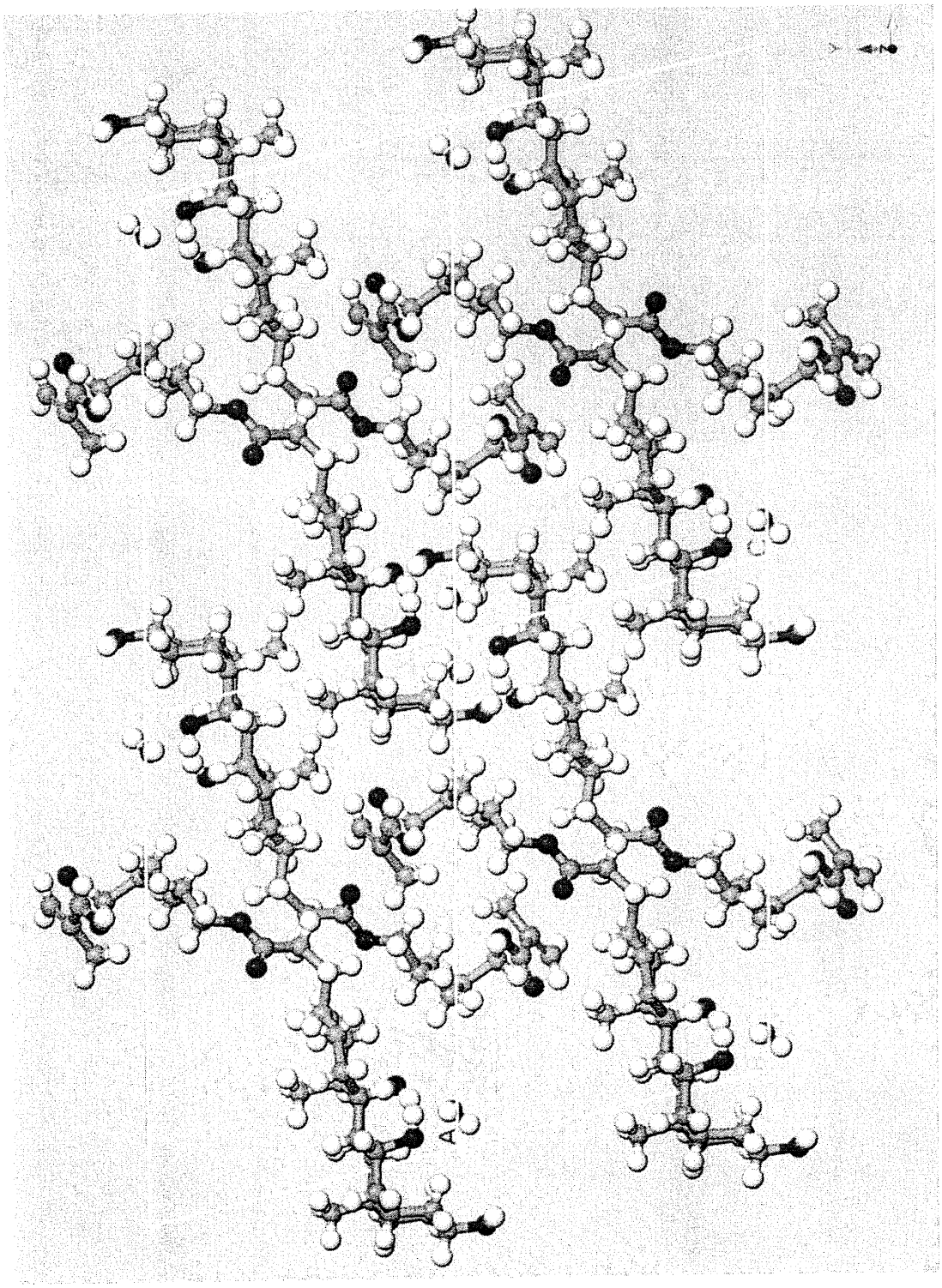

Figure 3.21 (a) Disposition of the cholic acid derivative **26** in its monoclinic unit cell (*ac* projection).

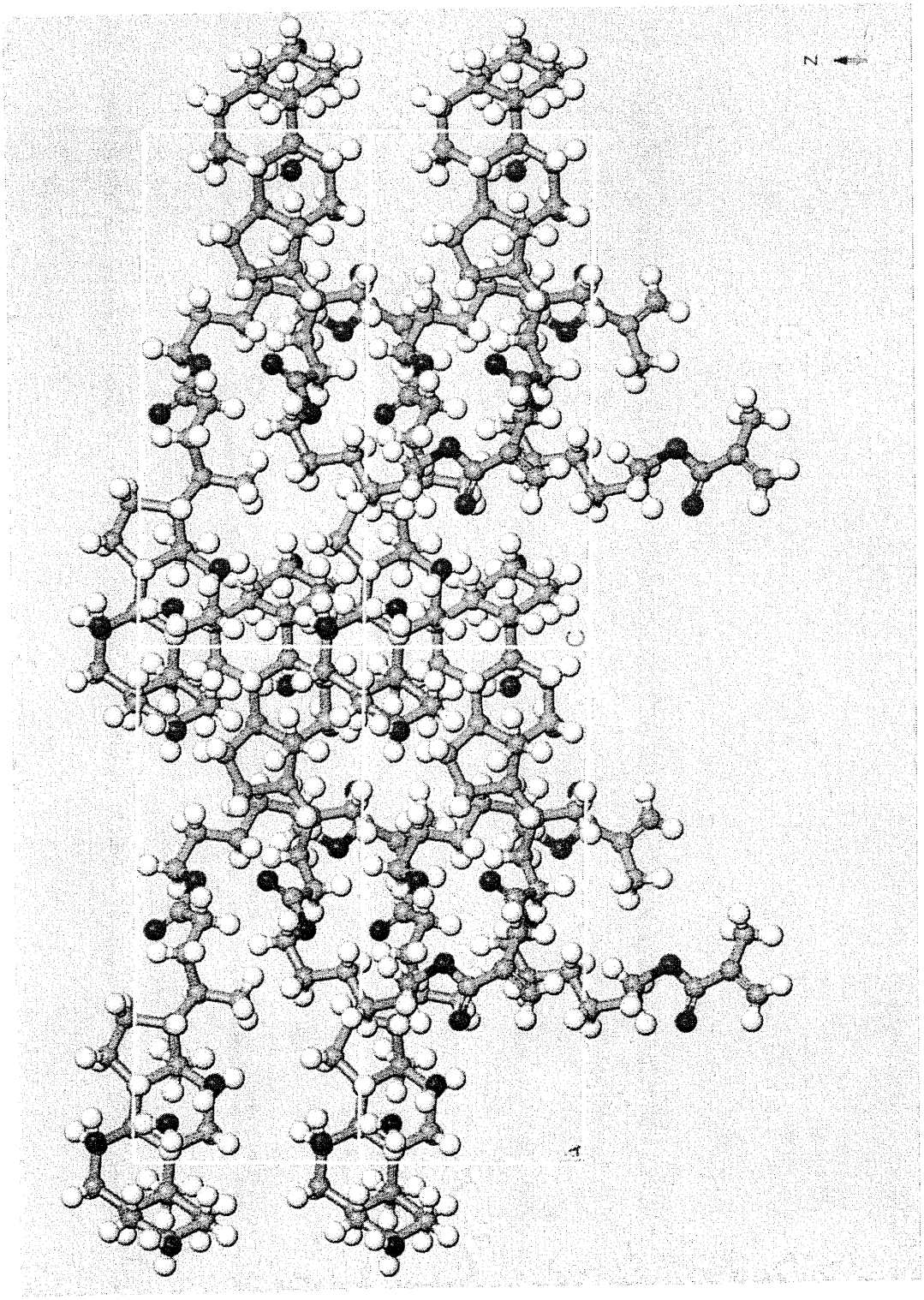

Figure 3.21 (b) Disposition of the cholic acid derivative **26** in its monoclinic unit cell. (*bc* projection)

Table 3.7 Selected bond distances, Å, in the molecule of monomer **26**

O3-C3	1.433(7)	C20-C21	1.499(12)
O7-C7	1.444(7)	C20-C22	1.541(11)
O12-C12	1.443(8)	C22-C23	1.524(11)
C1-C2	1.497(9)	C23-C24	1.516(13)
C1-C10	1.550(11)	C24-O24	1.157(11)
C2-C3	1.547(10)	C24-O25	1.337(9)
C3-C4	1.484(10)	O25-C26	1.483(11)
C4-C5	1.543(9)	C26-C27	1.535(8)
C5-C10	1.549(11)	C27-C28	1.537(8)
C5-C6	1.552(11)	C28-C29	1.535(8)
C6-C7	1.507(11)	C29-C30	1.556(9)
C7-C8	1.549(10)	C30-C311	1.548(10)
C8-C14	1.502(9)	C30-C312	1.516(13)
C8-C9	1.560(9)	C311-O311	1.496(10)
C9-C11	1.487(10)	O311-C321	1.334(9)
C9-C10	1.554(9)	C321-O321	1.216(8)
C10-C19	1.563(9)	C321-C331	1.459(8)
C11-C12	1.544(10)	C331-C341	1.384(9)
C12-C13	1.492(11)	C331-C351	1.478(9)
C13-C18	1.538(8)	C312-O312	1.488(10)
C13-C17	1.544(9)	O312-C322	1.345(9)
C13-C14	1.589(10)	C322-O322	1.221(9)
C14-C15	1.539(10)	C322-C332	1.457(9)
C15-C16	1.493(11)	C332-C342	1.389(9)
C16-C17	1.613(12)	C332-C352	1.481(9)

Table 3. 8 Hydrogen-bonding geometry (Å,°) in the molecule of monomer **26**

D—H···O	D—H	H···A	D···A	D—H···A
O3—H3···O12 [i]	0.82	2.02	2.828(7)	166
O12—H12···O3 [i]	0.82	2.03	2.773(7)	150
O12—H12···O1	0.82	2.02	2.771(11)	153
O1—H1C···O7	0.82	2.35	3.067(15)	147
O1—H1D···O7 [ii]	0.82	2.11	2.864(13)	153

Symmetry codes: (i) $2-x, \frac{1}{2}+y, 2\ z$; (ii) $2\ x, y-\frac{1}{2}, 2-z$

Table 3. 9 Selected bond angles, degree, in the molecule of monomer **26**

C2-C1-C10	113.7(6)	C15-C14-C13	102.0(5)
C1-C2-C3	108.8(6)	C16-C15-C14	106.1(7)
O3-C3-C4	112.4(6)	C15-C16-C17	107.7(6)
C4-C3-C2	107.7(6)	C20-C17-C13	120.1(7)
C3-C4-C5	113.5(6)	C13-C17-C16	101.7(6)
C4-C5-C10	112.7(6)	C21-C20-C17	112.2(7)
C4-C5-C6	112.2(6)	C21-C20-C22	111.6(6)
C7-C6-C5	115.1(6)	C23-C22-C20	115.0(8)
O7-C7-C6	108.6(5)	C24-C23-C22	112.7(8)
O7-C7-C8	110.8(6)	O24-C24-O25	124.8(10)
C6-C7-C8	111.2(6)	O24-C24-C23	125.9(9)
C14-C8-C7	111.3(6)	O25-C24-C23	109.3(8)
C7-C8-C9	110.9(5)	O25-C26-C27	105.1(7)
C11-C9-C10	113.4(6)	C26-C27-C28	112.8(8)
C10-C9-C8	112.0(6)	C28-C29-C30	112.5(7)
C5-C10-C1	108.2(5)	C311-C30-C29	114.0(10)
C5-C10-C9	109.0(6)	C29-C30-C312	111.5(8)
C1-C10-C9	113.4(6)	O311-C311-C30	116.3(14)
C5-C10-C19	110.7(6)	C321-O311-C311	109.8(12)
C1-C10-C19	105.0(6)	O321-C321-O311	119.5(12)
C9-C10-C19	110.5(5)	O321-C321-C331	124.3(12)
C9-C11-C12	114.3(6)	O311-C321-C331	115.7(11)
O12-C12-C13	112.5(6)	C341-C331-C321	116.6(12)
O12-C12-C11	110.2(6)	C341-C331-C351	119.5(13)
C13-C12-C11	112.8(6)	C321-C331-C351	119.0(11)
C12-C13-C18	110.1(6)	O312-C312-C30	125.2(15)
C12-C13-C17	117.8(6)	C322-O312-C312	103.2(11)
C18-C13-C14	111.2(6)	O312-C322-C332	119.4(12)
C17-C13-C14	101.3(5)	C342-C332-C352	119.2(12)

Table 3.10 Selected torsion angles, degree, in the molecule of monomer **26**

C10-C1-C2-C3	60.4(8)	C1-C2-C3-O3	178.5(5)
C1-C2-C3-C4	-58.4(7)	O3-C3-C4-C5	175.5(6)
C2-C3-C4-C5	55.2(8)	C3-C4-C5-C10	-52.1(8)
C5-C6-C7-C8	50.9(7)	O7-C7-C8-C14	-56.0(7)
C11-C9-C10-C19	-63.9(8)	O25-C26-C27-C28	65.4(1)
C8-C9-C10-C19	64.5(8)	C26-C27-C28-C29	77.2(9)
C9-C11-C12-O12	72.0(8)	C27-C28-C29-C30	-175.2(1)
C9-C11-C12-C13	-54.7(8)	C28-C29-C30-C311	82.6(2)
O12-C12-C13-C18	170.1(6)	C28-C29-C30-C312	36(2)
C11-C12-C13-C18	-64.3(8)	C29-C30-C311-O311	-158.3(1)
O12-C12-C13-C17	43.8(9)	C312-C30-C311-O311	-61.9(2)
C11-C12-C13-C17	169.3(6)	C30-C311-O311-C321	-93(2)
O12-C12-C13-C14	-69.1(7)	C311-O311-C321-O321	-3(3)
C11-C12-C13-C14	56.4(7)	C311-O311-C321-C331	-175.8(2)
C7-C8-C14-C15	-59.6(8)	O321-C321-C331-C341	7(4)
C9-C8-C14-C15	176.2(6)	O311-C321-C331-C341	179(2)
C7-C8-C14-C13	179.7(5)	O321-C321-C331-C351	163(3)
C17-C13-C14-C8	176.9(5)	O311-C321-C331-C351	-25(3)
C12-C13-C17-C20	78.9(8)	C311-C30-C312-O312	81(2)
C18-C13-C17-C20	-47.8(9)	C29-C30-C312-O312	-176(2)
C15-C16-C17-C20	149.6(7)	C30-C312-O312-C322	-49(3)
C13-C17-C20-C21	-58.2(10)	C312-O312-C322-O322	7(4)
C16-C17-C20-C21	-178.7(8)	C312-O312-C322-C332	169(2)
C13-C17-C20-C22	175.7(6)	O322-C322-C332-C342	-11(4)
C16-C17-C20-C22	55.3(9)	O312-C322-C332-C342	-170(3)
C21-C20-C22-C23	68.5(10)	O322-C322-C332-C352	-162(3)
C17-C20-C22-C23	-165.1(7)	O312-C322-C332-C352	39(4)
C20-C22-C23-C24	78.3(10)	C22-C23-C24-O24	-1.8(2)
C22-C23-C24-O25	175.9(8)	O24-C24-O25-C26	-1.1(2)
C23-C24-O25-C26	-178.8(8)	C24-O25-C26-C27	178.7(8)

in the *ac* and *bc*-projections of Figure 3.21. The crystal structure is stabilized by intermolecular hydrogen bonds of the O—H···O type (Table 3.8). The hydrogen bonding involves the O3, O7 and O12 hydroxyl groups as well as the water molecules.

Two molecules of **26** and two water molecules are held by many hydrogen bonds. The flexible spacer and methacrylate group extend out. The small molecules of water can be seen near the hydroxyl group at position 7 in the *ac*-projection. There are six hydrogen bonds (O—H···O). The hydroxyl groups at positions 3 and 12 act as donors towards the hydroxyl groups at positions 12 and 3 respectively of another molecule. The other four hydrogen bonds involve the water molecule. Two of them are formed between the hydroxyl group at position 7 as donor and the water molecule as acceptor. The other two hydrogen bonds are formed between the water molecule as donors and the hydroxyl group at position 7 as acceptor. All of the hydrogen bonds are moderately bent. The O12—H12 and O3—H3 of two symmetrically related molecules form two pairs of hydrogen bonds: O12—H12···O3 and O3—H3···O12, where O3 and O12 are both acceptors and donors. The hydrogen bond scheme is shown as Figure 3. 22.

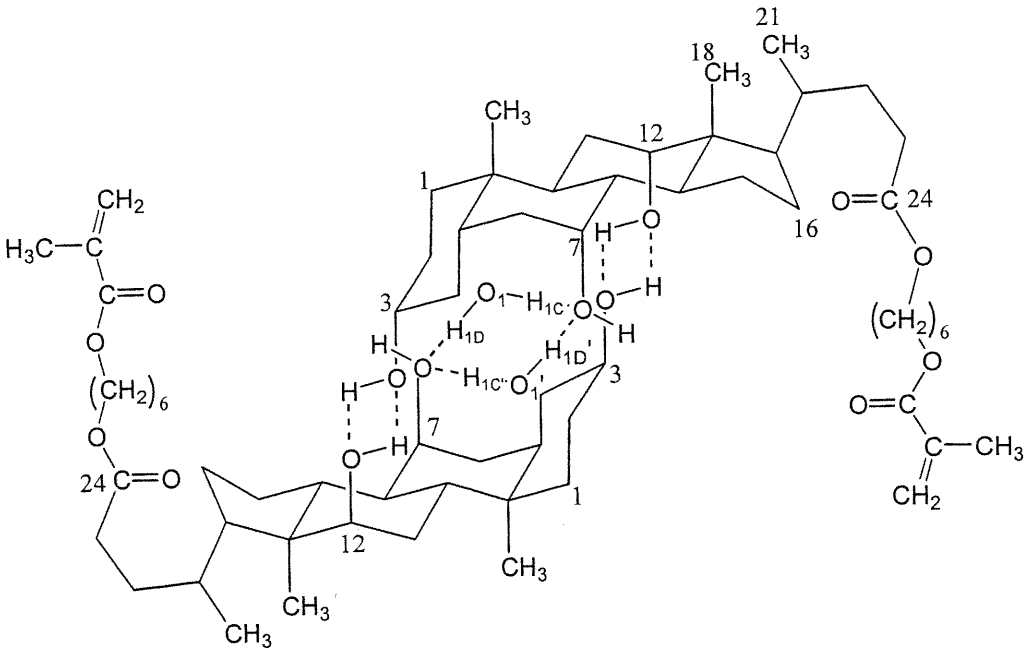

Figure 3.22 The hydrogen bond scheme in the crystal structure of molecule **26**

There is no ordered layer organization as in the crystal of molecule **11**. The rigid frameworks of cholic acid fused-ring aggregate together.

3.4 Physical properties of the polymers

3.4.1 Molecular weight of polymers

The molecular weight and the polydispersity are important variables which can affect both the liquid-crystalline behavior and phase morphology of side chain LC polymers. The average molecular weight of all homopolymers and copolymers was analyzed by SEC, and the results are listed in Tables 2.4, 2.5 and 2.6.

The number-average molecular weight of polymers ranged approximately from 5000 to 9000. Since the monomer's molecular weight is above 500, we can say the degree of polymerization is not very high. It is just about 10-18 repeat units. In the polymerization reaction of this thesis, the amount of initiator AIBN is 3% mole of monomer. The proportion amount of AIBN is the same as the previous experiments [60, 83].

The degree of polymerization[84] $\overline{DP}_{n,o}$ is given by the relation:

$$\overline{DP}_{n,o} = f_t \frac{k_p\left(2k_d/k_t\right)^{1/2}[A]^{1/2}[M]}{2k_d[A]} \qquad (3.1)$$

that is $$\overline{DP}_{n,o} \propto \frac{[M]}{[A]^{1/2}} \qquad (3.2)$$

and polymerization rate $$V_P \propto [A]^{1/2}[M] \qquad (3.3)$$

Here, $f_t = 1$ if the reaction is terminated only by a dismutation reaction.

$f_t = 2$ if the reaction is terminated only by a combination reaction

k_p is the propagation rate constant,

k_d is the initiator decomposition rate constant,

k_t is termination rate constant, [A] is the concentration of the initiator, [M] is the concentration of the monomer.

It is concluded from the above formula that in order to obtain long polymer chains, that is high molecular weight polymer, the condition of [A] << [M] should be fulfilled. Consequently, the proportion of AIBN should be lowered to increase the molecular weight. However, in this condition the polymerization rate will be slower.

Although we could decrease the amount of AIBN to increase the molecular weight, the methacrylate polymers' molecular weight does not increase significantly[48] by standard radical polymerization when the monomers have long spacers and bulky structures. Furthermore, it is observed that the molecular weight decreases as the spacer length increases. For example, when the spacer length n increases from 2 to 6, the molecular weight of a polymethacrylate decreases from 12700 to 7600[85]. It is reported [48] that the molecular weight is not very high (M_n: 13000) when monomer has longer spacers even when using anionic polymerization, although the polydispersity is narrow (1.05). In my case, the polydispersity of the polymers is broader. The polydispersity distributes broadly from 1.37 to 2.24.

From the above result, the equation of (3.2) seems that it can not hold exactly. That is because this equation is applied much better to small molecules than big monomers which have much lower reactivity and limited flexibility due to the bulky cholic acid structure. The lower reactivity makes these big molecules difficult to polymerize into long chain polymer. Generally speaking, this equation can tell us some information about the molecular weight of polymer qualitatively, but not quantitatively precisely.

Moreover, the lower reactivity of big molecules also caused a longer polymerization time. 60 hours were required to make sure all double bonds polymerized for both homopolymers and copolymers due to the slow kinetics of the propagating substituted methacrylate main chain[83, 86]. The presence of a spacer, especially with increased spacer length, leads to further reduction of the reactivity of the methacrylate monomer of bile acid derivatives.

Although the molecular weight of the polymers is relatively low, their properties differ from those of the monomers. For example, the polymers cannot be dissolved in many organic solvents which can dissolve monomers such as methanol, ethyl acetate, chloroform etc. They can only be dissolved in THF and DMF. Another important change is the appearance of glass transition temperature T_g of polymers. The T_g of polymers and other thermal properties of all polymers will be discussed later.

3.4.2 Glass transition temperature

3.4.2.1 Homopolymers

The glass transition temperatures, T_g, were obtained by DSC from a second heating at a 10 °C / min rate. The T_g for every polymer was measured three times. Every time the T_g has a small difference due to the slightly different M_w of the sample. The average values of T_g are listed in Table 3.11, 3.12 and 3.13. Once the series of homopolymers DSC trace plots are shown in Figure 3.23.

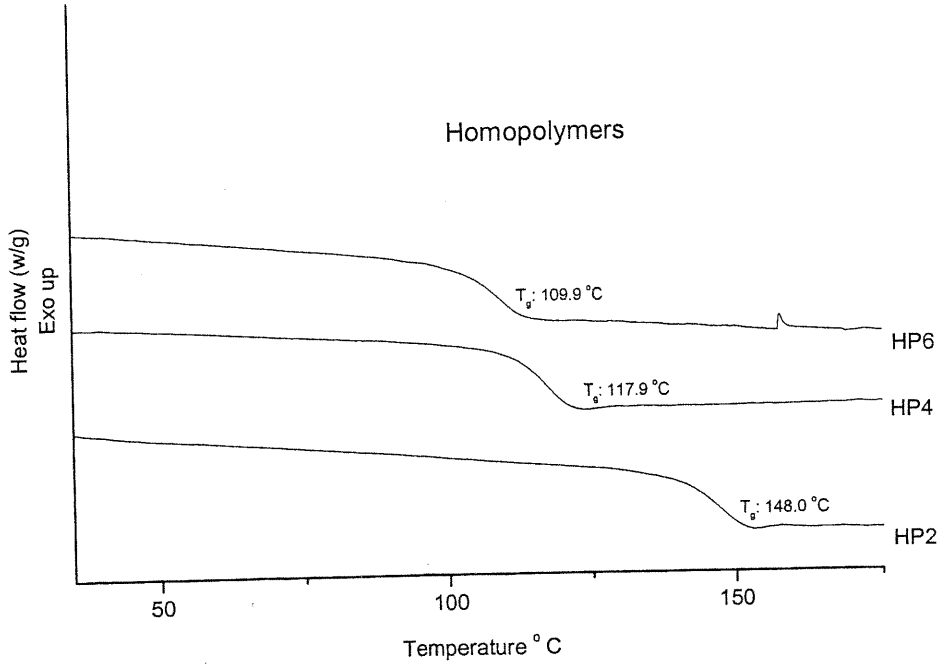

Figure 3.23 The DSC traces of homopolymers showing different T_g's

The variation of T_g as a function of spacer length is shown in Figure 3.24. Examination of the Figure 3.23 clearly reveals the strong influence of the spacer length on the glass transition of temperature, T_g, of the homopolymers. The T_g of these homopolymers is 148.6 ± 0.6 °C, 117.3 ± 0.6 °C and 108.2 ± 1.8 °C respectively for HP2, HP4 and HP6. The error was obtained by selecting the greatest error value in the three times. The glass transition temperature decreases with increasing spacer chain length as shown in Figure 3.24. A similar behavior was observed for the mesogenic polystyrene containing cyanobiphenyl[87- 90] and other mesogenic groups.[91, 92] The T_g decreased rapidly when spacer length changed from n = 2 to n = 4. When the spacer length changed from n = 4 to n = 6, the T_g did not decrease as much.

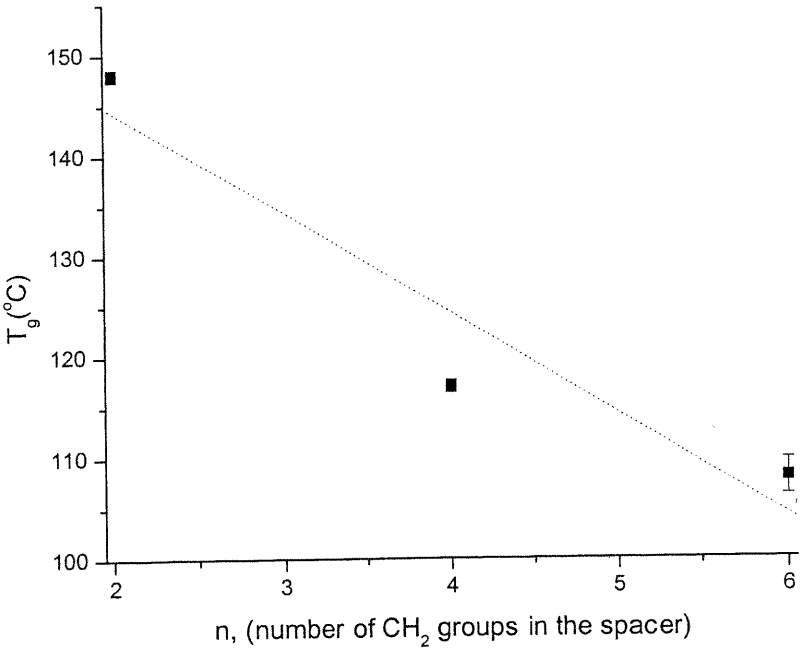

Figure 3.24 Variation of T_g of the homopolymers as a function of the spacer length

3.4.2.2 Copolymers

The glass transition temperatures of the copolymers were also established by DSC. The traces are shown in Figures 3.25, 3.26 and 3.27 for the CP24, CP26 and CP46

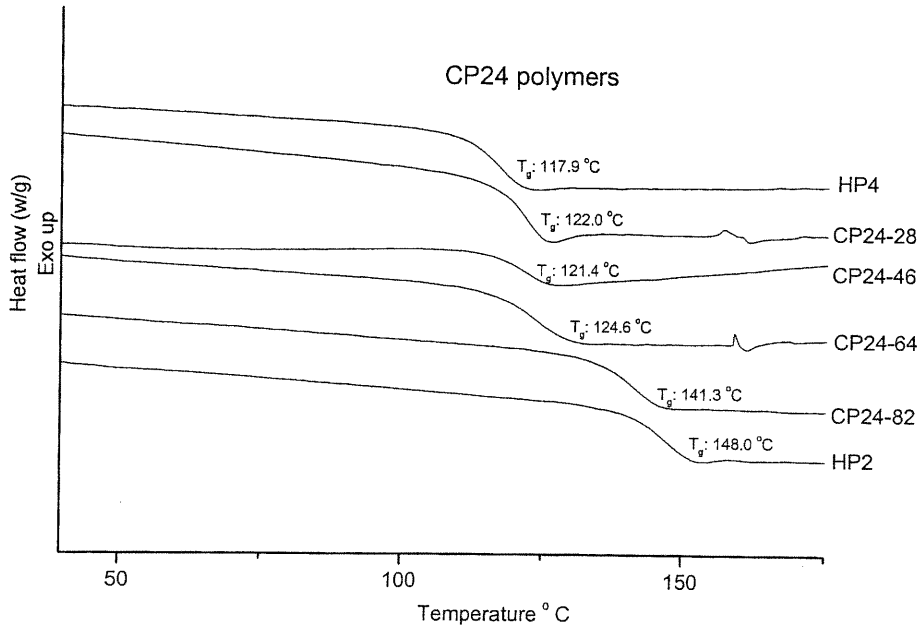

Figure 3.25 DSC traces of copolymers CP24 showing the changes in T_g

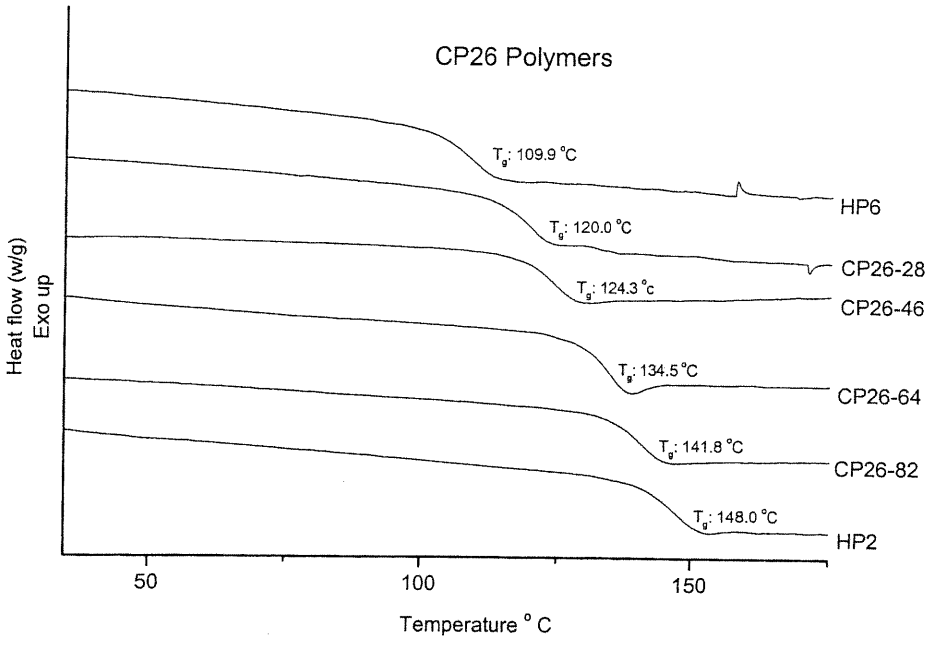

Figure 3.26 DSC traces of copolymers CP26 showing different T_g

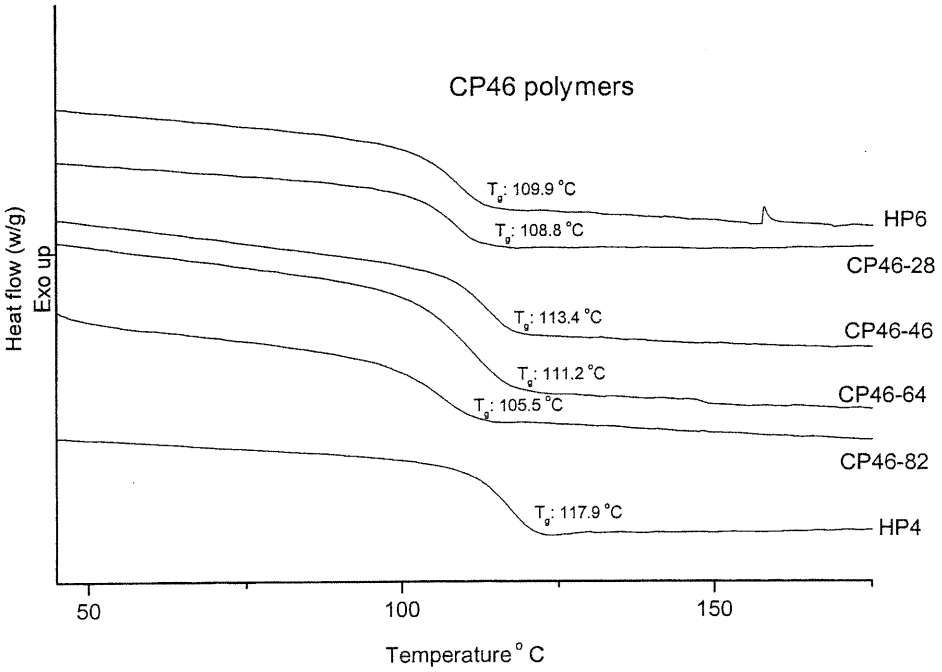

Figure 3.27 DSC traces of copolymers CP46 showing different T_g

Table 3.11 The glass transition temperature of CP24 copolymers and homopolymers

Monomers composition	Ratio	Name	T_g (°C)
24 (n = 2), **25** (n = 4)	**24**: **25** = 0: 100	HP4	117.3 ± 0.6
	24: **25** = 20: 80	CP24-28	123.6 ± 5.1
	24: **25** = 40: 60	CP24-46	118.0 ± 3.6
	24: **25** = 60: 40	CP24-64	126.3 ± 2.5
	24: **25** = 80: 20	CP24-82	141.3 ± 0
	24: **25** = 100: 0	HP2	148.6 ± 0.6

Table 3.12 The glass transition temperature of CP26 copolymers and homopolymers

Monomers composition	Ratio	Name	T_g (°C)
24 (n = 2), **26** (n = 6)	**24**: **26** = 0: 100	HP6	108.2 ± 1.8
	24: **26** = 20: 80	CP26-28	119.8 ± 0.2
	24: **26** = 40: 60	CP26-46	124.3 ± 0
	24: **26** = 60: 40	CP26-64	134.5 ± 0
	24: **26** = 80: 20	CP26-82	141.5 ± 0.3
	24: **26** = 100: 0	HP2	148.6 ± 0.6

Table 3.13 The glass transition temperature of CP46 copolymers and homopolymers

Monomers composition	Ratio	Name	T_g (°C)
25 (n = 4), **26** (n = 6)	**25**: **26** = 0: 100	HP6	108.2 ± 1.8
	25: **26** = 20: 80	CP46-28	107.3 ± 1.5
	25: **26** = 40: 60	CP46-46	113.1 ± 0.3
	25: **26** = 60: 40	CP46-64	110.1 ± 1.2
	25: **26** = 80: 20	CP46-82	103.0 ± 3.1
	25: **26** = 100: 0	HP4	117.3 ± 0.6

copolymers respectively. Their variations as a function of different spacer length composition are shown in Figures 3.29, 3.28 and 3.30.

From the DSC curves in Figures 3.25, 3.26, 3.27, it can be said the copolymers are statistic since they are characterized by only one glass transition temperature. The DSC plot reveals the existence of a linear relationship between the glass transition temperature T_g, and the composition of different spacer length in CP26 copolymers (Figure 3.28). As the content of monomers **24** (spacer length n = 2) decreases, the glass transition temperature decreases linearly. This is the ideal case when T_g follows a relation with composition of the comonomers. In most case, the T_g of copolymers should follow this equation[93]:

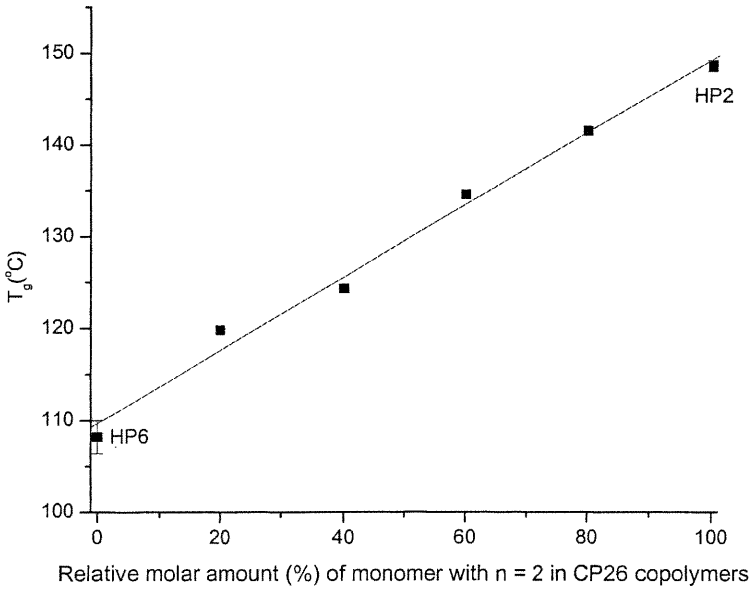

Figure 3.28 The relationship of glass transition temperature with different spacer length composition in CP26 copolymers

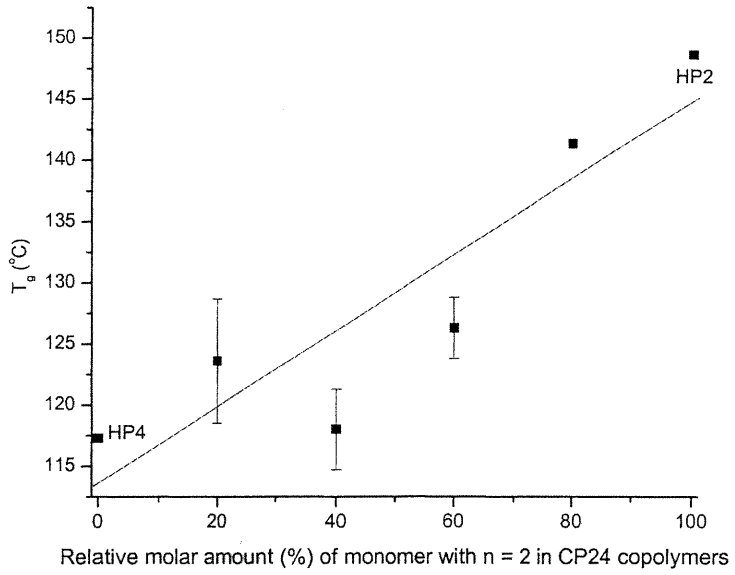

Figure 3.29 The relationship of glass transition temperature with different spacer length composition in CP24 copolymers

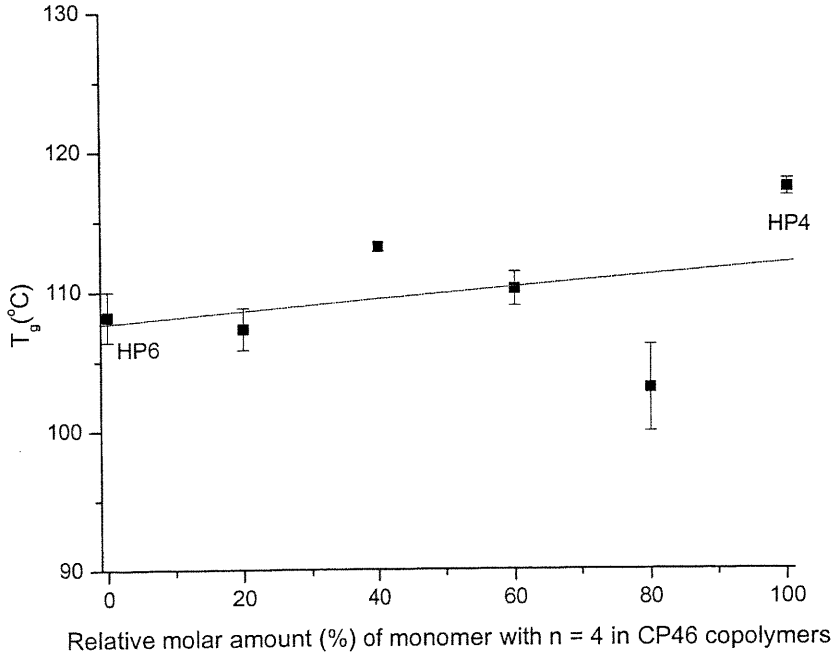

Figure 3.30 The relationship of glass transition temperature with different spacer length composition in CP46 copolymers

$$T_g = \frac{\omega_1 T_{g1} + k\omega_2 T_{g2}}{\omega_1 + k\omega_2} \qquad (3.4)$$

ω_1, ω_2: The fractional mole of two comonomers

T_{g1}, T_{g2}: The glass transition temperature of the corresponding homopolymer

k is a constant and $k = 1$ in the ideal case. In most cases, k is larger than unity.

According to the calculation, the k values of CP26 copolymers approach nearly to 1. The two other CP24 and CP46 copolymers deviate 1 much more. This can also reflect from the Figures 3.28, 3.29 and 3.30. The relationship in Figure 3.28 is linear. However, there are no obvious linear relationships in the case of the CP24 and CP46 copolymers (Figures 3.29 and 3.30). In Figure 3.29, we can see that the glass transition temperature

decreases with increasing spacer length in CP24 copolymers. However, this trend is weaker in CP46 copolymers as shown in Figure 3.30. An explanation may be drawn from a comparison of three homopolymers HP2, HP4 and HP6. The T_g difference between HP4 and HP6 is only 8°C (109.9°C and 117.9°C). So the composition of different monomers **25** (n = 4) and **26** (n = 6) will not affect T_g very much. However, in CP26 copolymers, the T_g difference between HP2 and HP6 is about 40°C (109.9°C and 148.0°C), so the different contents of monomers **24** (n = 2) and **25** (n = 4) in CP26 copolymers will cause obvious change. The more ratio of monomer 24, the higher the glass transition temperature.

Because the feed ratio of different monomers can not completely stand for the ratio of different spacer in the polymer, so the linearity of T_g and spacer composition can not be established very well for CP24 and CP46 copolymers. Meanwhile, the molecular weight of sample is not exactly same every time, so the T_g will change more or less. In addition, the incertitude of measurement also cause the T_g fluctuate a little bit.

3.4.3 Thermogravimetric analysis

The thermal stability of some selected polymers was established by TGA measurements. The TGA decomposition curves are shown in Figure 3.31.

It was found, as shown in Table 3.14, that all polymers are stable up to 300°C.

Table 3.14 The temperature corresponding to 10% decomposition of the polymers and that of the second derivative

Polymer	10% decomposition temperature (°C)	The temperature at the highest derivative weight loss (°C)
HP2	351	397
HP4	353	401
CP24-28	354	397
CP46-28	359	402
HP6	360	410

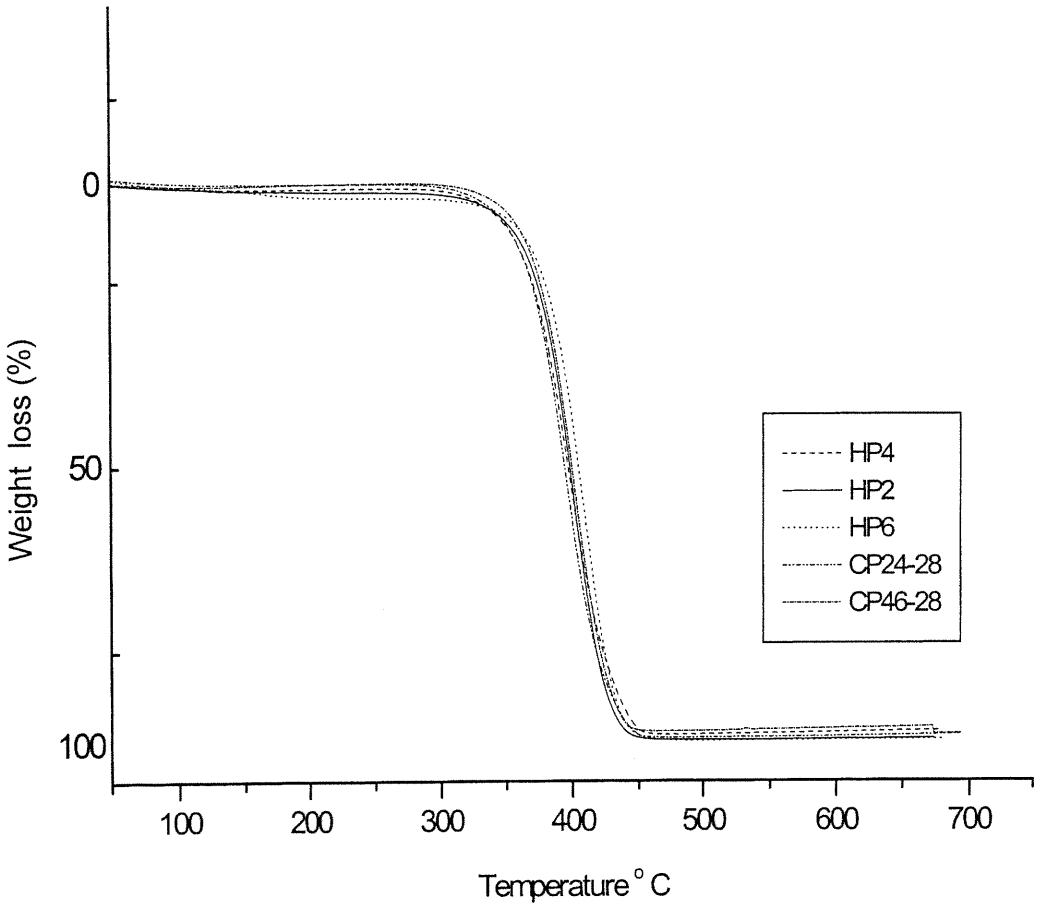

Figure 3.31 Typical thermograms of homopolymers and copolymers The heating rate was 20°C/min for all specimens.

It can be said the peaks at temperature 139.8, 152.2 and 165.9°C for CP24-46 polymer; 155.5 and 160.4°C for CP24-28 polymer; 145.1 and 158.3°C for CP46-28 polymers in the first heating cycle of DSC curve (Figure in Appendix A2, Page 143) are not due to the thermal decomposition of the homopolymers or the copolymers. The temperature at 10 % weight loss for all polymers is above 350°C. The temperature of 10% decomposition increased with increasing the length of methylene spacer. It is same as the literature [92]. The temperature at the highest derivative weight loss is at about 400°C. It tells us that at this temperature, the rate of polymer decomposition is the fastest. The TGA experiment indicates the decomposition is smooth and the LC polymers have good thermal stability.

3.4.4 FTIR spectra of polymers

The homopolymers and some selected copolymers were analyzed by FTIR. The FTIR spectra were shown in Figure 3.32. First of all, the infrared spectra for homopolymers and copolymers are almost identical. No peaks were observed at 1633 cm^{-1} (due to the stretch of alkene double bonds) confirming the absence of double bond in the polymers. The broad bands, ranging from 3600 to 3300 cm^{-1}, are due to the characteristic OH bond and hydrogen bond absorption[94]. The two peaks at 2928 and 2863 cm^{-1} are attributed to the C-H asymmetric and symmetric stretching vibrations. The slightly split peaks of the C=O group visible in monomer **26** are now merged into a single peak at 1720 cm^{-1} in the IR spectra of the polymers. That indicates the differences of two kinds of carbonyl groups in polymers has disappeared. The peaks in the 500 to 1500 cm^{-1} region are quite similar for both the homopolymers and the copolymers.

The FTIR spectra indicate that all the polymers have identical absorption patterns. It is not surprising since they are chemically related. The difference only lies in that they have different spacer lengths. Because the peak from 2750 to 3100 cm^{-1} reflects the absorption of $\gamma_{C\text{-}H}$ and the peak from 3100 to 3750 cm^{-1} stands for the absorption of $\gamma_{O\text{-}H}$, the absorption of $\gamma_{O\text{-}H}$ is invariable in these five polymers, so it is possible that the information of spacer contribution can be obtained if we compare the integration of these two peaks. Table 3.15 listed the integration value of different polymers and compared the spacer contribution. From the result, it can be seen that HP6 have the highest ratio of C-H.

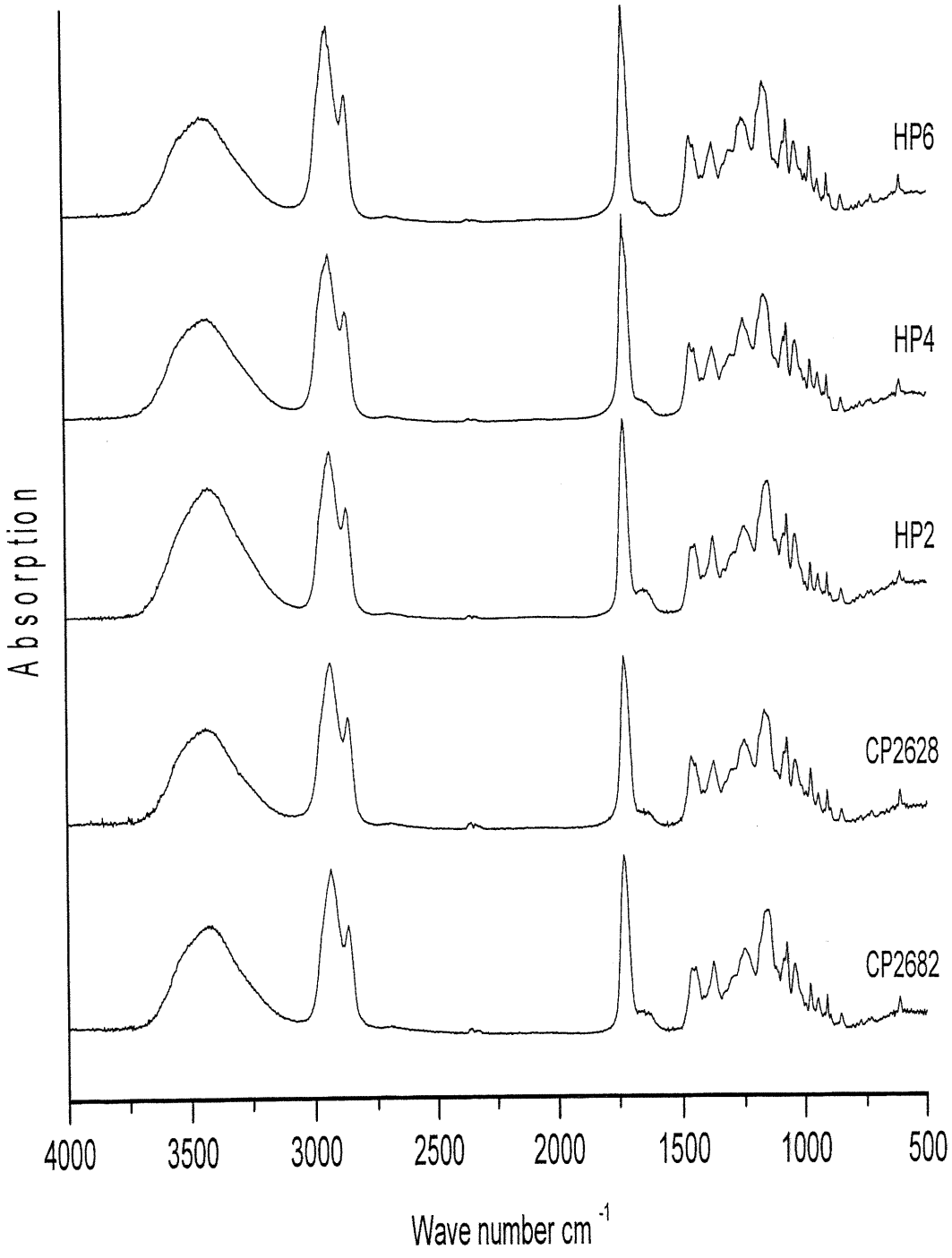

Figure 3.32 FTIR spectra of homopolymers and some copolymers

groups to O-H groups. Then it decreased in order from HP6 to CP2628, HP4, CP2682, HP2. And the spacer contribution of CP2628 is a little bit higher than HP4. From the experimental result, it is reasonable.

Table 3.15 The comparison of integration of spacer contribution in polymers

Polymers name	Integration of γ_{O-H}	Integration of γ_{C-H}	Integration ratio of γ_{C-H}: γ_{O-H}
HP6	1263	914	0.72
CP2628	1222	804	0.66
HP4	1292	810	0.63
CP2682	1336	765	0.57
HP2	1706	784	0.46

3.4.5 X-ray diffraction of polymers

X-ray diffraction was used to determine whether the polymers were crystalline or not. If it is a crystalline material, its X-ray fiber pattern would reveal the fiber repeat of the polymer. Other structure information would be derived from a detailed analysis of the intensity data. And we tried to determine the role of those structural elements of the side chains and mesogenic groups who are responsible for the liquid crystalline state. The liquid crystalline side chains can be packed in several arrangement, even considering only the smectic A mesophase. The schematic packing of side chain mesogenic groups in anisotropic (smectic A) and isotropic films is shown in Figure 3.33.

In order to establish the polymers' structure by X-ray diffraction, films of the polymers were made. The diffraction patterns were recorded in the transmission mode using the Bruker CCD diffractometer. The diffraction patterns only contain one or two diffuse rings showing no preferential orientation. The patterns are characteristic of an amorphous material. It indicates that the polymer main chains are not long enough and there is no ordered arrangement among the polymer main chain and side chain. Because the cholic acid units are so huge, it requires that both the main chain and the flexible side chains are long enough so that the alkyl spacer can decouple the motion of side chains

with cholic acid mesogenic groups and the polymethacrylate main chain to get an ordered arrangement.

In this work, because the cholic acid is a very large group that is not rigid rod-like, the ordered liquid crystalline packing of the mesogenic groups is hindered by the steric requirement. A longer spacer is needed to decouple the main chain and the side chain. So all the effects of main chain type, spacer length and mesogenic groups have to be considered together in order that the polymer has liquid crystalline state. The X-ray diffraction patterns of films of the HP6 polymer are reproduced in Figure 3.34. The films were recorded under different conditions: the stationary specimen is exposed to the X-ray beam for 60 and 240 seconds. In another experiment the specimen is rotated 240 seconds so as to resemble a fiber pattern. There are no significant differences between the various recordings. As shown in Figure 3.34, the patterns which consist of one or two diffuse halos at d_1 = 6.8 Å (intensity $\leq$ 5) and d_2 = 5.6 Å (intensity = 100) are typical of an amorphous specimen. That indicates there is no liquid crystallinity at room temperature.

The reasons why there is no liquid crystalline state probably are caused by the following factors:

The polymer backbone is polymethacrylate structure, so that the chemical repeat unit is quite short as compared to the bulky cholic acid group (see Figure 3.35). Because of the steric requirements, the cholic acid mesogenic groups may easily overlap each other or stack in a disordered manner instead of arranging orderly. The polymer main chains can not be in the fully extended conformation. Most likely it adopts a helicoidal conformation as shown in Figure 3.36. Furthermore the side chains could adopt many different orientations.

So the method to solve this problem is probably that we may increase the length of backbone between two cholic acid groups so that they have more space to extend fully and configure parallel each other in the same layer to form liquid crystalline state. According to this hypothesis, we can use methacrylic acid or styrene to copolymerize the cholic acid derivative monomers. As the reactivity of these lower molecular weight monomers is much higher than cholic acid monomers, the length of backbone between two cholic acid groups will be longer. At the same time, the copolymers' molecular weight will be much higher than that of homopolymer made from cholic acid derivative

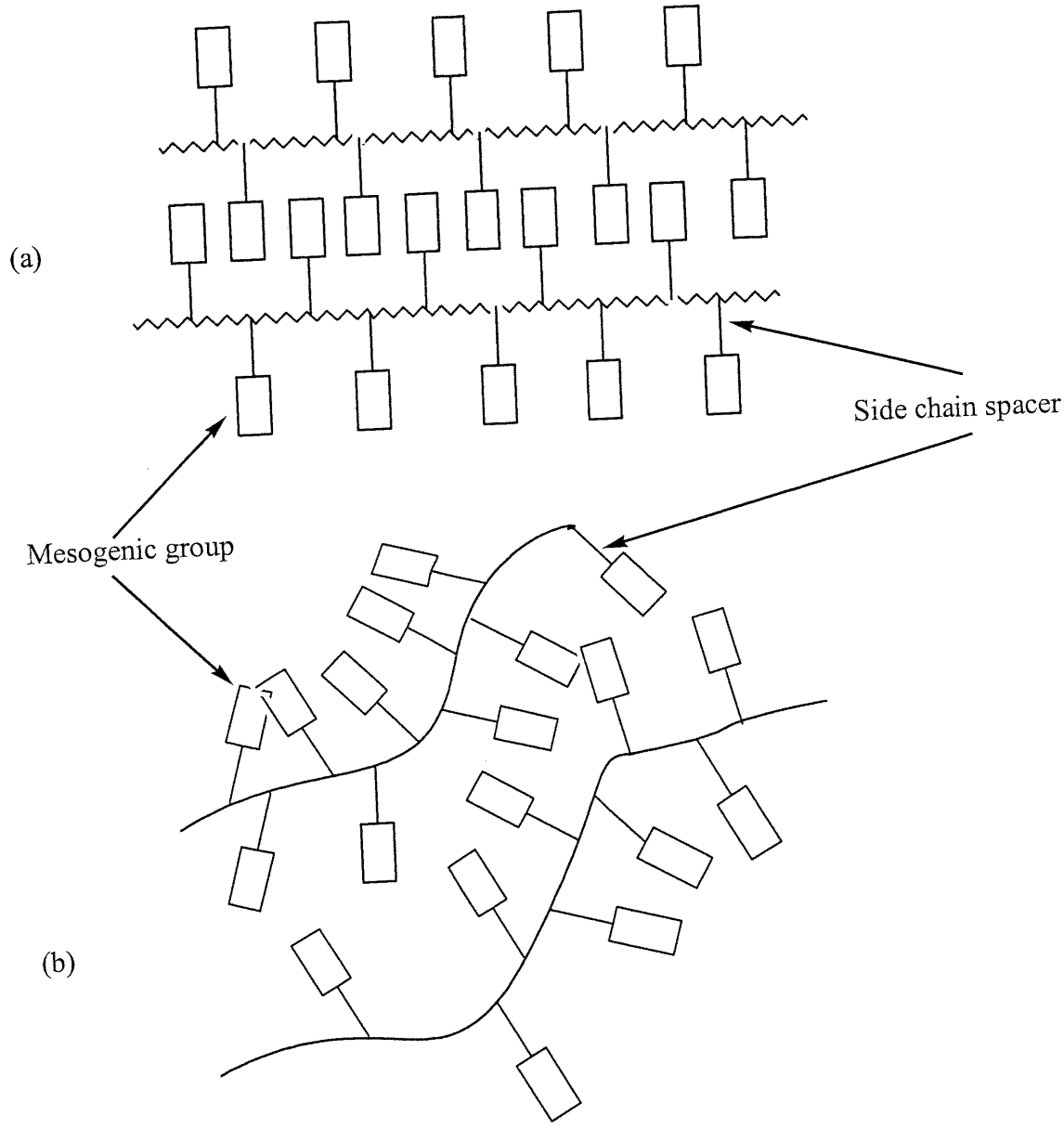

Figure 3.33 Schematic packing of side chain mesogenic group in anisotropic (a) and isotropic films (b)

(a) 60 s without rotation

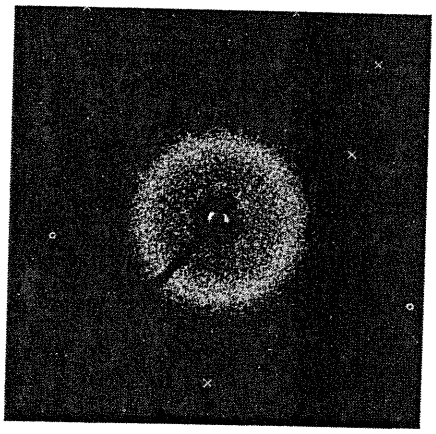

(b) 240 s without rotation

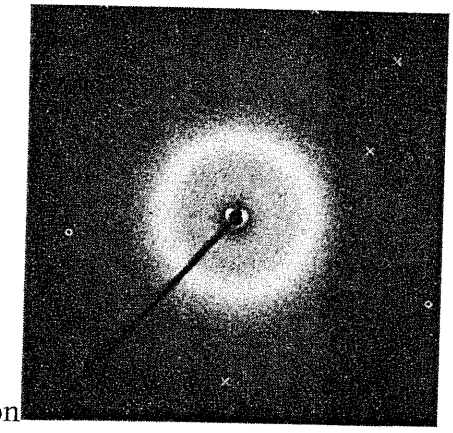

(c) 240 s with rotation

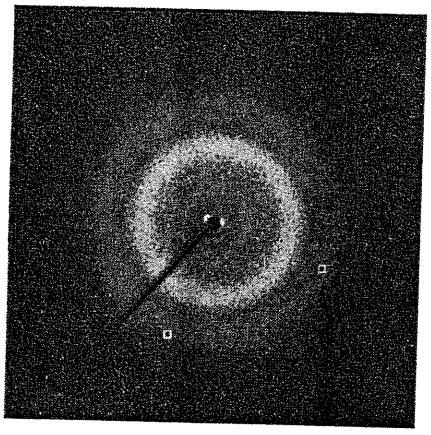

Figure 3.34 X-ray diffraction of an unstretched polymer film of HP6 showing diffuse halos

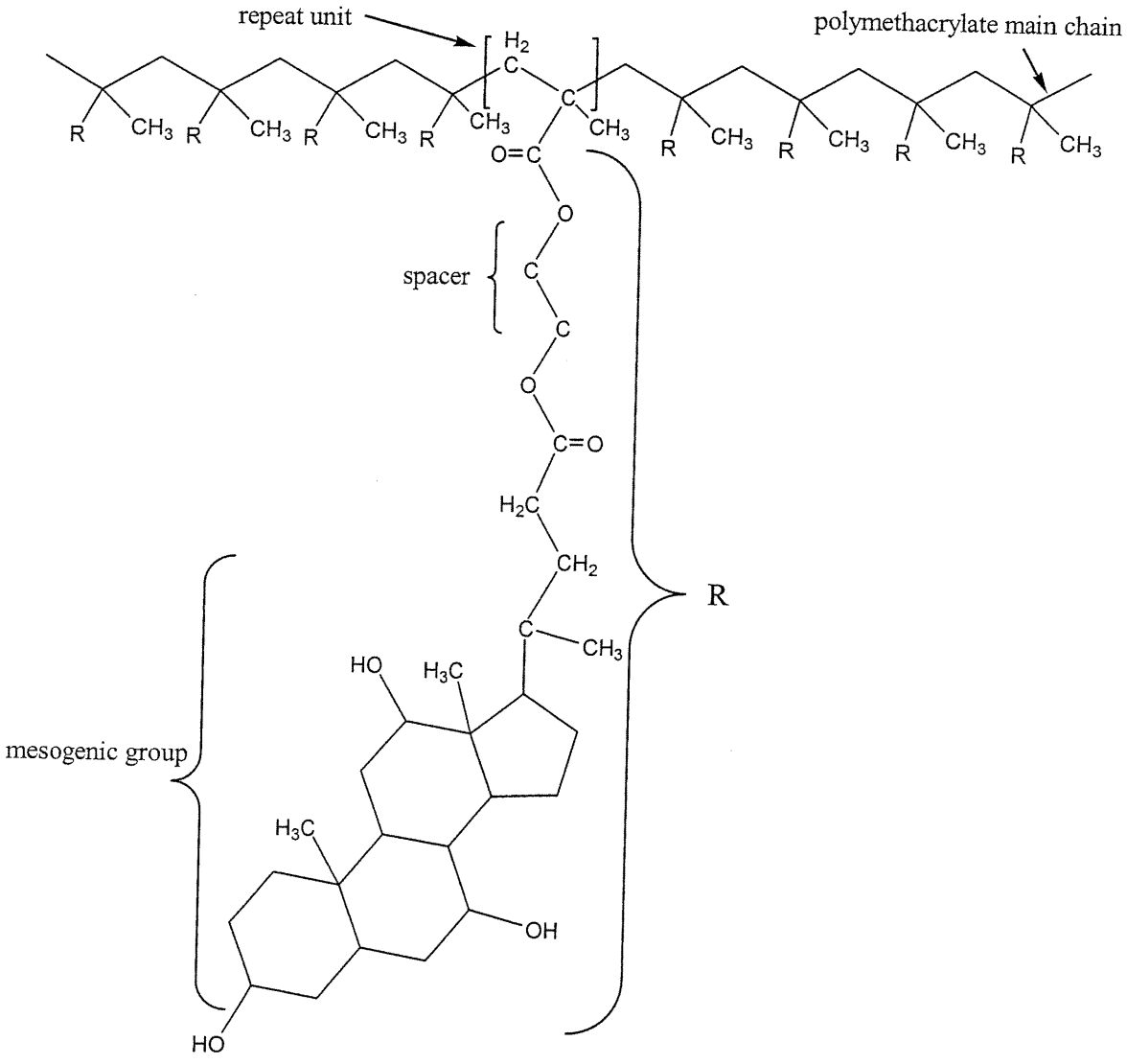

Figure 3. 35 The structure of liquid crystalline polymers with bile acid mesogenic group.

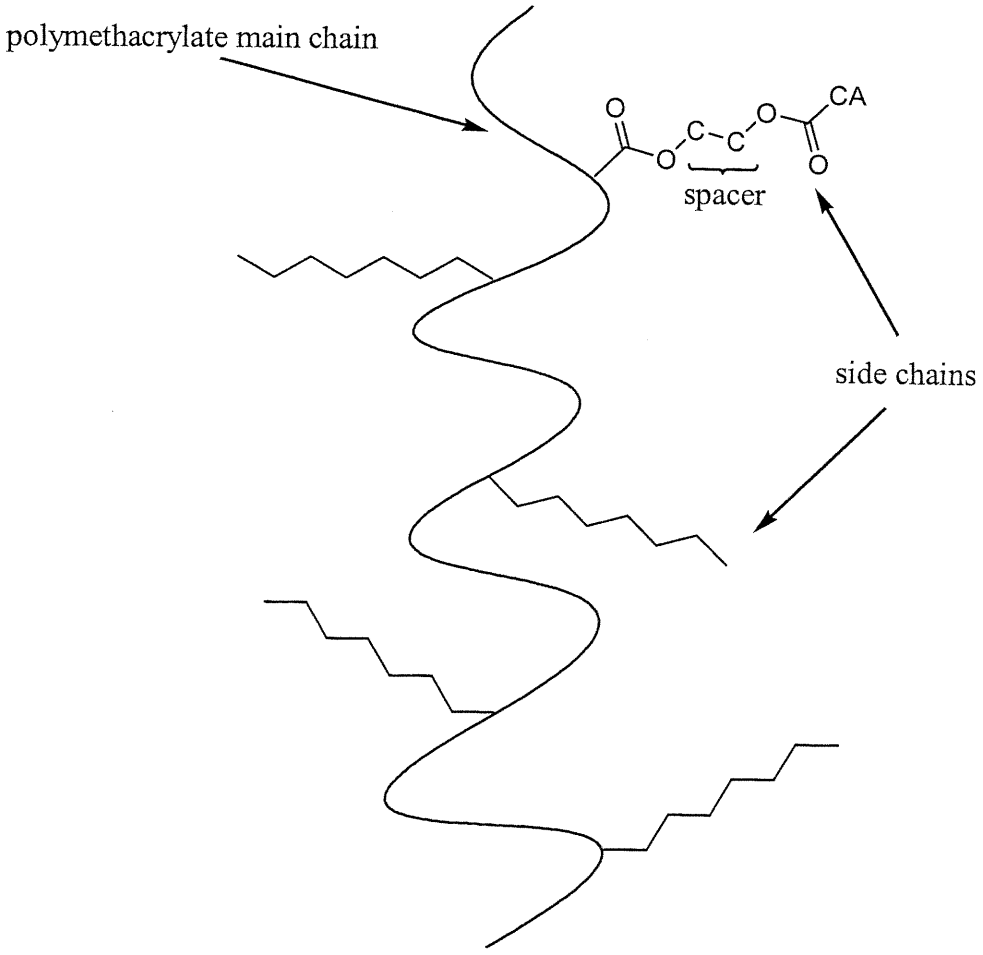

Figure 3.36 The polymethacrylate main chain adopts helical conformation and cholic acid side chains have many orientations (longer spacer will be more accessible to decouple the motion of main chain and side chain to form LC polymers)

monomers. So the mechanical property of films or fibers will be stronger and more flexible than that of lower molecular weight polymers. When they are drawn or oriented, they will move easily to form liquid crystalline state.

Secondly, as the length of spacer group is increased, the low enthalpies of phase transformation of the nematic polymers become larger. The better ordered smectic phases form. The entropy change of isotropization also increases in tendency by increasing the length of flexible spacer. So longer spacers will be very beneficial for polymers to decouple the motion of main chain and side chain. And the mesogenic groups will arrange more orderly. Moreover, the massive cholic acid groups really need longer spacer too. Now the longest spacer length in this research project is n = 6. And the experiment result indicates that it is still not long enough. So it should be tried to increase the spacer length to n = 10 or 12 in future. It is expected that there will be better result.

Furthermore, the structure of cholic acid derivative monomers may be modified a little bit further in order to improve its property to form liquid crystalline state more easily. For example, an alkyl tail can be attached to the end of cholic acid monomers. So the monomer has the structure of double bond and alkyl tail at the two ends, the flexible spacer and cholic acid in the middle of monomer. At the same time, we can also introduce an asymmetric carbon in the molecule so that the corresponding polymer may form the cholesteric or S_c liquid crystalline phase. Moreover, the ester link between cholic acid and spacer can be modified to ether bond type. It is more flexible than ester bond to decouple the motion of main chain and side chain. The idea was tried to synthesize ether monomers, but the yield was so low that no pure monomers were obtained. So other new methods are to be adopted to synthesize this type of monomers with higher yield.

3.4.6 Liquid crystallinity

Liquid crystalline phases may appear or are induced under different temperatures or other physical conditions such as magnetic field, electric field, pressure, etc. When the temperature increases, the polymer goes through one or multiple first-order transitions after glass transition temperature from a more ordered to a less ordered state[41, 95] as shown in Figure 1.9. It has been established that these various mesophasic transitions are first-order transitions, because the volume and the heat capacity go through discontinuities when they are plotted against the temperature or pressure. These

transitions should be reversible when the liquid crystalline polymers are cooled down to room temperature.

As for the liquid crystal property of the polymers in this project, we do not observe any mesophases from the above DSC traces of Figures 3.23, 3.25, 3.26, and 3.27. The very small peaks after the glass transition temperatures in the above plots are probably due to the remaining slight crystallinity in polymers after the first heating and cooling. DSC experiments proved that these minor peaks disappear after three or four heating cycles. The DSC plots show that the polymers do not have reversible liquid crystallinity, the first heating indicates polymers CP24-46, CP24-28 and CP46-28 may have liquid crystalline structures. There are several peaks at temperature 139.8°C, 152.2°C and 165.9°C for CP24-46 polymer; 155.5°C and 160.4°C for CP24-28 polymer; 145.1°C and 158.3°C for CP46-28 polymers. And these transitions vanished irreversibly when the polymer was heated above its glass transition temperature, T_g. After the polymers were cooled down below T_g, isotropic glass state polymers were obtained, even when a very slow cooling rate (1°C / min) was adopted.

Although the mesophases of unsubstituted cholic acid or lithocholic acid have never been reported, the cholesteryl nonanoate and many other cholesterol derivatives have been reported to have cholesteric phase[96-102]. Considering the fact that the bile acids and cholesterol have similar structures, it is possible for bile acids derivatives and their related polymers to have liquid crystalline properties. One possible reason why my polymers do not exhibit liquid crystalline properties could be that the flexible polymethylene $-(CH_2)_n-$, n = 2, 4, 6 spacers are not long enough, although there is a literature report indicating that two or four methylene groups are sufficient to achieve the required decoupling[4]. However, their mesogenic groups are not as bulky as the bile acid derivatives of this project. Other reports indicate that short spacers cannot exhibit mesophases[89, 102]. From my experiments, it seems that excessively large cholic acid mesogenic groups seem to require much longer flexible spacer to decouple the polymethacrylate backbone than rod-like mesogenic groups do. So the main chain needs to subscribe more configuration entropy and yield to the action of side chain. Then the mesogenic groups can self-assemble and the polymers display liquid crystalline properties. From the above discussion, we can say the flexible spacers are not always

long enough to obtain a liquid crystalline polymer. The mesogenic groups are also very important. Whether a mesophase appears, depends on which of the main chain or the side chain, plays the most important role. If the mesogenic groups and side chains yield to backbone motion, they will adopt a disordered state and the polymer will be amorphous. X-ray diffraction and polarized microscopy could help elucidate whether mesophases exist or not. In our polarizing microscopy experiments, mesophases were not observed.

CHAPTER 4

CONCLUSIONS

4.1 The syntheses of monomers

New monomers with bile acids derivatives were successfully prepared with the intention of synthesizing liquid crystalline polymers. The monomers contain methacrylate double bonds, bile acid derivatives and spacers of different lengths. With the spacers of 2, 4, or 6 methylene groups, the influence of their length on the property of polymers have been studied.

All the monomers which were purified by column chromatography were identified by nuclear magnetic resonance, mass spectrometry, elemental analysis, Fourier transform infrared and X-ray diffraction etc. The above spectra and experimental data indicate that the monomers have the expected structures and that they are pure enough for the polymerization.

4.2 The structure of the model compounds 11 and 26

The two compounds: methyl 3α-tosyloxy-5β-cholan-24-ate **11** and methacryloyloxy-hexyloxy 3α,7α,12α-trihydroxy-5β-cholan-24-ate **26** were crystallized. Their crystal structure were established by single crystal X-ray diffraction analysis.

The X-ray diffraction experiments revealed that compound **11** has an orthorhombic unit cell of dimension $a = 11.6982$, $b = 22.1349$, $c = 71.1604$ Å. The very large unit cell volume, V = 18426.2(2) $Å^3$, contains 24 molecules. Hence there are 6 independent molecules per asymmetric unit of the $P2_12_12_1$ space group. The junctions of cholic acid fused ring and C18, C19 methyl substitutions at position C13, C10 provided the torsion barriers so that the framework of bile acids had more ordered configuration. Otherwise, they have to overcome the torsion barriers if they change their conformation. That is, for the six-membered rings, the lowest energy structures adopt approximate chair conformation, while the five-membered ring is in an approximate envelope conformation.

The flexible part of the side chain from C13 to C25 is nearly in the fully extended conformation. The average deviation from *t* = *trans* = 180° is only ±10°. The *para*-toluenesulfonyl substitute is disordered over two positions in the 57:43, 51:49, 63:37, 52:48, 51:49 and 53:47 ratios for molecules A, B, C, D, E and F, respectively. These twelve orientations may be regrouped into two distinct conformations.

The packing of the rigid lithocholic acid moieties (LA) are nearly parallel to one another and inclined by 30° with respect to the *bc*-face of the unit cell. They constitute layers parallel to the *ab*-face. This disposition of the molecules is similar to that of the liquid crystal phases of the S_C-type. The methyl ester groups (ME) are located between two consecutive layers while the *para*-toluenesulfonyl terminals (MS) occupy the space between the next layers and so on. Four such layers are observed in one unit cell, perpendicular to the *c*-axis. The packing sequence along the *c*-direction is: ME-LA-MS MS-LA-ME ME-LA-MS MS-LA-ME, etc.

Compound **26** has a monoclinic $P2_1$ unit cell with *a* = *11.5401, b* = *7.8751, c* = *18.5539* Å and β = 103.4°. There is only one independent molecule in the monoclinic unit cell. The structure determination indicates that the rigid cholic acid framework is ordered and crystallizes with one water molecule. The three six-membered rings were in an approximate chair conformation while the five-membered ring adopted an approximate envelope conformation. However, there is 53:47 disorder at the end of the long terminal, from C31 to C35. The aliphatic segment from C23 to C32 is not in the fully extended conformation. The crystal structure of (methacryloyloxy)hexyloxy 3α,7α,12α-trihydroxy-5β-cholan-24-ate is stabilized by intermolecular hydrogen bonds. They are linked by intermolecular hydrogen bonds of the O—H···O type. There are six hydrogen bonds (O—H···O). The hydroxyl groups on position 3 and 7 act as donors towards the hydroxyl groups on position 12 and 3 respectively of another molecule. The other four hydrogen bonds involve the water molecules. One of them is formed between the hydroxyl group on position 12 as donor and the water molecule as acceptor. The other two hydrogen bonds are formed between the water molecule as donors and the hydroxyl group on position 7 as acceptor. All of the hydrogen bonds are moderately bent. The O12—H12 and O3—H3 of two symmetrically related molecules form two pairs of

hydrogen bonds: O12—H12···O3 and O3—H3···O12, where O3 and O12 are both acceptors and donors.

The packing of the molecules **26** seems to be no ordered layer organization as for molecule **11**. The flexible spacer and methacrylate extend out.

4.3 The properties of polymers

Homopolymers and copolymers with bile acids derivatives were synthesized by free radical polymerization. They were characterized by size exclusion chromatography, differential scanning calorimetry, Fourier transformation infrared spectroscopy, thermogravimetric analysis, polarized microscopy and X-ray diffraction. The SEC experiments indicated the molecular weights of polymers were not very high and polydispersity was broad. Hence, the polymer main chain contained approximately 10-15 monomer units. The low reactivity of the monomers is probably due to the steric hindrance associated with the large bile acid derivatives. The glass transition temperature decreased with increasing the length of spacer. When the spacer length n is 2, the homopolymer HP2 has the highest T_g (148°C); and the homopolymer HP6 has the lowest T_g (108°C). This is an interesting property since T_g can be adjusted according to the composition of different spacer lengths. The TGA experiments indicated the polymers had good thermal stability.

Since bile acids are bulky, longer spacers may be needed in the polymers mesophases. Polymers with shorter spacers were not able to exhibit mesophases. X-ray diffraction patterns showed diffuse scattering characteristic of an amorphous material. New monomers with longer spacers up to n = 10 or 12 units should be synthesized. So the main chain and side chain with bile acids mesogenic groups can be decoupled. The monomers containing bile acids can be copolymerized with other mesogenic monomers. It will be possible then to obtain higher molecular weight polymers with liquid crystalline properties.

REFERENCE

[1] A. M. Donald, A. H. Windle, "*Liquid Crystalline Polymers*", Cambridge University Press (1992)

[2] J. A. Castellano, *Mol.Cryst. Liq. Cryst.*, **165**, 289 (1988)

[3] A. Ciferri, W. R. Krigbaum, R. B. Meyer, " *Polymer Liquid Crystals* ", Academic Press (1982)

[4] F. Reinitzer, *Monatsch*, **9**, 421 (1888)

[5] F. Reinitzer, *Ann. Physique,* **18**, 273 (1922)

[6] G. W. Gray, J. W. G. Goodby,"*Smectic Liquid Crystals* ", Leonard Hill, Glasgow (1984)

[7] G. W. Gray, *Mol. Cryst. Liq. Cryst.*, **21**, 161 (1973)

[8] F. C. Bawden, N. W. Pirie, *Proc. Roy. Soc. London* Ser. B, **123**, 274 (1937)

[9] D. G. H. Ballard Courtaulds Ltd, UK Patent BP 864, 962 (1958)

[10] S. L. Kwolek, Du Pont, US Patent 3 600 350 (1971)

[11] L. Onsager, *Ann. NY Acad. Sci.*, **51**, 627 (1949)

[12] O. J. Flory, *Proc. Roy. Soc. London* Ser. A, **234**, 66 (1956)

[13] H. Finkelmann, G. Rohage, *Adv. Polym. Sci.*, **60/61** 99 (1984)

[14] A.V. Volokhina, G. I. Kudryavtsev in *" Liquid-Crystal Polymers"* N.A. Platé, Plenum, New York (1993)

[15] A. J. East, L. F. Charbonneau, G. W.Calundann, U.S. Pat. No. 4 330 457 (1982)

[16] G. Huynh-Ba, E. F. Cluff, *" Polymeric Liquid Crystals "*, A. Blumstein, Ed., Plenum, New York (1985)

[17] C. K. Ober, J. I. Jin, R. W. Lenz, *" Liquid Crystal Polymers I "* N. A. Platé, Ed., *Advances in Polymer Science,* **59**, Springer-Verlag, Berlin (1984)

[18] W. J. Jackson, F. H. Kuhfuss, *J. Polym. Sci. Polym. Chem. Ed.*, **14**, 2043 (1976)

[19] A.Blumstein, E. C. Hsu, *" Liquid Crystalline Order in Polymers "* Academic Press, New York (1978)

[20] V. P. Shibaev, N. A. Platé, *Polym. Sci USSR (English transl.),* **19**, 1065 (1978)

[21] H. Finkelmann, M.Happ, M. Portugall, H. Ringsdorf, *Makromol. Chem.,* **179**, 2541 (1978)

[22] A. F. Hofmann, *" The Bile acids "*, Ed by P. P. Mair and D. Kritchevsky, Plenum Press, New York (1971)

[23] U. Maitra, S. Balasubramanian, *J. Chem. Soc Perkin Trans*, **1**, 83 (1995)

[24] R.P. Bonar-Law, A.P. Davis, *Tetrahedron*, **49**, 9829 (1993)

[25] R.P. Bonar-Law, A.P. Davis, *Tetrahedron*, **49**, 9845 (1993)

[26] R.P. Bonar-Law, A.P. Davis, *Tetrahedron*, **49**, 9855 (1993)

[27] G. Wess, W. Kramer, G. Schubert, A. Enhsen, K. H. Baringhaus, H. Glomobil, S. K. Müllner, H. Bock, M. Kleine, G. John, A. Neckermann, A. Hoffmann, *Tetrahedron Lett.*, **34**, 819 (1993)

[28] U. Maitra, B. G. Bag, *J. Org. Chem.,* **57**, 6979 (1992)

[29] U. Maitra, P. Mathivanan, *J. Chem. Soc., Chem. Commun.*, 1469 (1993)

[30] U. Maitra, P. Mathivanan,. *Tetrahedron : Asymmetry*, **5**, 1171 (1994)

[31] A. P. Davis, *Chem. Soc. Rev.,* **243** (1993)

[32] M. Ahlheim, M.L. Hallensleben, *Makromol. Chem., Rapid Commun.*, **9**, 299 (1988)

[33] N. Ghedini, P. Ferruti, *Synth. Commun.*, **13**, 701 (1983)

[34] M. Ahlheim, M.L. Hallensleben, *Polym. Bull.*, **15**, 497 (1986)

[35] X. X. Zhu, M. Moslova, J. K. Denike, *Polymer*, **37**,493 (1996)

[36] J. K. Denike, X. X. Zhu, *Macromol. Rapid Commun.,* **15,** 459 (1994)

[37] Y. H. Zhang, X. X. Zhu, *Macromol. Chem. Phys.,* **197**, 3473 (1996)

[38] Y. H. Zhang, M. Akram, H. Y. Liu, X. X. Zhu, *Macromol. Chem. Phys.,* **199**, 1399 (1998)

[39] J. K. Denike, M. Moskova, X. X. Zhu, *Chem. Phys. Lipids,* **77**, 261 (1995)

[40] A. Benrebouh, D. Avoce, X. X. Zhu, *Polymer,* **42**, 4031 (2001)

[41] P. W. Atkins, *" Physcial Chemistry "* 4th Edition, W. H. Freeman and Company, New York (1990)

[42] G. H. Stout, L. H. Jensen, *" X-ray Structure Determination "*, The Macmillan Company, London (1968)

[43] X. D. Li, Ph. D. thesis ''Structural studies of some mesogenic aromatic polyesters and their model compounds'' Université de Montréal (1993)

[44] M. Kakudo, N. Kasai, *" X-ray Diffraction by Polymers "*, Elsevier Publishing Company (1972)

[45] T. Suzuki, T. Okawa, T. Ohnuma, Y. Sakon, *Makromol. Chem., Rapid. Comm.*, **9**, 755 (1988)

[46] F. Herman, D. Mark, F.Othmer, *" Encyclopedia of Chemical Technology "* 3rd Edition, A Wiley-Interscience Publication (1981)

[47] G. H. Brown, J. J Wolken, *" Liquid Crystal and Biological Structures "*, Academic Press, New York (1979)

[48] W. Y. Zheng, P. T. Hammond, *Macromol. Rapid Commun.*, **17**, 814 (1996)

[49] H. Finkleman, J. Koldehoff, H. Ringsdorf, *Angew. Chem. Int. Ed. Engl.*, **17**, 935 (1978)

[50] V. P. Shibaev, V. M. Moiseenko, Y. S. Freidzon, N. A. Platé, *Eur. Polym. J.*, **16,** 277 (1979)

[51] J. Horvath, K. Nyitrai, F. Cser, G. Hardy, *Eur. Polym. J.*, **21**, 251 (1985)

[52] R. Zentel, H. Ringsdorf, *Makrol. Chem. Rapid Commun.*, **5**, 393 (1984)

[53] Sadtler Research Laboratories Inc. *The Sadtler Standard Spectra.* J213, J214 (1976).

[54] G. H. Stempel, P. P. Cross, R. P. Mariella, *J. Am. Chem. Soc.*, **72**, 2299 (1950)

[55] S. Gouin, Ph. D. thesis '' Synthèse et caractérisation de nouveaux polymères biodégradables dérivés des acides biliaires '' Université de Montréal (1998)

[56] S. Gouin, X.X. Zhu, *Steroids,* **61**, 667 (1996)

[57] G. Wess, W. Kramer, W. Bartmann, A. Enhsen, H. Glombik, S. Mullner, K. Bock, A. Dries, H. Kleine, W. Schmitt, *Tetrahedron* Letter, **33**, 195 (1992)

[58] C. H. Brieskorn, H. Mosandl, *Arch. Pharm.*, **314**, 118 (1981)

[59] K. Yamasaki, V. Rosnati, M. Frieser, L. F. Fieser, *J. Am. Chem. Soc.*, **77**, 3308 (1955)

[60] A. Benrebouh, Y. H. Zhang, X. X. Zhu, *Macromol. Rapid Commun.*, **21**, 685 (2000)

[61] H. D. Flack, *Acta Cryst.*, **A39**, 876 (1983)

[62] *International Tables for Crystallography* Vol. C. Tables 4.2.6.8 and 6.1.1.4, Dordrecht: Kluwer Academic Publishers (1992)

[63] *Integration Software for Single Crystal Data.* Bruker AXS Inc., Madison, WI 53719 -1173. SAINT (1999)

[64] G. M. Sheldrick, SADABS, *Bruker Area Detector Absorption Corrections.* Bruker AXS Inc., Madison, WI 53719-1173 (1996)

[65] G. M. Sheldrick, SHELXS97, *Program for the Solution of Crystal Structures.* Univ. of Gottingen, Germany (1996)

[66] G. M. Sheldrick, SHELXS96, *Program for the Refinement of Crystal Structures.* Univ. of Gottingen, Germany (1996)

[67] Release 5.10 ; *The Complete Software Package for Single Crystal Structure Determination.* Bruker AXS Inc., Madison, WI 53719-1173. SHELXTL (1997)

[68] Release 5.059 ; *Bruker Molecular Analysis Research Tool.* Bruker AXS Inc., Madison, WI 53719-1173. SMART (1999)

[69] A. L. Spek, *Molecular Geometry Program,* July 1995 version. University of Utrecht, Utrecht, Holland. PLATON (1995)

[70] Release 5.10; *X-ray data Preparation and Reciprocal Space Exploration Program.* Bruker AXS Inc., Madison, WI 53719-1173. XPREP (1997)

[71] H. D. Flack, D. Schwarzenbach, *Acta Cryst.*, **A44**, 499 (1988)

[72] L. M. Arnett, *J. Am. Chem. Soc.*, **74**, 2027 (1952)

[73] The Merck Index, 11th edition published by MERCK & CO., INC (1989)

[74] T. Kodaira, K. Mori, *Makromol. Chem.*, **193**, 1331 (1992)

[75] G. Galli, E. Chiellini, *Makromol. Chem., Rapid Commun.*, **14**, 185 (1993)

[76] M. Hefft, J. Springer, *Makromol. Chem., Rapid Commun.*, **11**, 397 (1990)

[77] S. Czapla, R. Ruhmann, *Makromol. Chem.*, **194**, 243 (1993)

[78] M. Portugall, H. Ringsdirf, R. Zentel, *Makromol. Chem.*, **183**, 2311 (1982)

[79] Seyhan Ege, ''*Organic Chemistry* '' 3rd edition, D. C. Heath and Company (1994)

[80] K. D. R. Setchell, D. Kritchevsky, P. P. Nair, *'' The Bile acids, Chemistry, Physiology, and Metabolism ''*, Vol. 4: Methods and applications Ed by P. P. Mair and D. Kritchevsky, Plenum Press, New York (1988)

[81] L. F. Fieser, M. Fieser, ''*Steroids* '', Reinhold, New York (1959)

[82] M. Karplus, *J. Chem. Phys.*, **30**, 11 (1959)

[83] H.Y. Liu, D. Avoce, X. X. Zhu, *Macromol. Rapid Commun.*, **22**, 675 (2001)

[84] M. Ranger, J. Zhu, ''*Introduction à la chimie macromoléculaire*'' Notes de Cours, Université de Montréal (2000-2001)

[85] A. Benrebouh, Master thesis '' Synthèse de polymère hydrophiles et thermosensibles dérivés de l'acide cholique '' Université de Montreal (1998)

[86] J. Horváth, K. Nyitrai, *Eur. Polym. J.*, **21**, No. 3, 251 (1985)

[87] C. T. Imrie, F. E. Karasz, G. S. Attard, *Macromolecules* **26**, 3803 (1993)

[88] C. T. Imrie, F. E. Karasz, G. S. Attard, *J. Macromol. Sci., Pure Appl. Chem.*, **A31**, 1221 (1994)

[89] C. T. Imrie, F. E. Karasz, G. S. Attard, *Macromolecules*, **28**, 3617 (1995)

[90] C. T. Imrie, F. E. Karasz, G. S. Attard, *Macromolecules,* **25**, 1278 (1993)

[91] C. T. Imrie, F. E. Karasz, G. S. Attard, *Macromolecules,* **26**, 545 (1993)

[92] K. M. Kim, Y. Imai, K. Naka, Y. Chujo, *Polymer Journal,* **32**, No. 8, 657 (2000)

[93] J. Mark, A. Eisenberg, W. W. Graessley, L. Mandelkern, T. E. Samulski, J. L. Koening, *Physical Properties of Polymers,* 2nd edition 87 ACS Professional Reference Book, American Chemical Society, Washington (1993)

[94] G. M. Loudon, ''*Organic chemistry* '' *2n*d edition, Benjamin/Cummings publishing Company, Inc. (1988)

[95] V. T. Arthur, F. M. Herman, '' *Polymer Science and Materials* '' Wiley-Interscience, a Divison of John Wiley & Sons, Inc. (1971)

[96] B. Q. Chen, A. Kameyama, T. Nishikubo, *Macromolecules*, **32,** 6485 (1999)

[97] H. Finkelmann, H. Ringsdorf, W. Siol, J. H. Wendorff, *Makromol. Chem.*, **179**, 829 (1977)

[98] Ya. S. Freidzon, A. V. Kharitonov, V. P. Shibaev, N. A. Platé, *Mol. Cryst. Liq.*

Cryst., **88**, 87 (1982)

[99] H. Finkelmann, J. Koldehoff, H. Ringsdorf, *Angew. Chem. Int. Ed. Engl.*, **17**, No. 12 935 (1978)

[100] V. P. Shibaev, N. A. Platé, Ya. S. Freidzon, *J. Polym. Sci., Polym. Chem. Ed.* **17** (1979)

[101] A. M. Mousa, Ya. S. Freidzon, V. P. Shibaev, N. A. Platé, *Polym. Bull.* **6**, 485 (1982)

[102] Ya. S. Freidzon, N. I. Boiko, V. P. Shibaev, N. A. Platé, *Eur. Polym. J.*, **22**, No.1, 13 (1986)

APPENDICES

A1 (1) Atomic coordinates ($\times 10^4$) and equivalent isotropic displacement parameters ($Å^2 \times 10^3$) for $C_{32}H_{48}O_5S$.

U(eq) is defined as one third of the trace of the Orthogonalized Uij tensor.

	Occ.	x	y	z	U(eq)
O(24A)	1	3990(4)	5201(3)	182(1)	124(2)
O(25A)	1	2994(4)	5185(3)	-79(1)	112(2)
C(1A)	1	-1792(4)	5445(3)	1529(1)	77(1)
C(2A)	1	-775(4)	5129(2)	1621(1)	65(1)
C(3A)	1	-134(4)	5555(2)	1748(1)	64(1)
C(4A)	1	208(4)	6128(2)	1651(1)	62(1)
C(5A)	1	-786(5)	6440(2)	1553(1)	72(1)
C(6A)	1	-382(5)	7007(2)	1447(1)	77(1)
C(7A)	1	328(5)	6857(2)	1276(1)	69(1)
C(8A)	1	-262(4)	6427(2)	1142(1)	63(1)
C(9A)	1	-685(4)	5855(2)	1248(1)	62(1)
C(10A)	1	-1446(4)	6012(2)	1420(1)	73(1)
C(11A)	1	-1189(4)	5392(2)	1111(1)	70(1)
C(12A)	1	-397(4)	5226(2)	949(1)	67(1)
C(13A)	1	-8(4)	5799(2)	839(1)	63(1)
C(14A)	1	531(4)	6238(2)	985(1)	60(1)
C(15A)	1	1072(5)	6720(2)	862(1)	77(1)
C(16A)	1	1493(5)	6382(2)	687(1)	74(1)
C(17A)	1	1040(4)	5727(2)	705(1)	63(1)
C(18A)	1	-1013(4)	6069(2)	734(1)	74(1)
C(19A)	1	-2574(5)	6310(3)	1351(1)	106(2)
C(20A)	1	892(4)	5407(2)	513(1)	68(1)
C(21A)	1	523(6)	4759(2)	532(1)	91(2)
C(22A)	1	1996(5)	5441(3)	401(1)	80(1)
C(23A)	1	1926(5)	5237(4)	199(1)	96(2)
C(24A)	1	3104(6)	5206(3)	107(1)	84(2)
C(25A)	1	4049(8)	5143(5)	-181(1)	142(3)
S(1A)	0.57	1383(6)	5224(3)	2013(1)	74(1)
O(1A)	0.57	2466(10)	4925(9)	1995(2)	88(3)
O(2A)	0.57	1395(7)	5788(4)	2110(1)	79(2)
O(3A)	0.57	934(8)	5262(5)	1807(1)	74(1)
C(31A)	0.57	420(5)	4751(3)	2127(1)	58(2)
C(32A)	0.57	117(7)	4204(3)	2045(1)	69(2)
C(33A)	0.57	-651(7)	3822(3)	2134(1)	73(2)

C(34A)	0.57	-1117(5)	3986(2)	2307(1)	62(2)
C(35A)	0.57	-814(5)	4533(3)	2389(1)	70(2)
C(36A)	0.57	-46(5)	4915(2)	2299(1)	63(2)
C(37A)	0.57	-1947(9)	3585(5)	2409(2)	87(3)
S(1G)	0.43	1268(9)	5277(5)	2020(1)	74(1)
O(1G)	0.43	2356(14)	4993(12)	2034(4)	88(3)
O(2G)	0.43	1104(10)	5889(5)	2069(2)	79(2)
O(3G)	0.43	938(11)	5247(6)	1804(2)	74(1)
C(31G)	0.43	206(6)	4871(4)	2135(1)	58(2)
C(32G)	0.43	169(8)	4251(5)	2104(1)	69(2)
C(33G)	0.43	-660(9)	3902(3)	2193(2)	73(2)
C(34G)	0.43	-1452(7)	4173(3)	2312(1)	62(2)
C(35G)	0.43	-1415(6)	4793(3)	2342(1)	70(2)
C(36G)	0.43	-586(6)	5142(3)	2253(1)	63(2)
C(37G)	0.43	-2408(12)	3811(7)	2397(3)	87(3)
O(24B)	1	8972(5)	8289(4)	119(1)	149(3)
O(25B)	1	7875(5)	8096(3)	-127(1)	124(2)
C(1B)	1	4522(6)	7606(3)	1579(1)	118(3)
C(2B)	1	5554(5)	7871(4)	1674(1)	134(3)
C(3B)	1	5210(4)	8469(4)	1761(1)	114(3)
C(4B)	1	4678(4)	8877(3)	1626(1)	86(2)
C(5B)	1	3651(4)	8611(3)	1523(1)	76(1)
C(6B)	1	3168(4)	9063(3)	1384(1)	89(2)
C(7B)	1	3925(5)	9142(2)	1212(1)	82(2)
C(8B)	1	4203(4)	8555(2)	1116(1)	66(1)
C(9B)	1	4716(4)	8097(2)	1255(1)	67(1)
C(10B)	1	3947(4)	8002(3)	1431(1)	79(1)
C(11B)	1	5072(5)	7516(2)	1155(1)	82(2)
C(12B)	1	5830(5)	7609(2)	984(1)	77(1)
C(13B)	1	5292(4)	8045(2)	844(1)	65(1)
C(14B)	1	5027(4)	8629(2)	953(1)	68(1)
C(15B)	1	4751(6)	9083(3)	798(1)	89(2)
C(16B)	1	5567(6)	8905(3)	636(1)	94(2)
C(17B)	1	6075(4)	8289(2)	684(1)	70(1)
C(18B)	1	4187(5)	7773(3)	756(1)	85(2)
C(19B)	1	2813(5)	7695(4)	1374(1)	121(3)
C(20B)	1	6263(5)	7908(2)	505(1)	79(1)
C(21B)	1	6687(7)	7280(3)	547(1)	118(3)
C(22B)	1	7103(5)	8231(3)	375(1)	87(2)
C(23B)	1	7020(5)	8032(4)	169(1)	101(2)
C(24B)	1	8066(6)	8157(3)	56(1)	94(2)
C(25B)	1	8852(8)	8154(5)	-246(1)	139(3)
S(1B)	0.51	6509(2)	8626(2)	2051(1)	68(1)
O(1B)	0.51	6055(10)	8094(4)	2138(1)	108(2)
O(2B)	0.51	7687(5)	8766(4)	2062(1)	93(2)
O(3B)	0.51	6275(9)	8729(6)	1830(1)	165(3)
C(31B)	0.51	5705(5)	9278(3)	2128(1)	63(2)
C(32B)	0.51	4705(6)	9211(3)	2232(1)	102(4)
C(33B)	0.51	4110(5)	9719(4)	2292(1)	124(5)
C(34B)	0.51	4513(6)	10293(3)	2249(1)	86(3)
C(35B)	0.51	5513(6)	10359(2)	2146(1)	89(3)
C(36B)	0.51	6109(5)	9852(3)	2085(1)	87(2)
C(37B)	0.51	3906(11)	10862(5)	2308(2)	101(3)
S(1H)	0.49	6588(2)	9022(1)	2032(1)	68(1)

O(1H)	0.49	6477(11)	8431(4)	2128(2)	108(2)
O(2H)	0.49	7663(5)	9333(4)	2025(1)	93(2)
O(3H)	0.49	6267(10)	8785(6)	1823(2)	165(3)
C(31H)	0.49	5549(5)	9501(3)	2125(1)	63(2)
C(32H)	0.49	5060(6)	9333(3)	2295(1)	102(4)
C(33H)	0.49	4251(7)	9704(4)	2380(1)	124(5)
C(34H)	0.49	3931(6)	10242(4)	2294(1)	86(3)
C(35H)	0.49	4419(7)	10411(3)	2124(1)	89(3)
C(36H)	0.49	5228(6)	10040(3)	2039(1)	87(2)
C(37H)	0.49	3136(11)	10684(6)	2389(2)	101(3)
O(24C)	1	8896(6)	1648(5)	121(1)	185(4)
O(25C)	1	7865(5)	1361(3)	-116(1)	137(2)
C(1C)	1	4480(5)	1045(2)	1594(1)	80(2)
C(2C)	1	5471(5)	1361(2)	1681(1)	69(1)
C(3C)	1	5065(4)	1960(2)	1761(1)	67(1)
C(4C)	1	4471(4)	2337(2)	1616(1)	69(1)
C(5C)	1	3480(4)	2013(3)	1517(1)	79(1)
C(6C)	1	2958(4)	2410(3)	1366(1)	91(2)
C(7C)	1	3729(4)	2492(2)	1195(1)	74(1)
C(8C)	1	4072(4)	1889(2)	1112(1)	71(1)
C(9C)	1	4633(4)	1477(2)	1261(1)	69(1)
C(10C)	1	3860(5)	1394(2)	1440(1)	82(2)
C(11C)	1	5045(5)	887(2)	1172(1)	78(1)
C(12C)	1	5807(5)	968(2)	999(1)	79(1)
C(13C)	1	5228(4)	1363(2)	849(1)	72(1)
C(14C)	1	4894(4)	1965(2)	950(1)	68(1)
C(15C)	1	4579(5)	2386(2)	788(1)	75(1)
C(16C)	1	5425(5)	2202(2)	629(1)	82(2)
C(17C)	1	5988(5)	1608(2)	689(1)	72(1)
C(18C)	1	4162(5)	1051(3)	766(1)	87(2)
C(19C)	1	2782(6)	1019(4)	1389(1)	113(2)
C(20C)	1	6249(5)	1198(2)	519(1)	83(2)
C(21C)	1	6749(8)	593(3)	567(1)	117(3)
C(22C)	1	7044(6)	1530(3)	382(1)	95(2)
C(23C)	1	6997(6)	1289(3)	182(1)	99(2)
C(24C)	1	8014(7)	1456(4)	64(1)	101(2)
C(25C)	1	8829(8)	1465(5)	-235(1)	145(4)
S(1C)	0.63	6414(3)	2254(1)	2041(1)	60(1)
O(1C)	0.63	6316(9)	1654(3)	2117(1)	81(2)
O(2C)	0.63	7480(6)	2553(2)	2048(1)	74(2)
O(3C)	0.63	6061(8)	2292(4)	1827(1)	75(1)
C(31C)	0.63	5375(5)	2732(3)	2145(1)	75(2)
C(32C)	0.63	4744(8)	2562(3)	2302(1)	145(5)
C(33C)	0.63	3948(8)	2957(3)	2378(1)	130(6)
C(34C)	0.63	3782(6)	3523(3)	2298(1)	67(2)
C(35C)	0.63	4413(6)	3694(2)	2141(1)	83(3)
C(36C)	0.63	5209(6)	3298(3)	2065(1)	78(2)
C(37C)	0.63	2895(10)	3929(5)	2382(2)	97(4)
S(1I)	0.37	6388(6)	2449(2)	2030(1)	60(1)
O(1I)	0.37	6428(18)	1850(5)	2117(3)	81(2)
O(2I)	0.37	7403(10)	2766(5)	2027(2)	74(2)
O(3I)	0.37	6063(12)	2311(6)	1820(2)	75(1)
C(31I)	0.37	5210(8)	2784(6)	2143(1)	75(2)
C(32I)	0.37	4420(14)	2452(5)	2246(2)	145(5)

C(33I)	0.37	3513(13)	2744(6)	2334(2)	130(6)
C(34I)	0.37	3396(9)	3367(6)	2318(2)	67(2)
C(35I)	0.37	4187(11)	3698(5)	2215(2)	83(3)
C(36I)	0.37	5094(9)	3407(6)	2128(2)	78(2)
C(37I)	0.37	2440(17)	3718(8)	2405(3)	97(4)
O(24D)	1	4066(5)	1833(3)	170(1)	138(2)
O(25D)	1	3105(5)	1752(3)	-94(1)	135(2)
C(1D)	1	-1609(6)	2070(3)	1520(1)	90(2)
C(2D)	1	-518(6)	1867(3)	1616(1)	112(3)
C(3D)	1	-51(5)	2373(3)	1733(1)	106(2)
C(4D)	1	140(4)	2925(2)	1618(1)	83(2)
C(5D)	1	-939(4)	3135(2)	1516(1)	70(1)
C(6D)	1	-642(5)	3694(2)	1399(1)	83(2)
C(7D)	1	107(4)	3552(2)	1230(1)	77(1)
C(8D)	1	-382(4)	3054(2)	1106(1)	61(1)
C(9D)	1	-660(4)	2488(2)	1222(1)	63(1)
C(10D)	1	-1462(4)	2630(2)	1392(1)	72(1)
C(11D)	1	-1075(6)	1965(2)	1096(1)	85(2)
C(12D)	1	-242(6)	1823(2)	935(1)	81(2)
C(13D)	1	8(4)	2388(2)	814(1)	66(1)
C(14D)	1	450(4)	2880(2)	950(1)	63(1)
C(15D)	1	897(5)	3370(2)	821(1)	83(2)
C(16D)	1	1387(5)	3019(2)	654(1)	84(2)
C(17D)	1	1040(4)	2349(2)	676(1)	70(1)
C(18D)	1	-1063(5)	2584(3)	710(1)	93(2)
C(19D)	1	-2647(4)	2828(4)	1328(1)	101(2)
C(20D)	1	935(5)	1997(3)	490(1)	82(2)
C(21D)	1	633(7)	1342(3)	517(1)	102(2)
C(22D)	1	2054(5)	2046(3)	380(1)	94(2)
C(23D)	1	2021(6)	1845(4)	178(1)	108(2)
C(24D)	1	3193(6)	1821(3)	89(1)	95(2)
C(25D)	1	4168(8)	1702(5)	-197(1)	155(4)
S(1D)	0.52	1529(4)	2236(3)	2009(1)	84(1)
O(1D)	0.52	2738(6)	2133(4)	2018(1)	91(2)
O(2D)	0.52	1022(13)	2781(5)	2078(2)	84(2)
O(3D)	0.52	1131(9)	2191(6)	1794(2)	153(3)
C(31D)	0.52	756(5)	1619(3)	2092(1)	66(2)
C(32D)	0.52	1206(5)	1045(3)	2063(1)	96(3)
C(33D)	0.52	622(7)	540(2)	2129(1)	120(5)
C(34D)	0.52	-412(6)	609(3)	2222(1)	75(2)
C(35D)	0.52	-862(5)	1183(3)	2251(1)	92(2)
C(36D)	0.52	-278(6)	1688(2)	2185(1)	76(3)
C(37D)	0.52	-963(11)	40(4)	2292(2)	99(3)
S(1J)	0.48	1210(5)	2046(3)	2019(1)	84(1)
O(1J)	0.48	2312(6)	1771(4)	2011(1)	91(2)
O(2J)	0.48	1193(15)	2630(5)	2102(2)	84(2)
O(3J)	0.48	1047(10)	2168(6)	1805(2)	153(3)
C(31J)	0.48	230(5)	1573(3)	2131(1)	66(2)
C(32J)	0.48	223(6)	954(3)	2099(1)	96(3)
C(33J)	0.48	-600(8)	593(2)	2185(1)	120(5)
C(34J)	0.48	-1416(6)	852(3)	2302(1)	75(2)
C(35J)	0.48	-1409(6)	1472(3)	2333(1)	92(2)
C(36J)	0.48	-586(7)	1833(2)	2248(1)	76(3)
C(37J)	0.48	-2360(10)	479(6)	2387(2)	99(3)

O(24E)	1	4058(5)	8510(3)	168(1)	128(2)
O(25E)	1	3044(5)	8436(3)	-92(1)	136(2)
C(1E)	1	-1529(4)	8772(2)	1533(1)	80(2)
C(2E)	1	-475(6)	8534(3)	1628(1)	93(2)
C(3E)	1	77(5)	9014(4)	1743(1)	107(2)
C(4E)	1	314(5)	9576(3)	1631(1)	110(3)
C(5E)	1	-727(5)	9812(2)	1529(1)	89(2)
C(6E)	1	-405(7)	10371(3)	1417(1)	136(3)
C(7E)	1	332(6)	10212(3)	1246(1)	112(2)
C(8E)	1	-222(4)	9734(2)	1122(1)	80(1)
C(9E)	1	-531(4)	9169(2)	1238(1)	65(1)
C(10E)	1	-1318(4)	9321(2)	1408(1)	71(1)
C(11E)	1	-988(5)	8662(2)	1110(1)	82(2)
C(12E)	1	-185(5)	8511(2)	947(1)	80(2)
C(13E)	1	107(4)	9057(2)	827(1)	70(1)
C(14E)	1	590(4)	9546(2)	964(1)	74(1)
C(15E)	1	1050(7)	10027(3)	834(1)	118(2)
C(16E)	1	1494(5)	9677(2)	663(1)	90(2)
C(17E)	1	1123(4)	9013(2)	689(1)	71(1)
C(18E)	1	-962(5)	9290(4)	725(1)	112(2)
C(19E)	1	-2483(5)	9547(5)	1342(1)	135(3)
C(20E)	1	978(5)	8680(3)	502(1)	84(2)
C(21E)	1	648(7)	8019(3)	525(1)	102(2)
C(22E)	1	2087(5)	8712(3)	389(1)	92(2)
C(23E)	1	2013(6)	8510(4)	186(1)	101(2)
C(24E)	1	3155(6)	8483(3)	91(1)	94(2)
C(25E)	1	4095(8)	8387(5)	-196(1)	150(4)
S(1E)	0.51	1544(2)	8946(2)	2016(1)	72(1)
O(1E)	0.51	2736(6)	8801(4)	2022(1)	99(2)
O(2E)	0.51	1101(9)	9463(4)	2104(1)	96(2)
O(3E)	0.51	1238(9)	8823(6)	1798(1)	171(4)
C(31E)	0.51	787(5)	8299(2)	2091(1)	61(2)
C(32E)	0.51	1267(4)	7732(3)	2062(1)	90(2)
C(33E)	0.51	700(6)	7217(2)	2124(1)	95(3)
C(34E)	0.51	-347(6)	7269(2)	2215(1)	84(2)
C(35E)	0.51	-827(4)	7836(3)	2244(1)	73(2)
C(36E)	0.51	-260(5)	8351(2)	2182(1)	74(2)
C(37E)	0.51	-946(12)	6708(5)	2294(2)	105(3)
S(1K)	0.49	1478(2)	8530(1)	2020(1)	72(1)
O(1K)	0.49	2563(6)	8226(4)	2007(1)	99(2)
O(2K)	0.49	1396(10)	9105(4)	2116(1)	96(2)
O(3K)	0.49	1151(9)	8760(6)	1813(2)	171(4)
C(31K)	0.49	472(5)	8048(3)	2126(1)	61(2)
C(32K)	0.49	188(6)	7498(3)	2044(1)	90(2)
C(33K)	0.49	-568(7)	7110(3)	2135(1)	95(3)
C(34K)	0.49	-1040(5)	7273(3)	2307(1)	84(2)
C(35K)	0.49	-756(5)	7823(3)	2388(1)	73(2)
C(36K)	0.49	1(5)	8211(2)	2298(1)	74(2)
C(37K)	0.49	-1796(12)	6837(6)	2409(2)	105(3)
O(24F)	1	8954(6)	5015(4)	121(1)	167(3)
O(25F)	1	7893(5)	4762(3)	-120(1)	131(2)
C(1F)	1	4308(5)	4253(3)	1574(1)	85(2)
C(2F)	1	5346(5)	4519(3)	1671(1)	101(2)
C(3F)	1	5045(5)	5107(4)	1762(1)	118(3)

C(4F)	1	4527(5)	5528(3)	1623(1)	105(2)
C(5F)	1	3491(5)	5278(3)	1516(1)	86(2)
C(6F)	1	3053(6)	5736(3)	1373(1)	107(2)
C(7F)	1	3843(6)	5817(3)	1206(1)	92(2)
C(8F)	1	4121(4)	5222(2)	1111(1)	69(1)
C(9F)	1	4594(4)	4757(2)	1254(1)	67(1)
C(10F)	1	3770(4)	4666(2)	1424(1)	77(1)
C(11F)	1	4965(5)	4179(2)	1155(1)	83(2)
C(12F)	1	5745(5)	4269(2)	986(1)	79(1)
C(13F)	1	5231(4)	4707(2)	843(1)	69(1)
C(14F)	1	4968(4)	5296(2)	951(1)	69(1)
C(15F)	1	4694(6)	5748(3)	797(1)	91(2)
C(16F)	1	5551(6)	5582(3)	637(1)	89(2)
C(17F)	1	6056(5)	4958(2)	690(1)	78(1)
C(18F)	1	4131(5)	4452(3)	752(1)	89(2)
C(19F)	1	2640(5)	4372(3)	1362(1)	104(2)
C(20F)	1	6271(5)	4567(2)	513(1)	85(2)
C(21F)	1	6682(8)	3941(3)	551(1)	132(3)
C(22F)	1	7108(6)	4889(3)	382(1)	99(2)
C(23F)	1	7018(6)	4692(4)	177(1)	111(2)
C(24F)	1	8067(7)	4844(4)	63(1)	98(2)
C(25F)	1	8885(8)	4846(5)	-239(1)	145(3)
S(1F)	0.53	6213(3)	5533(2)	2049(1)	76(1)
O(1F)	0.53	6208(9)	4937(4)	2130(2)	76(2)
O(2F)	0.53	7278(5)	5835(4)	2054(1)	93(2)
O(3F)	0.53	6044(10)	5415(6)	1836(1)	153(3)
C(31F)	0.53	5195(4)	6010(3)	2153(1)	66(3)
C(32F)	0.53	4322(5)	5732(2)	2253(1)	77(2)
C(33F)	0.53	3462(5)	6078(3)	2334(1)	94(2)
C(34F)	0.53	3476(5)	6703(3)	2315(1)	76(2)
C(35F)	0.53	4349(7)	6982(2)	2214(1)	106(3)
C(36F)	0.53	5209(6)	6635(3)	2133(1)	90(2)
C(37F)	0.53	2501(9)	7070(6)	2392(2)	97(3)
S(1L)	0.47	6519(3)	5310(3)	2044(1)	76(1)
O(1L)	0.47	5940(10)	4786(5)	2123(2)	76(2)
O(2L)	0.47	7721(5)	5430(5)	2060(1)	93(2)
O(3L)	0.47	6133(11)	5375(6)	1830(2)	153(3)
C(31L)	0.47	5724(6)	5935(3)	2118(1)	66(3)
C(32L)	0.47	4666(6)	5877(3)	2205(1)	77(2)
C(33L)	0.47	4070(5)	6389(3)	2262(1)	94(2)
C(34L)	0.47	4531(7)	6959(3)	2231(1)	76(2)
C(35L)	0.47	5589(7)	7017(3)	2144(1)	106(3)
C(36L)	0.47	6185(5)	6505(4)	2088(1)	90(2)
C(37L)	0.47	3923(11)	7518(5)	2308(2)	97(3)

(2) Hydrogen coordinates ($\times 10^4$) and isotropic displacement parameters ($Å^2 \times 10^3$) for C32 H48 O5 S.

	Occ.	x	y	z	U(eq)
H(1A)	1	-2339	5557	1626	92
H(1B)	1	-2166	5165	1444	92
H(2A)	1	-1045	4787	1694	78
H(2B)	1	-264	4979	1525	78
H(3A)	0.57	-600	5650	1859	77
H(3G)	0.43	-593	5648	1860	77
H(4A)	1	793	6036	1559	75
H(4B)	1	536	6402	1742	75
H(5A)	1	-1320	6572	1650	87
H(6A)	1	-1044	7240	1409	92
H(6B)	1	67	7255	1532	92
H(7A)	1	1044	6678	1317	83
H(7B)	1	507	7228	1210	83
H(8A)	1	-924	6633	1087	76
H(9A)	1	4	5666	1300	75
H(11A)	1	-1376	5027	1180	83
H(11B)	1	-1895	5552	1060	83
H(12A)	1	-790	4953	865	80
H(12B)	1	269	5018	998	80
H(14A)	1	1162	6018	1044	71
H(15A)	1	1705	6913	927	92
H(15B)	1	516	7026	828	92
H(16A)	1	2322	6384	682	89
H(16B)	1	1200	6571	574	89
H(17A)	1	1620	5498	774	75
H(18A)	1	-1300	5780	645	111
H(18B)	1	-770	6426	669	111
H(18C)	1	-1607	6172	821	111
H(19A)	1	-2966	6037	1268	159
H(19B)	1	-2401	6677	1285	159
H(19C)	1	-3053	6398	1457	159
H(20A)	1	300	5623	442	82
H(21A)	1	-180	4740	601	137
H(21B)	1	1103	4535	597	137
H(21C)	1	411	4588	409	137
H(22A)	1	2264	5855	403	96
H(22B)	1	2566	5196	465	96
H(23A)	1	1447	5516	129	115
H(23B)	1	1570	4841	194	115
H(25A)	1	3892	5128	-313	213
H(25B)	1	4448	4783	-144	213
H(25C)	1	4513	5490	-154	213
H(32A)	0.57	429	4095	1929	82
H(33A)	0.57	-854	3457	2079	87
H(35A)	0.57	-1126	4643	2505	84
H(36A)	0.57	157	5280	2355	76

H(37A)	0.57	-1792	3600	2542	131
H(37B)	0.57	-1866	3177	2366	131
H(37C)	0.57	-2713	3721	2386	131
H(32G)	0.43	699	4069	2025	82
H(33G)	0.43	-684	3487	2173	87
H(35G)	0.43	-1945	4974	2421	84
H(36G)	0.43	-561	5557	2274	76
H(37D)	0.43	-2308	3793	2531	131
H(37E)	0.43	-2400	3409	2347	131
H(37F)	0.43	-3126	4000	2369	131
H(1C)	1	3960	7508	1674	142
H(1D)	1	4747	7230	1519	142
H(2C)	1	6162	7933	1583	161
H(2D)	1	5829	7599	1771	161
H(3B)	0.51	4688	8398	1866	136
H(3H)	0.49	4700	8401	1868	136
H(4C)	1	5247	8998	1535	103
H(4D)	1	4433	9238	1693	103
H(5B)	1	3057	8533	1617	91
H(6C)	1	3079	9450	1446	107
H(6D)	1	2417	8929	1344	107
H(7C)	1	3544	9407	1124	98
H(7D)	1	4632	9335	1250	98
H(8B)	1	3489	8385	1066	79
H(9B)	1	5425	8281	1302	81
H(11C)	1	5474	7260	1244	99
H(11D)	1	4388	7303	1116	99
H(12C)	1	5961	7223	923	92
H(12D)	1	6565	7766	1024	92
H(14B)	1	5752	8760	1009	81
H(15C)	1	4896	9493	840	107
H(15D)	1	3959	9049	759	107
H(16C)	1	5150	8885	519	113
H(16D)	1	6170	9204	624	113
H(17B)	1	6830	8362	739	84
H(18D)	1	3855	8059	671	127
H(18E)	1	3651	7682	855	127
H(18F)	1	4374	7409	690	127
H(19D)	1	2973	7314	1315	182
H(19E)	1	2405	7950	1288	182
H(19F)	1	2356	7629	1485	182
H(20B)	1	5529	7873	440	95
H(21D)	1	6786	7064	431	178
H(21E)	1	6140	7073	624	178
H(21F)	1	7405	7304	612	178
H(22C)	1	7874	8157	420	105
H(22D)	1	6965	8662	382	105
H(23C)	1	6865	7601	166	121
H(23D)	1	6377	8237	112	121
H(25D)	1	8629	8082	-374	209
H(25E)	1	9421	7864	-210	209
H(25F)	1	9161	8554	-235	209
H(32B)	0.51	4435	8827	2261	122
H(33B)	0.51	3441	9674	2362	149

H(35B)	0.51	5783	10743	2117	107
H(36B)	0.51	6778	9896	2016	104
H(37G)	0.51	3849	11130	2203	151
H(37H)	0.51	4329	11054	2407	151
H(37I)	0.51	3154	10763	2352	151
H(32H)	0.49	5275	8973	2352	122
H(33H)	0.49	3925	9591	2494	149
H(35H)	0.49	4205	10771	2067	107
H(36H)	0.49	5555	10153	1926	104
H(37J)	0.49	3540	11052	2415	151
H(37K)	0.49	2862	10513	2505	151
H(37L)	0.49	2501	10768	2308	151
H(1E)	1	3934	949	1692	95
H(1F)	1	4747	666	1541	95
H(2E)	1	6058	1432	1587	82
H(2F)	1	5794	1113	1780	82
H(3C)	0.63	4545	1885	1867	80
H(3I)	0.37	4557	1890	1869	80
H(4E)	1	5027	2461	1522	83
H(4F)	1	4179	2699	1676	83
H(5C)	1	2886	1938	1611	95
H(6E)	1	2792	2804	1419	109
H(6F)	1	2240	2233	1325	109
H(7E)	1	3330	2728	1101	89
H(7F)	1	4409	2713	1232	89
H(8C)	1	3382	1688	1065	85
H(9C)	1	5321	1689	1303	83
H(11E)	1	4383	648	1137	94
H(11F)	1	5466	660	1266	94
H(12E)	1	6523	1153	1036	95
H(12F)	1	5977	575	945	95
H(14C)	1	5602	2125	1004	81
H(15E)	1	4683	2806	823	90
H(15F)	1	3793	2325	749	90
H(16E)	1	5017	2148	511	99
H(16F)	1	5999	2513	612	99
H(17C)	1	6726	1714	745	86
H(18G)	1	3818	1309	674	131
H(18H)	1	3622	972	865	131
H(18I)	1	4383	677	708	131
H(19G)	1	2357	1224	1293	169
H(19H)	1	2312	972	1498	169
H(19I)	1	3010	628	1344	169
H(20C)	1	5526	1126	453	100
H(21G)	1	6879	367	454	176
H(21H)	1	6227	376	647	176
H(21I)	1	7461	649	632	176
H(22E)	1	6841	1955	381	114
H(22F)	1	7822	1498	428	114
H(23E)	1	6935	853	186	118
H(23F)	1	6313	1443	122	118
H(25G)	1	8638	1356	-362	218
H(25H)	1	9461	1223	-193	218
H(25I)	1	9037	1884	-230	218

H(32C)	0.63	4855	2183	2355	174
H(33C)	0.63	3526	2843	2483	156
H(35C)	0.63	4302	4073	2088	100
H(36C)	0.63	5631	3412	1960	93
H(37M)	0.63	3085	4342	2356	146
H(37N)	0.63	2868	3868	2516	146
H(37O)	0.63	2162	3836	2329	146
H(32I)	0.37	4498	2035	2256	174
H(33I)	0.37	2984	2522	2403	156
H(35I)	0.37	4109	4115	2205	100
H(36I)	0.37	5623	3629	2059	93
H(37P)	0.37	2234	4047	2324	146
H(37Q)	0.37	2681	3874	2525	146
H(37R)	0.37	1791	3458	2423	146
H(1G)	1	-2175	2161	1616	108
H(1H)	1	-1901	1738	1445	108
H(2G)	1	-673	1520	1695	134
H(2H)	1	41	1749	1522	134
H(3D)	0.52	-544	2457	1841	127
H(3J)	0.48	-572	2462	1837	127
H(4G)	1	735	2844	1527	99
H(4H)	1	407	3248	1700	99
H(5D)	1	-1507	3252	1610	84
H(6G)	1	-1345	3880	1356	99
H(6H)	1	-250	3983	1479	99
H(7G)	1	857	3430	1274	92
H(7H)	1	200	3916	1156	92
H(8D)	1	-1090	3202	1048	73
H(9D)	1	67	2354	1277	76
H(11G)	1	-1176	1606	1172	102
H(11H)	1	-1813	2071	1043	102
H(12G)	1	-566	1510	856	97
H(12H)	1	469	1672	987	97
H(14D)	1	1120	2707	1012	76
H(15G)	1	1486	3606	883	99
H(15H)	1	286	3638	782	99
H(16G)	1	2213	3056	652	100
H(16H)	1	1086	3180	538	100
H(17D)	1	1660	2156	747	84
H(18J)	1	-1306	2267	628	140
H(18K)	1	-901	2941	638	140
H(18L)	1	-1658	2670	799	140
H(19J)	1	-2978	2518	1251	152
H(19K)	1	-2584	3194	1256	152
H(19L)	1	-3123	2897	1436	152
H(20D)	1	330	2185	415	99
H(21J)	1	560	1150	397	153
H(21K)	1	-78	1312	584	153
H(21L)	1	1225	1146	588	153
H(22G)	1	2301	2465	383	112
H(22H)	1	2629	1810	445	112
H(23G)	1	1543	2121	107	130
H(23H)	1	1675	1447	171	130
H(25J)	1	4006	1641	-328	232

H(25K)	1	4600	1366	-150	232
H(25L)	1	4602	2067	-181	232
H(32D)	0.52	1898	998	2001	115
H(33D)	0.52	923	156	2110	144
H(35D)	0.52	-1554	1230	2313	111
H(36D)	0.52	-579	2072	2204	91
H(37S)	0.52	-1773	100	2301	149
H(37T)	0.52	-658	-62	2413	149
H(37U)	0.52	-809	-282	2205	149
H(32J)	0.48	768	780	2021	115
H(33J)	0.48	-605	179	2164	144
H(35J)	0.48	-1955	1646	2412	111
H(36J)	0.48	-581	2247	2269	91
H(37V)	0.48	-3082	672	2365	149
H(37W)	0.48	-2238	444	2520	149
H(37X)	0.48	-2361	84	2332	149
H(1I)	1	-2083	8881	1629	95
H(1J)	1	-1861	8453	1458	95
H(2I)	1	-678	8196	1708	112
H(2J)	1	59	8391	1534	112
H(3E)	0.51	-386	9107	1854	128
H(3K)	0.49	-418	9114	1850	128
H(4I)	1	910	9491	1540	132
H(4J)	1	594	9888	1715	132
H(5E)	1	-1279	9939	1625	106
H(6I)	1	11	10649	1497	163
H(6J)	1	-1095	10573	1375	163
H(7I)	1	465	10575	1173	135
H(7J)	1	1067	10065	1290	135
H(8E)	1	-921	9901	1066	96
H(9E)	1	187	9020	1291	78
H(11I)	1	-1106	8301	1185	99
H(11J)	1	-1724	8783	1060	99
H(12I)	1	516	8340	997	95
H(12J)	1	-541	8207	868	95
H(14E)	1	1256	9364	1025	89
H(15I)	1	1663	10251	893	141
H(15J)	1	451	10306	797	141
H(16I)	1	2321	9705	657	108
H(16J)	1	1174	9841	549	108
H(17E)	1	1744	8810	756	85
H(18M)	1	-1242	8982	642	168
H(18N)	1	-770	9644	654	168
H(18O)	1	-1542	9388	815	168
H(19M)	1	-2954	9633	1449	202
H(19N)	1	-2842	9242	1266	202
H(19O)	1	-2385	9908	1269	202
H(20E)	1	376	8882	430	101
H(21M)	1	549	7838	404	154
H(21N)	1	-55	7991	594	154
H(21O)	1	1241	7810	592	154
H(22I)	1	2359	9125	392	111
H(22J)	1	2655	8465	452	111
H(23I)	1	1661	8114	181	122

H(23J)	1	1524	8788	118	122
H(25M)	1	3927	8349	-328	226
H(25N)	1	4509	8038	-155	226
H(25O)	1	4550	8742	-176	226
H(32E)	0.51	1967	7697	2001	108
H(33E)	0.51	1022	6838	2105	114
H(35E)	0.51	-1528	7871	2305	87
H(36E)	0.51	-582	8730	2201	89
H(37Y)	0.51	-1598	6614	2217	157
H(37Z)	0.51	-1191	6786	2420	157
H(370)	0.51	-425	6373	2293	157
H(32K)	0.49	504	7389	1929	108
H(33K)	0.49	-758	6742	2080	114
H(35K)	0.49	-1071	7932	2503	87
H(36K)	0.49	191	8579	2353	89
H(371)	0.49	-1968	6994	2532	157
H(372)	0.49	-1411	6456	2421	157
H(373)	0.49	-2493	6782	2340	157
H(1K)	1	3734	4162	1668	102
H(1L)	1	4527	3875	1515	102
H(2K)	1	5624	4240	1765	121
H(2L)	1	5951	4582	1580	121
H(3F)	0.53	4500	5034	1864	142
H(3L)	0.47	4520	5040	1867	142
H(4K)	1	5109	5642	1533	126
H(4L)	1	4294	5892	1689	126
H(5F)	1	2879	5209	1608	103
H(6K)	1	2310	5606	1328	128
H(6L)	1	2954	6123	1435	128
H(7K)	1	4547	6005	1248	110
H(7L)	1	3486	6085	1116	110
H(8F)	1	3410	5059	1059	83
H(9F)	1	5292	4937	1305	80
H(11K)	1	5355	3924	1245	100
H(11L)	1	4287	3964	1114	100
H(12K)	1	5881	3883	926	95
H(12L)	1	6475	4425	1029	95
H(14F)	1	5690	5427	1008	83
H(15K)	1	4815	6159	841	109
H(15L)	1	3909	5706	755	109
H(16K)	1	5159	5561	517	106
H(16L)	1	6152	5882	629	106
H(17F)	1	6798	5029	750	93
H(18P)	1	4311	4088	685	133
H(18Q)	1	3820	4744	667	133
H(18R)	1	3581	4364	849	133
H(19P)	1	2796	3991	1303	155
H(19Q)	1	2256	4633	1275	155
H(19R)	1	2163	4309	1470	155
H(20F)	1	5542	4533	446	102
H(21P)	1	6150	3739	632	198
H(21Q)	1	7418	3958	611	198
H(21R)	1	6743	3723	435	198
H(22K)	1	7880	4814	426	119

H(22L)	1	6972	5321	390	119
H(23K)	1	6893	4260	172	133
H(23L)	1	6360	4887	120	133
H(25P)	1	8685	4759	-367	217
H(25Q)	1	9484	4579	-199	217
H(25R)	1	9144	5257	-229	217
H(32F)	0.53	4313	5314	2266	92
H(33F)	0.53	2878	5892	2401	113
H(35F)	0.53	4359	7400	2202	127
H(36F)	0.53	5794	6822	2066	108
H(374)	0.53	2771	7315	2495	146
H(375)	0.53	1912	6803	2437	146
H(376)	0.53	2197	7325	2295	146
H(32L)	0.47	4358	5495	2226	92
H(33L)	0.47	3362	6350	2320	113
H(35L)	0.47	5897	7399	2124	127
H(36L)	0.47	6893	6544	2029	108
H(377)	0.47	3126	7431	2326	146
H(378)	0.47	4005	7846	2221	146
H(379)	0.47	4255	7629	2427	146

(3) Anisotropic parameters ($Å^2 \times 10^3$) for C32 H48 O5 S.

The anisotropic displacement factor exponent takes the form:

$$-2\,\pi^2\,[\,h^2\,a^{*2}\,U11 + \ldots + 2\,h\,k\,a^*\,b^*\,U12\,]$$

	U11	U22	U33	U23	U13	U12
O(24A)	78(3)	203(6)	91(3)	-13(3)	3(2)	8(4)
O(25A)	114(4)	151(4)	70(2)	-9(2)	32(2)	-15(3)
C(1A)	55(3)	104(4)	71(3)	-5(3)	21(2)	-21(3)
C(2A)	73(3)	60(3)	63(3)	1(2)	21(2)	-20(2)
C(3A)	78(3)	56(2)	57(2)	4(2)	23(2)	-5(2)
C(4A)	80(3)	46(2)	61(2)	3(2)	13(2)	-9(2)
C(5A)	96(4)	67(3)	55(3)	1(2)	13(2)	13(3)
C(6A)	113(4)	49(3)	68(3)	0(2)	2(3)	15(3)
C(7A)	96(4)	48(2)	64(3)	10(2)	-4(2)	-9(2)
C(8A)	75(3)	60(3)	54(2)	-2(2)	1(2)	-1(2)
C(9A)	60(3)	68(3)	60(3)	-3(2)	13(2)	-3(2)
C(10A)	65(3)	86(3)	69(3)	-7(2)	21(2)	5(3)
C(11A)	63(3)	68(3)	77(3)	4(2)	12(2)	-19(2)
C(12A)	81(3)	60(3)	61(3)	0(2)	7(2)	-12(2)
C(13A)	69(3)	58(2)	60(2)	1(2)	8(2)	-1(2)
C(14A)	63(3)	61(3)	54(2)	5(2)	0(2)	-3(2)
C(15A)	96(4)	71(3)	63(3)	7(2)	0(3)	-19(3)
C(16A)	84(3)	79(3)	60(3)	8(2)	8(2)	-17(3)
C(17A)	67(3)	65(3)	57(2)	7(2)	1(2)	0(2)
C(18A)	71(3)	83(3)	67(3)	-3(2)	-5(2)	5(3)
C(19A)	79(4)	129(6)	110(5)	-9(4)	22(3)	29(4)
C(20A)	79(3)	64(3)	63(3)	9(2)	5(2)	3(2)
C(21A)	124(5)	75(3)	75(3)	-10(3)	16(3)	-11(3)
C(22A)	81(3)	96(4)	62(3)	-1(3)	15(3)	-6(3)
C(23A)	84(4)	130(5)	73(3)	5(3)	9(3)	10(4)
C(24A)	98(4)	89(4)	66(3)	-10(3)	18(3)	-7(3)
C(25A)	156(8)	183(9)	88(5)	-22(5)	42(5)	-43(7)
S(1A)	73(1)	76(1)	73(1)	7(1)	10(1)	-14(1)
O(1A)	63(3)	103(5)	97(7)	16(5)	14(3)	1(2)
O(2A)	87(3)	78(2)	71(3)	-16(2)	6(2)	5(2)
O(3A)	76(2)	70(2)	76(2)	10(2)	22(2)	6(2)
C(31A)	30(3)	87(5)	57(3)	7(3)	10(2)	9(3)
C(32A)	80(4)	70(4)	55(6)	-1(3)	23(4)	11(3)
C(33A)	99(4)	73(4)	46(6)	-17(3)	-17(4)	-15(3)
C(34A)	63(5)	74(5)	49(3)	-12(3)	6(3)	-2(4)
C(35A)	64(5)	101(6)	46(3)	-4(3)	10(3)	1(4)
C(36A)	74(5)	70(5)	45(3)	-11(3)	9(3)	8(3)
C(37A)	76(8)	102(9)	84(4)	-4(6)	16(6)	-23(6)
S(1G)	73(1)	76(1)	73(1)	7(1)	10(1)	-14(1)
O(1G)	63(3)	103(5)	97(7)	16(5)	14(3)	1(2)
O(2G)	87(3)	78(2)	71(3)	-16(2)	6(2)	5(2)
O(3G)	76(2)	70(2)	76(2)	10(2)	22(2)	6(2)
C(31G)	30(3)	87(5)	57(3)	7(3)	10(2)	9(3)

C(32G)	80(4)	70(4)	55(6)	-1(3)	23(4)	11(3)
C(33G)	99(4)	73(4)	46(6)	-17(3)	-17(4)	-15(3)
C(34G)	63(5)	74(5)	49(3)	-12(3)	6(3)	-2(4)
C(35G)	64(5)	101(6)	46(3)	-4(3)	10(3)	1(4)
C(36G)	74(5)	70(5)	45(3)	-11(3)	9(3)	8(3)
C(37G)	76(8)	102(9)	84(4)	-4(6)	16(6)	-23(6)
O(24B)	102(4)	237(8)	109(4)	5(4)	16(3)	-27(5)
O(25B)	127(4)	173(5)	72(3)	-15(3)	14(3)	27(4)
C(1B)	120(6)	134(6)	99(5)	40(4)	38(4)	27(5)
C(2B)	77(4)	248(11)	77(4)	40(5)	16(3)	59(6)
C(3B)	43(3)	224(9)	74(4)	-16(5)	9(3)	2(4)
C(4B)	56(3)	132(5)	71(3)	-10(3)	10(2)	-15(3)
C(5B)	37(2)	111(4)	80(3)	-8(3)	12(2)	-4(2)
C(6B)	54(3)	101(4)	112(4)	-19(3)	3(3)	11(3)
C(7B)	73(3)	85(4)	87(3)	-9(3)	-5(3)	19(3)
C(8B)	48(2)	74(3)	77(3)	-11(2)	-7(2)	-1(2)
C(9B)	45(2)	82(3)	75(3)	-5(2)	-2(2)	-5(2)
C(10B)	59(3)	93(4)	83(3)	-3(3)	8(3)	-8(3)
C(11B)	94(4)	70(3)	82(3)	12(2)	1(3)	6(3)
C(12B)	83(3)	69(3)	79(3)	-3(2)	4(3)	14(3)
C(13B)	60(3)	63(3)	71(3)	-8(2)	-4(2)	-3(2)
C(14B)	59(3)	58(3)	86(3)	-7(2)	-3(2)	-2(2)
C(15B)	103(4)	78(4)	86(4)	10(3)	9(3)	17(3)
C(16B)	110(5)	79(4)	94(4)	17(3)	11(4)	1(3)
C(17B)	70(3)	70(3)	71(3)	-3(2)	-3(2)	-1(2)
C(18B)	86(4)	85(4)	84(3)	-9(3)	-12(3)	-23(3)
C(19B)	87(4)	147(7)	131(6)	-20(5)	30(4)	-56(5)
C(20B)	86(4)	80(3)	70(3)	-6(2)	0(3)	-3(3)
C(21B)	156(7)	91(5)	108(5)	-25(4)	40(5)	15(5)
C(22B)	85(4)	102(4)	74(3)	-8(3)	12(3)	-6(3)
C(23B)	95(4)	146(6)	62(3)	-22(3)	-2(3)	5(4)
C(24B)	97(5)	109(5)	77(4)	6(3)	8(3)	5(4)
C(25B)	157(8)	171(8)	89(5)	6(5)	44(5)	48(7)
S(1B)	49(1)	90(2)	66(1)	-6(1)	5(1)	-11(1)
O(1B)	148(7)	79(6)	98(4)	6(4)	1(4)	-21(4)
O(2B)	48(2)	139(5)	92(3)	-18(4)	1(2)	-25(4)
O(3B)	47(2)	381(10)	67(2)	-43(4)	13(2)	-13(4)
C(31B)	57(3)	64(6)	67(3)	20(4)	-4(3)	-25(4)
C(32B)	59(6)	85(6)	161(9)	9(6)	41(6)	-45(4)
C(33B)	61(4)	104(6)	208(15)	-17(7)	17(7)	-9(4)
C(34B)	63(6)	91(5)	103(6)	14(4)	-18(5)	-22(5)
C(35B)	129(7)	79(5)	60(4)	20(3)	4(5)	-25(6)
C(36B)	98(6)	113(6)	49(4)	12(4)	24(4)	-10(5)
C(37B)	98(7)	97(7)	107(8)	3(5)	6(5)	22(6)
S(1H)	49(1)	90(2)	66(1)	-6(1)	5(1)	-11(1)
O(1H)	148(7)	79(6)	98(4)	6(4)	1(4)	-21(4)
O(2H)	48(2)	139(5)	92(3)	-18(4)	1(2)	-25(4)
O(3H)	47(2)	381(10)	67(2)	-43(4)	13(2)	-13(4)
C(31H)	57(3)	64(6)	67(3)	20(4)	-4(3)	-25(4)
C(32H)	59(6)	85(6)	161(9)	9(6)	41(6)	-45(4)
C(33H)	61(4)	104(6)	208(15)	-17(7)	17(7)	-9(4)
C(34H)	63(6)	91(5)	103(6)	14(4)	-18(5)	-22(5)
C(35H)	129(7)	79(5)	60(4)	20(3)	4(5)	-25(6)
C(36H)	98(6)	113(6)	49(4)	12(4)	24(4)	-10(5)

C(37H)	98(7)	97(7)	107(8)	3(5)	6(5)	22(6)
O(24C)	120(5)	307(11)	128(5)	24(6)	7(4)	-64(6)
O(25C)	146(5)	189(6)	76(3)	-25(3)	15(3)	14(4)
C(1C)	102(4)	70(3)	67(3)	-4(2)	7(3)	-25(3)
C(2C)	94(4)	52(2)	59(3)	-4(2)	0(2)	0(2)
C(3C)	84(3)	55(3)	60(3)	-8(2)	6(2)	-2(2)
C(4C)	74(3)	57(3)	76(3)	-9(2)	11(2)	5(2)
C(5C)	58(3)	97(4)	82(3)	-8(3)	11(3)	0(3)
C(6C)	52(3)	120(5)	101(4)	-11(4)	-3(3)	19(3)
C(7C)	59(3)	73(3)	90(3)	0(2)	-3(3)	9(2)
C(8C)	57(3)	71(3)	84(3)	-5(2)	-2(2)	-2(2)
C(9C)	72(3)	62(3)	73(3)	-12(2)	2(2)	-11(2)
C(10C)	83(4)	84(4)	79(3)	-12(3)	3(3)	-22(3)
C(11C)	97(4)	61(3)	77(3)	2(2)	-4(3)	-11(3)
C(12C)	91(4)	70(3)	75(3)	-12(2)	-13(3)	15(3)
C(13C)	70(3)	68(3)	79(3)	-12(2)	0(2)	-7(2)
C(14C)	53(2)	65(3)	85(3)	-6(2)	-11(2)	-3(2)
C(15C)	72(3)	71(3)	82(3)	-1(2)	-3(3)	-6(2)
C(16C)	94(4)	73(3)	80(3)	4(3)	-3(3)	-8(3)
C(17C)	71(3)	72(3)	73(3)	-10(2)	-3(2)	-11(2)
C(18C)	85(4)	78(3)	98(4)	-12(3)	-6(3)	-22(3)
C(19C)	99(5)	138(6)	100(4)	5(4)	0(4)	-48(5)
C(20C)	94(4)	89(4)	68(3)	-8(3)	4(3)	-13(3)
C(21C)	167(7)	89(5)	96(4)	-8(3)	37(5)	15(5)
C(22C)	97(4)	105(5)	84(4)	-17(3)	9(3)	-12(4)
C(23C)	94(4)	120(5)	81(4)	-13(3)	-1(3)	-6(4)
C(24C)	106(5)	109(5)	87(5)	1(4)	-2(4)	0(4)
C(25C)	138(7)	210(10)	89(5)	16(5)	40(5)	35(7)
S(1C)	90(1)	21(2)	68(1)	-4(1)	-12(1)	22(1)
O(1C)	128(4)	35(4)	81(2)	28(4)	18(3)	-18(4)
O(2C)	86(3)	44(4)	93(3)	-7(4)	-34(2)	24(3)
O(3C)	82(2)	76(2)	67(2)	-13(2)	-1(2)	-3(2)
C(31C)	59(3)	94(4)	72(3)	-22(3)	-22(3)	33(3)
C(32C)	256(13)	146(7)	32(6)	32(5)	50(7)	107(8)
C(33C)	200(13)	122(9)	68(6)	22(6)	52(7)	76(9)
C(34C)	62(6)	98(6)	42(3)	7(3)	13(4)	15(4)
C(35C)	84(6)	90(4)	75(7)	-20(5)	15(5)	29(4)
C(36C)	63(4)	67(5)	102(7)	-38(4)	26(4)	-1(3)
C(37C)	112(10)	103(8)	77(5)	11(6)	26(6)	24(7)
S(1I)	90(1)	21(2)	68(1)	-4(1)	-12(1)	22(1)
O(1I)	128(4)	35(4)	81(2)	28(4)	18(3)	-18(4)
O(2I)	86(3)	44(4)	93(3)	-7(4)	-34(2)	24(3)
O(3I)	82(2)	76(2)	67(2)	-13(2)	-1(2)	-3(2)
C(31I)	59(3)	94(4)	72(3)	-22(3)	-22(3)	33(3)
C(32I)	256(13)	146(7)	32(6)	32(5)	50(7)	107(8)
C(33I)	200(13)	122(9)	68(6)	22(6)	52(7)	76(9)
C(34I)	62(6)	98(6)	42(3)	7(3)	13(4)	15(4)
C(35I)	84(6)	90(4)	75(7)	-20(5)	15(5)	29(4)
C(36I)	63(4)	67(5)	102(7)	-38(4)	26(4)	-1(3)
C(37I)	112(10)	103(8)	77(5)	11(6)	26(6)	24(7)
O(24D)	107(4)	213(7)	93(3)	-19(4)	0(3)	0(4)
O(25D)	128(4)	208(6)	69(3)	8(3)	15(3)	-45(4)
C(1D)	112(5)	79(4)	79(3)	-19(3)	20(3)	-19(3)
C(2D)	178(8)	81(4)	76(4)	9(3)	38(4)	45(4)

C(3D)	111(5)	149(6)	57(3)	-4(3)	-5(3)	76(5)
C(4D)	75(3)	100(4)	74(3)	-24(3)	-21(3)	34(3)
C(5D)	56(2)	71(3)	82(3)	-22(2)	-10(2)	7(2)
C(6D)	85(4)	56(3)	108(4)	-20(3)	-9(3)	17(2)
C(7D)	67(3)	53(3)	109(4)	-6(2)	-13(3)	-9(2)
C(8D)	56(2)	55(2)	71(3)	0(2)	-21(2)	-3(2)
C(9D)	64(3)	68(3)	58(3)	-8(2)	-8(2)	-12(2)
C(10D)	62(3)	79(3)	76(3)	-10(2)	-4(2)	-21(2)
C(11D)	121(5)	71(3)	65(3)	-4(2)	6(3)	-41(3)
C(12D)	121(5)	61(3)	61(3)	-9(2)	4(3)	-25(3)
C(13D)	76(3)	66(3)	58(2)	3(2)	-13(2)	-15(2)
C(14D)	52(2)	59(3)	79(3)	14(2)	-17(2)	-11(2)
C(15D)	89(4)	68(3)	91(4)	15(3)	1(3)	-23(3)
C(16D)	84(4)	87(4)	80(3)	18(3)	-7(3)	-21(3)
C(17D)	69(3)	77(3)	63(3)	16(2)	-5(2)	-7(2)
C(18D)	74(3)	132(5)	74(3)	-5(3)	-18(3)	-14(4)
C(19D)	58(3)	143(6)	102(4)	-11(4)	-2(3)	-17(3)
C(20D)	93(4)	92(4)	61(3)	15(3)	-2(3)	-9(3)
C(21D)	138(6)	87(4)	81(4)	-12(3)	20(4)	-18(4)
C(22D)	99(4)	110(5)	72(3)	7(3)	9(3)	-13(4)
C(23D)	102(5)	159(7)	64(3)	8(4)	0(3)	-1(5)
C(24D)	100(5)	110(5)	75(4)	2(3)	7(3)	-7(4)
C(25D)	145(8)	225(11)	95(5)	-4(6)	39(5)	-45(8)
S(1D)	70(3)	113(4)	70(1)	7(2)	6(2)	35(2)
O(1D)	56(4)	98(6)	119(4)	-21(4)	-10(3)	18(3)
O(2D)	79(5)	77(5)	96(4)	33(4)	-15(3)	35(4)
O(3D)	151(5)	235(6)	71(3)	-1(3)	15(3)	137(5)
C(31D)	82(7)	66(4)	51(4)	12(3)	20(4)	4(5)
C(32D)	94(6)	99(6)	95(5)	-45(5)	-12(5)	37(6)
C(33D)	184(13)	79(6)	97(7)	-32(5)	-41(8)	5(8)
C(34D)	64(4)	98(6)	64(4)	-3(4)	-9(4)	13(4)
C(35D)	78(6)	112(7)	87(6)	4(5)	0(4)	21(5)
C(36D)	76(6)	71(5)	80(7)	-1(4)	-3(5)	25(4)
C(37D)	112(7)	79(6)	108(6)	9(5)	-32(5)	-9(5)
S(1J)	70(3)	113(4)	70(1)	7(2)	6(2)	35(2)
O(1J)	56(4)	98(6)	119(4)	-21(4)	-10(3)	18(3)
O(2J)	79(5)	77(5)	96(4)	33(4)	-15(3)	35(4)
O(3J)	151(5)	235(6)	71(3)	-1(3)	15(3)	137(5)
C(31J)	82(7)	66(4)	51(4)	12(3)	20(4)	4(5)
C(32J)	94(6)	99(6)	95(5)	-45(5)	-12(5)	37(6)
C(33J)	184(13)	79(6)	97(7)	-32(5)	-41(8)	5(8)
C(34J)	64(4)	98(6)	64(4)	-3(4)	-9(4)	13(4)
C(35J)	78(6)	112(7)	87(6)	4(5)	0(4)	21(5)
C(36J)	76(6)	71(5)	80(7)	-1(4)	-3(5)	25(4)
C(37J)	112(7)	79(6)	108(6)	9(5)	-32(5)	-9(5)
O(24E)	99(3)	197(6)	89(3)	-10(3)	2(3)	11(4)
O(25E)	127(4)	213(6)	67(3)	11(3)	9(3)	-58(4)
C(1E)	73(3)	90(4)	76(3)	-5(3)	5(3)	-38(3)
C(2E)	130(6)	87(4)	61(3)	-1(3)	15(3)	9(4)
C(3E)	58(3)	191(8)	71(3)	-39(4)	-2(3)	24(4)
C(4E)	63(3)	151(6)	118(5)	-75(5)	30(3)	-40(4)
C(5E)	73(3)	72(3)	121(4)	-16(3)	42(3)	-7(3)
C(6E)	156(7)	54(3)	199(7)	-20(4)	96(6)	-5(4)
C(7E)	134(5)	55(3)	149(6)	-14(3)	68(5)	-25(3)

C(8E)	62(3)	64(3)	114(4)	15(3)	19(3)	3(2)
C(9E)	42(2)	67(3)	85(3)	8(2)	0(2)	-10(2)
C(10E)	39(2)	80(3)	93(3)	10(2)	5(2)	-3(2)
C(11E)	76(3)	89(4)	82(3)	15(3)	-4(3)	-27(3)
C(12E)	97(4)	71(3)	71(3)	5(2)	-4(3)	-30(3)
C(13E)	58(3)	78(3)	74(3)	21(2)	-1(2)	-9(2)
C(14E)	61(3)	59(3)	102(4)	13(2)	8(3)	-2(2)
C(15E)	130(6)	69(4)	153(6)	19(4)	68(5)	-17(4)
C(16E)	83(4)	82(4)	107(4)	14(3)	21(3)	-7(3)
C(17E)	56(3)	72(3)	84(3)	23(2)	0(2)	0(2)
C(18E)	60(3)	188(7)	89(4)	37(4)	1(3)	27(4)
C(19E)	52(3)	224(10)	127(5)	44(6)	14(3)	27(5)
C(20E)	87(4)	96(4)	71(3)	26(3)	-11(3)	1(3)
C(21E)	134(6)	92(4)	82(4)	3(3)	-2(4)	-18(4)
C(22E)	96(4)	107(5)	74(3)	12(3)	3(3)	-8(4)
C(23E)	94(4)	141(6)	70(4)	1(4)	-10(3)	-7(4)
C(24E)	103(5)	96(4)	83(4)	10(3)	-1(4)	-1(4)
C(25E)	154(8)	206(10)	91(5)	-10(5)	38(5)	-73(7)
S(1E)	59(1)	86(1)	71(1)	5(1)	1(1)	17(1)
O(1E)	67(3)	126(5)	103(4)	10(4)	6(3)	24(4)
O(2E)	119(6)	97(6)	70(3)	-1(5)	11(3)	2(5)
O(3E)	73(3)	375(11)	66(3)	-16(4)	12(2)	79(5)
C(31E)	52(4)	55(5)	76(4)	-12(4)	-9(3)	13(4)
C(32E)	112(7)	92(6)	66(4)	-23(4)	18(5)	16(5)
C(33E)	135(8)	68(5)	82(5)	-26(4)	-23(6)	22(5)
C(34E)	60(5)	86(5)	104(7)	-5(5)	-11(4)	10(4)
C(35E)	58(4)	84(5)	77(4)	2(4)	5(4)	7(3)
C(36E)	64(4)	69(4)	90(6)	-10(4)	12(4)	28(3)
C(37E)	119(8)	85(6)	110(8)	9(5)	-11(6)	-10(6)
S(1K)	59(1)	86(1)	71(1)	5(1)	1(1)	17(1)
O(1K)	67(3)	126(5)	103(4)	10(4)	6(3)	24(4)
O(2K)	119(6)	97(6)	70(3)	-1(5)	11(3)	2(5)
O(3K)	73(3)	375(11)	66(3)	-16(4)	12(2)	79(5)
C(31K)	52(4)	55(5)	76(4)	-12(4)	-9(3)	13(4)
C(32K)	112(7)	92(6)	66(4)	-23(4)	18(5)	16(5)
C(33K)	135(8)	68(5)	82(5)	-26(4)	-23(6)	22(5)
C(34K)	60(5)	86(5)	104(7)	-5(5)	-11(4)	10(4)
C(35K)	58(4)	84(5)	77(4)	2(4)	5(4)	7(3)
C(36K)	64(4)	69(4)	90(6)	-10(4)	12(4)	28(3)
C(37K)	119(8)	85(6)	110(8)	9(5)	-11(6)	-10(6)
O(24F)	113(4)	282(10)	106(4)	22(5)	12(3)	-41(6)
O(25F)	135(4)	175(5)	84(3)	-28(3)	12(3)	26(4)
C(1F)	76(3)	100(4)	78(3)	17(3)	-3(3)	-35(3)
C(2F)	78(4)	163(6)	63(3)	22(4)	-9(3)	-50(4)
C(3F)	80(4)	216(8)	58(3)	-4(4)	-2(3)	-99(5)
C(4F)	119(5)	125(5)	70(3)	-18(3)	18(3)	-61(4)
C(5F)	68(3)	110(4)	78(3)	2(3)	13(3)	-20(3)
C(6F)	116(5)	98(5)	107(5)	-8(4)	27(4)	-1(4)
C(7F)	114(5)	80(4)	82(4)	-3(3)	15(3)	9(3)
C(8F)	72(3)	64(3)	72(3)	-1(2)	-8(2)	-1(2)
C(9F)	61(3)	74(3)	66(3)	5(2)	-10(2)	-20(2)
C(10F)	58(3)	94(4)	78(3)	7(3)	-7(2)	-33(3)
C(11F)	94(4)	64(3)	91(4)	17(3)	-16(3)	-2(3)
C(12F)	81(3)	70(3)	86(3)	-1(2)	1(3)	8(3)

C(13F)	70(3)	63(3)	73(3)	-5(2)	-9(2)	-7(2)
C(14F)	65(3)	75(3)	68(3)	-1(2)	-5(2)	-2(2)
C(15F)	121(5)	77(4)	75(3)	5(3)	13(3)	-1(3)
C(16F)	104(4)	79(4)	83(3)	10(3)	3(3)	-4(3)
C(17F)	80(3)	83(3)	69(3)	-3(2)	-3(3)	0(3)
C(18F)	87(4)	96(4)	84(3)	-6(3)	-14(3)	-16(3)
C(19F)	70(4)	124(5)	117(5)	0(4)	-3(3)	-46(4)
C(20F)	93(4)	83(4)	79(3)	-13(3)	0(3)	-6(3)
C(21F)	178(8)	94(5)	124(6)	-18(4)	45(6)	11(5)
C(22F)	104(5)	117(5)	76(4)	-15(3)	12(3)	-5(4)
C(23F)	109(5)	148(7)	75(4)	-26(4)	-1(4)	0(5)
C(24F)	111(5)	110(5)	73(4)	0(3)	0(4)	0(4)
C(25F)	183(9)	166(8)	85(4)	-3(5)	34(5)	49(7)
S(1F)	42(2)	118(3)	66(1)	-11(2)	5(1)	-23(2)
O(1F)	49(5)	82(5)	98(3)	-27(4)	-9(3)	-39(3)
O(2F)	32(3)	149(7)	99(3)	-10(5)	-9(3)	-25(3)
O(3F)	112(3)	289(7)	59(2)	-11(3)	15(2)	-143(4)
C(31F)	80(8)	66(4)	52(4)	-1(3)	4(5)	-13(5)
C(32F)	42(5)	88(6)	100(6)	-20(5)	12(4)	-28(4)
C(33F)	95(6)	95(7)	93(6)	-3(4)	25(5)	-1(5)
C(34F)	78(5)	76(5)	75(5)	3(4)	-10(4)	-11(4)
C(35F)	119(8)	105(7)	93(7)	33(6)	13(6)	-12(7)
C(36F)	98(6)	106(6)	67(4)	16(4)	19(4)	-3(5)
C(37F)	90(6)	102(7)	100(6)	-3(5)	2(5)	13(5)
S(1L)	42(2)	118(3)	66(1)	-11(2)	5(1)	-23(2)
O(1L)	49(5)	82(5)	98(3)	-27(4)	-9(3)	-39(3)
O(2L)	32(3)	149(7)	99(3)	-10(5)	-9(3)	-25(3)
O(3L)	112(3)	289(7)	59(2)	-11(3)	15(2)	-143(4)
C(31L)	80(8)	66(4)	52(4)	-1(3)	4(5)	-13(5)
C(32L)	42(5)	88(6)	100(6)	-20(5)	12(4)	-28(4)
C(33L)	95(6)	95(7)	93(6)	-3(4)	25(5)	-1(5)
C(34L)	78(5)	76(5)	75(5)	3(4)	-10(4)	-11(4)
C(35L)	119(8)	105(7)	93(7)	33(6)	13(6)	-12(7)
C(36L)	98(6)	106(6)	67(4)	16(4)	19(4)	-3(5)
C(37L)	90(6)	102(7)	100(6)	-3(5)	2(5)	13(5)

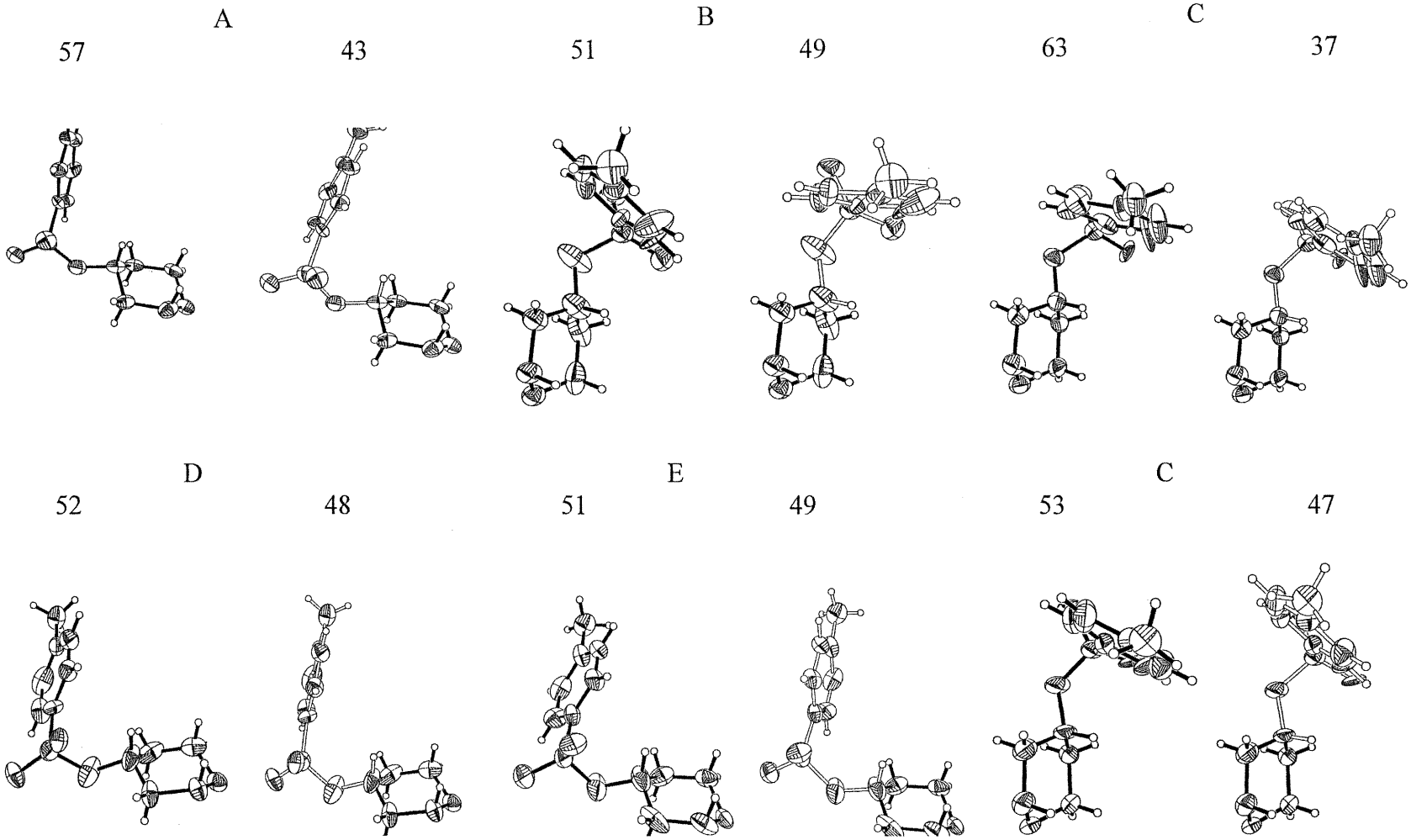

(4) The conformation of the para-methylphenylsulfonyl terminus in the six molecules. Every molecules has two possibilities at ratio: A(57:43), B(51:49), C(63:37), D(52:48),E(51:49), F(53:47). Therefore, there are 12 figures of conformation

(5) Fractional atomic coordinates and equivalent isotropic displacement parameters ($Å^2$) for $C_{34}H_{56}O_7.H_2O$

$$Ueq = (1/3) \sum_i \sum_j U^{ij} a^i a^j a_i a_j$$

	Occupancy	x	y	z	Ueq
O3	1	1.0922 (4)	0.334 (2)	1.1631 (3)	0.0603 (13)
H3	1	1.1199	0.4242	1.1522	0.090
O7	1	0.8559 (4)	0.674 (2)	0.9587 (3)	0.0607 (14)
H7	1	0.8567	0.6907	0.9152	0.091
O12	1	0.7999 (4)	0.153 (2)	0.8476 (3)	0.0732 (16)
H12	1	0.8462	0.1994	0.8822	0.110
C1	1	0.7752 (6)	0.201 (2)	1.1060 (4)	0.058 (2)
H1A	1	0.7582	0.2093	1.1547	0.070
H1B	1	0.7386	0.0969	1.0833	0.070
C2	1	0.9072 (6)	0.188 (2)	1.1149 (4)	0.058 (2)
H2A	1	0.9257	0.1764	1.0667	0.070
H2B	1	0.9377	0.0894	1.1444	0.070
C3	1	0.9659 (5)	0.351 (2)	1.1535 (3)	0.0527 (18)
H3A	1	0.9478	0.3596	1.2025	0.063
C4	1	0.9182 (5)	0.504 (2)	1.1097 (4)	0.0486 (18)
H4A	1	0.9426	0.5011	1.0631	0.058
H4B	1	0.9527	0.6042	1.1365	0.058
C5	1	0.7812 (6)	0.518 (2)	1.0934 (4)	0.0522 (19)
H5	1	0.7605	0.5316	1.1414	0.063
C6	1	0.7340 (6)	0.678 (2)	1.0471 (4)	0.0531 (19)
H6A	1	0.6532	0.6994	1.0515	0.064
H6B	1	0.7823	0.7742	1.0683	0.064
C7	1	0.7341 (5)	0.667 (2)	0.9661 (4)	0.0508 (18)
H7A	1	0.6909	0.7646	0.9404	0.061
C8	1	0.6723 (6)	0.502 (2)	0.9309 (4)	0.0483 (18)
H8	1	0.5881	0.5088	0.9325	0.058
C9	1	0.7267 (5)	0.343 (2)	0.9763 (3)	0.0439 (16)
H9	1	0.8119	0.3438	0.9772	0.053

C10	1	0.7177 (5)	0.354 (3)	1.0585 (4)	0.0541 (18)
C11	1	0.6789 (7)	0.181 (2)	0.9395 (4)	0.060 (2)
H11A	1	0.5978	0.1667	0.9446	0.072
H11B	1	0.7257	0.0877	0.9650	0.072
C12	1	0.6796 (6)	0.172 (2)	0.8565 (4)	0.0546 (19)
H12A	1	0.6363	0.0690	0.8367	0.066
C13	1	0.6163 (5)	0.318 (2)	0.8130 (4)	0.0452 (16)
C14	1	0.6781 (6)	0.486 (2)	0.8512 (4)	0.0448 (17)
H14	1	0.7626	0.4784	0.8505	0.054
C15	1	0.6226 (7)	0.623 (2)	0.7946 (4)	0.064 (2)
H15A	1	0.5471	0.6609	0.8032	0.076
H15B	1	0.6754	0.7201	0.7982	0.076
C16	1	0.6050 (8)	0.542 (2)	0.7201 (4)	0.069 (2)
H16A	1	0.6597	0.5900	0.6931	0.083
H16B	1	0.5242	0.5607	0.6917	0.083
C17	1	0.6297 (6)	0.341 (2)	0.7327 (4)	0.0545 (18)
H17	1	0.7139	0.3222	0.7333	0.065
C18	1	0.4832 (6)	0.313 (2)	0.8135 (4)	0.062 (2)
H18A	1	0.4513	0.2032	0.7982	0.093
H18B	1	0.4414	0.3978	0.7800	0.093
H18C	1	0.4739	0.3366	0.8627	0.093
C19	1	0.5844 (6)	0.353 (2)	1.0637 (4)	0.068 (2)
H19A	1	0.5802	0.3705	1.1142	0.102

A2 The DSC traces of some selected polymers showing the peaks only in the first heating cycle (heating rate: 10 ° C / min)